Authors' response on "Using depolarization to quantify ice nucleating particle concentrations: a new method" *by* Jake Zenker et al.

The authors thank the 4 anonymous reviewers for the detailed comments, all published on Aug 9. 2017. In the response below, we address each of the suggestions of the 4 reviews.

5 **Anonymous Referee #1 Received and published: 9 August 2017**

Referee Comment:

Review of "Using depolarization to quantify ice nucleating particle concentrations: a new method" by Zenker et al.

General Comment This manuscript introduces a new method to distinguish between ice particles, aerosol 10 particles, and liquid water droplets at the water droplet breakthrough (WDBT) line in a continuous flow diffusion chamber. The traditional method to determine the concentration of ice nucleating particles (i.e., particle size) is not accurate at the WDBT and therefore, the proposed method can be of high importance. The new proposed method agrees well with the traditional method before the WDBT and it improves the detection of INPs at and above this line. However, this new method cannot be applied to field 15 measurements given that the uncertainty is very high when low concentrations of INPs are present. Therefore, this new method is only valid for laboratory experiments where high concentrations of INPs are usually achieve. Although the scientific goals are interesting and the experiments/analysis were carefully performed, the presentation of the manuscript is not the best. There are too many typos, some parts are repeated along the manuscript, and there are key references missing. It would be nice if a senior 20 researcher from the team can proof-read the revised version. **The reviewer did not find a major point; however, the following minor comments need to be addressed before its publication in AMT.**

Authors' response: Thank you. As the reviewer notes, we have stated in the original text that this technique is best applied to laboratory measurements due to signal to noise. Nevertheless, we agree with 25 the reviewer that developing such a method is of high importance due to the need for such a method, and we thank the reviewer for supporting this work.

Authors' changes in manuscript: The manuscript has been carefully revised and the minor comments of the reviewer are addressed item by item below.

Minor Comments

5 *Referee Comment:*

P2 L6: "depositional freezing" is incorrect given that "freezing" refers to the transition from liquid to solid. In deposition ice nucleation the liquid phase is not present.

Authors' response: Corrected.

10 *Referee Comment:* P2 L9-10: In all clouds or Mixed-phase clouds only?

Authors' response: In general, immersion freezing is the dominant nucleation mechanism for producing ice crystals in all clouds containing ice.

Referee Comment: P2 L17: Why mixed-phase clouds exclusively? Heterogeneous ice nucleation can also

15 takes place in cirrus clouds, for example.

Authors' response: We did not mean to imply that ice nucleation mechanisms are only relevant to mixed phase clouds. Mixed phase clouds are mentioned here because the current study addresses the specific challenges of accurate detection of ice in the presence of droplets.

20 *Referee Comment:* P2 L18: Add references after "GCMs". P2 L20: There are many studies showing this. I will rather cite a review paper instead.

Authors' response: Added "(e.g. Tan et al., 2016; Pithan et al., 2014)".

Referee Comment: P2 L22: Atkinson et al. (2013) and Yakobi-Hancock et al. (2013) are not field studies.

25 *Authors' response:* True. We have changed "Field measurements" to "Measurements".

Referee Comment: P2 L24-25: Other groups working on ice nucleation (besides the two cited here) have done a significant contribution as well. It would be better to divide the references by aerosol type. The recent reviews by Coluzza et al. (2017) and Kanji et al. (2017) nicely fit here.

Authors' response: This is certainly true. We were focusing on the TAMU CFDC which is the topic of the manuscript and the CSU CFDC to which is it compared in this manuscript. But, we agree that other importance contributions should be mentioned.

Authors' changes in manuscript. We now include Coluzza et al. (2017) and Kanji et al. (2017).

Referee Comment: P3 L8: Add references after "crystals".

Authors' response: Reference to Bohren and Huffman, 1983 added.

Referee Comment: P3 L16: The Cziczo et al. (2017) review could be cited here.

Authors' response: Done.

Referee Comment: P6 L13: What do the authors mean with "processing chamber"?

Authors' response: Please refer to pg. 6 ln 4 which now reads "The aerosols then enter the CFDC processing chamber where temperature and supersaturation are controlled."

Referee Comment: P6 L14: Remove "TAMU". It was previously mentioned that CFDC will refer to the TAMU CFDC.

Authors' Comment: Done.

Referee Comment: P7 L4: Why were the flows changed? Should it not be constant?

Authors' response: Flow adjustments were made to maintain conditions within the critical flow regime, i.e. to ensue laminar flow, and avoid buoyancy effects under all operating temperature and supersaturations. Ideally, these flows would be constant; however in order to obtain the certain high supersaturation targets which were of interest during FIN02 evaluation of WDBT, adjustments were made.

Referee Comment: P7 L4: Please add the uncertainty for 2 L min-1.

Authors' response: Note that experimental uncertainty is not discussed in this sentence. This is variation
5 in selected operating flows (±0.5 L min^{-1}) during FIN02. In contrast, uncertainty in sample flow is ±0.1
L min^{-1} based on the experimental precision in the total and sheath mass flow controlled.
Authors' changes in manuscript: Added "±0.5 L min^{-1}."

Referee Comment: P7 L4: I found the 1.5°C value quite high. Other CFDC report much lower values.
10 What is the reason for this?
Authors' response: This is not an instrumental uncertainty, per se. It is a choice of data processing. All
CFDC data collected at a mean temperature of X ±1.5°C was included in the data set for a chosen
temperature X.

15 *Referee Comment:* P7 L10: Remove "and" after "pressure".
Authors' response: Done.

Referee Comment: P7 L15-16: "The concentration of particles measured while the filter is in place is
subtracted from the total concentration measured by the CASPOL." Both are measured by the CASPOL.
20 I think it would be better to say: Total concentration measured during the supersaturation scan. To account
for this, a filter is placed ahead of the sample inlet in order to determine background signal of the CFDC
chamber. The background period that is closest to a given 1-minute sample period is then applied by
subtracting that background concentration from the total concentration measured by the CASPOL at the
sample time.
25 *Authors' response*: We don't see exactly how the reviewer's suggestion would work, but we have revised
the sentence for clarity.
Authors' changes in the text: The text now reads, "… a filter is placed ahead of the sample inlet in order
to determine background signal of the CFDC chamber. The background period that is closest to a given

1-minute sample period is then applied by subtracting that background concentration from the total concentration measured by the CASPOL at the sample time."

Referee Comment: P7 L18: Add references after "crystals".

5 *Authors' response*: Added Bohren and Huffman, 1983.

Referee Comment: P7 L28: "Any droplets that remain larger than the 2 μm size cut will be miscounted as ice". This is based on who?

Authors' response: We are not certain what the Referee means to ask here. We feel it is clear as stated

10 that when the size-cut is set to 2 μm, any particles, be they ice or other composition, which are larger 2 μm will be counted as ice.

Referee Comment: P8 L7: "discern". Between what?

Authors' response: Changed to "determine".

15

Referee Comment: P8 L8: What do the authors mean with positive and negative artifacts?

Authors' response: This was a mistake on our part, because only positive artifacts are possible. "Positive artifacts" mean water droplets breaking through are counted as members of the ice crystal population. "Negative artifacts" would mean ice particles not counted because one thinks they are water droplets, but

20 in practice there is no way for that to occur.

Authors' changes in manuscript: "if the instrument is unintentionally operated at supersaturations above WDBT, droplets will be miscounted as ice crystals."

Referee Comment: P8 L11: This sound a bit awkward.

25 *Authors' response*: The original sentence was: "For the traditional analysis method to be successful, sample aerosols must not be larger than the applied size cut or they too will be miscounted as an INP."

Authors' changes in manuscript: Revised to: "In the traditional analysis, any sample aerosols larger than the applied size cut will also be miscounted as INPs."

Referee Comment: P8 L15: Add references after "signal".

Authors' response: This is based on empirical testing. There is no literature reference necessary.

5 *Referee Comment:* P8 L15: This is the fourth time the word "new" is used.

Authors' response: The topic of this manuscript is to compare one method, the "new method" developed here to the "traditional method", so we need to reserve the right to say "new" many times.

Referee Comment: P8 L16: What is "high" and "low"?

10 *Authors' response*: In the revised version of the document this sentence has been deleted due to other suggested revisions.

Referee Comment: P8 L16: Replace "our" with "the".

Authors' response: Removed "our" in the text.

15

Referee Comment: P9 L4: Add reference after "infinite"

Authors' response: This is a straightforward mathematical interpretation of Equation 2 above it. We do not feel it needs a reference.

20 *Referee Comment:* P9 L11: Delete "Using" after "…droplets."

Authors' response: Done.

Referee Comment: P9 L15: Add references for the 1.33 value.

Authors' response: Added Zajak and Hecht, 2002.

25

Referee Comment: P9 L16: Add the uncertainty for the droplet sizes.

Authors' response: Added.

Author's change in the manuscript: "As reported in Glen and Brooks (2013), the uncertainty in sizing due to differences in the complex refractive indices of oil and water are up to 30% based on a comparison of VOAG oil droplet calibrations of CASPOL to water-based calibrations performed by the manufacturer. For this project, droplets were generated with the diameters of 2 ± 0.6 μm, 6 ± 1.8 μm, 8 ± 2.4 μm, and

5 10 ± 1.5 μm."

Referee Comment: P9 L18: Remove "and" after "frequency".
Authors' response: Here the grammar is correct as written.

10 *Referee Comment:* P9 L22: "sample flow is split between flow to the CASPOL" sound a bit awkward. Remove one "the".
Authors' response: Done.

Referee Comment: P9 L22: Remove "and" after "controller".
15 *Authors' response*: Here the grammar is correct as written.

Referee Comment: P9 L24: Replacer "are" with "were".
Authors' response: Done.

20 *Referee Comment:* P10 L4: "in aerosols"?
Authors' response: Changed to "of aerosols"

Referee Comment: P10 L12-23: "in the absence of activated liquid droplets". Do the authors mean in the absence of INPs?
25 *Authors' response*: No. The referee is correct that homogenous freezing occurs without INP. However, the point we're making here is that the experiment under cold, dry temperatures to reduce the chance of any unwanted droplet formation.

Referee Comment: P10 L15: "-11 ± 1.5 % SSw"? Something is wrong here.

Authors' response: We have rearranged and simplified the sentence for clarify.

Authors' changes in manuscript: The text now reads, "the CFDC was operated at $-55 \pm 0.2\,°C$ and $51 \pm 2.3\,\%\ SS_i(-11 \pm 1.5\,\%\ SS_w)...$"

5

Referee Comment: P10 L26: Remove "TAMU". See comment on P6

Authors' response: Done.

Referee Comment: L14 P11 L16: "Fig.s 1" should be "Fig. 1".

10 *Authors' response*: Fixed.

Referee Comment: P12 L17 and P13 L6-8: Why did the authors choose dust-like as the model for aerosol particles? How about biological particles? Soot?

Authors' response: Indeed, aerosols come in a wide variety of compositions. Performing scattering

15 calculations on all atmospheric aerosol types would be beyond the scope of this study. We chose dust as a relevant choice due to its widespread presence in the atmosphere and the known action of many dusts as INPs. Also, many of the organic and inorganic salt particles in the atmosphere will be in the form of solution droplets. Since those will have similar scattering properties to the water droplets, which were already included, the non-spherical dust also provides a good compliment to the spherical particles.

20

Referee Comment: P13 L27: Please indicate to what Figure the authors are referring to.

Authors' response: Fig. 1a is now stated.

Referee Comment: P14 L23-24 and along the manuscript: Please use "WDBT" instead of "water droplet

25 breakthrough". This was defined in P8 L1.

Authors' response: True, but we find it helpful to write it out in full one more time for readers who are likely to be unfamiliar with the term.

Referee Comment: P15 L5: Please indicate to what Figure the authors are referring to.

Authors' response: Fig 1a is now included.

Referee Comment: P16 L24-26: Replace "um" with "μm" to be consistent.

5 *Authors' response*: Corrected.

Referee Comment: P17 L8: I think the year of the Pruppacher and Klett book is incorrect.

Authors' response: Thank you, we have corrected this oversight.

10 *Referee Comment:* P17 L23-24: "the geometry of the ice crystal can be modified leading to drastic differences in the observed depolarization ratio." Can the authors report the time scale under which this is valid? i.e., how many seconds/minutes are needed for an ice crystal to change its geometry?

Authors' response: This comment pertains to the study of Smith, 2016. . They grew ice crystals in the Manchester Ice Chamber which is similar in size and design to the AIDA chamber. They operated the

15 chamber at various temperatures and grew ice crystals in the chamber. The change in relative humidity reportedly causes the evolution of ice crystal geometry. To monitor the changes, sample were taken every minute over 5-6 minutes. There were visually noticeable changes in to the habit at each minute increment (e.g. hollow hexagonal columns evolve slowly into solid hexagonal columns, dendrites evolve into hexagonal plates). The paper does not report a specific timescale that is necessary for a detectable change

20 in ice crystal shape to occur, but their results suggest that changes may occur rather rapidly with changing conditions in the chamber (over a minute or less). While this is an interesting study, we feel it is beyond the scope of our study and interested readers are referred to the Smith paper.

Authors' changes in the manuscript: None.

25 *JAKE Referee Comment:* P17 L24 and 27: Add the year of the Smith et al. paper.

Authors' response: The year is now in the text "Smith et al. (2016)"

Referee Comment: P17 L28: "(2016)" is out of place.

Authors' response: Corrected.

Referee Comment: P18 L2: Add "field" before "campaign".

Authors' response: FIN-02 was a laboratory campaign, FIN-03 was a field campaign. These are now

5 correct everywhere in the text.

Referee Comment: P19 L25: Please indicate to what Figure the authors are referring to.

Authors' response: Fig. 7 is now mentioned in the text.

10 *Referee Comment:* P22 L3-4: How about to include kanji et al. (2017)?

Authors' response: Good idea. Done.

Referee Comment: P22 L8: "the Colorado State University (CSU) CFDC". This was defined already in

P3 L18.

15 *Authors' response*: True, but in discussion with coauthors we decided a little repetition for clarify was

helpful.

Referee Comment: P23 L19: Add "only" after "experiments".

Authors' response: Done.

20

Referee Comment: P25-30: Be consistent with the journal names in the references. Either add the full

name or their abbreviation.

Authors' response: Abbreviations are now used in accordance with the AMT manuscript preparation

guidance.

25

Jake Referee Comment: P25-30: The page numbers in several references are missing (e.g., DeMott et al.

(2017), Levin et al. (2016), McCluskey et al. (2016), McFarquhar et al. (2011)).

Authors' response: All page numbers are now included where applicable.

Referee Comment: P25-30: References need to be up to date.

Authors' response: We have added a few references from 2017 per the reviewer recommendations (Coluzza et al., 2017; Cziczo et al., 2017; Kanji et al., 2017).

5

Figure 2: Given that there is no extra-charge for colored-figures in AMT, I suggest to add color to this figure to improve its readability.

Authors' response: Since the symbols and colors on Fig. 2 were chosen to match the same data sets included on page. 6, we prefer to keep the original scheme.

10

Referee Comment: Figure 3: Blue circles in panel's b and c should be blue squares.

Authors' response: This has now been fixed.

Referee Comment: Figure 11: "TAMU CFDC versus CSU CFDC comparison."

15 Is written twice in the figure caption.

Authors' response: Corrected. Thank you.

Referee Comment: Table 1: Add ":" after "1" for consistency with the Figures.

Authors' response: Done.

20

References:

Coluzza, I., Creamean, J., Rossi, M. J., Wex, H., Alpert, P. A., Bianco, V., Y. Boose, C. Dellago, L. Felgitsch, J. Fröhlich-Nowoisky, H. Herrmann, S. Jungblut, Z.A. Kanji, G. Menzl, B. Moffett, C. Moritz, A. Mutzel, U. Pöschl, M. Schauperl, J. Scheel, E. Stopelli, F. Stratmann, H. Grothe, and D. Schmale III 25 (2017). Perspectives on the Future of Ice Nucleation Research: Research Needs and Unanswered Questions Identified from Two International Workshops. Atmosphere, 8(8), 138.

Cziczo, D. J., Ladino, L., Boose, Y., Kanji, Z. A., Kupiszewski, P., Lance, S., Mertes, S., and Wex, H. (2017). Measurements of Ice Nucleating Particles and Ice Residuals. Meteorological Monographs, 58, 8.1-8.13.

5   Kanji, Z.A., Ladino, L., Wex, H., Boose, Y., Burkert-Kohn, M., Cziczo, D.J., and Krämer, M. (2017). Overview of Ice Nucleating Particles. Meteorological Monographs, 58, 1.1-1.33

Anonymous Referee #2 Received and published: 9 August 2017

Referee Comment: The paper reports a new method, based on depolarization ratio, to enhance the calculation of ice nuclei concentrations in the occurrence of water droplet breakthrough. The method seems to be specific to the CFDC at Texas A&M University and to be applicable only in laboratory settings. For this reason, the wide applicability of the method might be limited. Despite that though, the issue to solve is an important one, especially considering the large uncertainties in the field of ice nucleation research. In addition, the technical work done for this comparison is considerable and involved also a modeling aspect. Therefore, I think the paper should be published. Overall the approach seems sound and well developed. Some clarification would be helpful in some instances, but overall the paper is well written.

Authors' response. Thank you for your positive review. We have revised the manuscript in order to provide clarification in the specific instances below.

Referee Comment: Some specific, rather minor comments:

1. Maybe I missed it, but I do not recall seeing mention of the specifications of the light source in the CASPOL (wavelength, polarization, source, e.g. laser etc.).

Authors' response. The light source is a linearly polarized 680 nm laser.

Authors' changes in manuscript. Added on pg 6 ln 20, "Laser light (680 nm) is scattered by single particles entering the CASPOL and detected by three detectors…"

Referee Comment 2: On page 5 the authors describe the APC chamber, how are clouds produced in it, also through adiabatic expansion?

Authors' response: No. To clarify, in this experiment, no clouds are produced in the APC chamber during the experiment. The APC is used to provide a uniform high concentration of aerosols generated by filling the APC chamber with aerosols produced by atomization and solid aerosol generation methods. The ice cloud particles sampled by the CFDC-CASPOL are produced within the CFDC's processing chamber

under conditions of controlled saturation conditions produced by varying the temperature gradient between the inner and outer iced walls of the chamber.

Authors' changes in manuscript: On pg 4, ln 28, the text now reads, "The APC was used during FIN02 to provide a uniform high concentration of aerosols of various compositions, which were generated by filling the APC chamber with aerosols produced by atomization and solid aerosol generation methods and were subsequently distributed to the participating ice nucleation instruments"

Referee Comment 3: It would help to have some more detail on what causes the water droplet breakthrough, in what conditions, why it happens at different conditions in different instrument etc. For example around page 8 or so.

Authors' response: Thanks for this good suggestion. Water droplet breakthrough is the term used to describe the arrival of droplets reaching the detector of an ice nucleation chamber where they will be miscounted by most as ice particles by most detection methods. This arises when the chamber is operated under supersaturation conditions and supercooled droplets form in the initial sections of the processing chamber. Most CFDC designs include a section following growth chamber, referred to as an evaporation region. The evaporation region is maintained under conditions at which the Bergeron process is active, that is conditions, which are subsaturated with respect to droplets. Thus, droplets shrink or evaporate entirely while at the same time the conditions are supersaturated with respect to ice, allowing ice crystals to grow.

The specific conditions of the evaporation chamber vary from instrument to instrument. Another cause of differences in WDBT between instruments is the selection of the size cut-off for distinguishing INPs by size alone. For example, using the traditional strategy of relying on a nominal size-cutoff to define INP, if an operator chooses 2 microns as the diameter above which all particles are presumed to be ice, then a water droplet need only be 2 microns in diameter to "break through," whereas if the operator chooses a 5 micron size cut-off same detector operating under all the same conditions, only water droplets will necessarily have to grow to 5 microns to break through and be miscounted as ice. So, it is the combination of chamber dimensions, flow rates, operating conditions (temperature and supersaturation)

14

in the growth and evaporation regions, and choice of detector and size cut-off which collectively determine WDBT for a certain instrument.

Authors' changes in manuscript: Page 8 has been revised to include addition details, "WDBT is a common issue in continuous flow ice nucleation instruments, although the point at which WDBT occurs varies between instruments of differing dimensions and even as a function of operating conditions (especially temperature) within a single instrument (Rogers et al., 2001, DeMott et al, 2015, Garimella et al., 2016). CFDCs in use today are custom-built instruments which vary in physical dimensions and choice of detector, although all operate under the same basic principles. Due to the combination of chamber dimensions, flow rates, operating conditions (temperature and supersaturation) in the growth and evaporation regions within the instrument, and the choice of detector and size cut-off, WDBT varies from instrument to instrument. In some cases, it can be difficult to determine when WDBT is occurring, and if the instrument is unintentionally operated at supersaturations above WDBT, droplets will be miscounted as ice crystals."

Referee Comment 4: On page 9 on the first line: "precisely" seems a bit too strong; also LIDARs will have some finite field of view.

Authors' response: We think our point is best made by keeping "precisely" here to emphasis the difference in backscattering angle of the lidar at 180° from the CASPOL backscatter at 168º to 176º.

Referee Comment 5: Still on page 9, the authors mention oil as having a similar real part of the imaginary index of refraction. I would think oil might have a different imaginary part of the index of refraction, with respect to water (also depending on the wavelength of the CASPOL). Maybe this is completely negligible, but could the absorption make any difference in the measurements or numerical simulations?

Authors' response: The uncertainty in sizing due to differences in the complex refractive indices of oil and water are up to 30% based on a comparison of VOAG oil droplet calibrations of CASPOL performed in our laboratory in comparison to the manufacturer's water-based CASPOL size calibrations (with the oil droplets being overestimated). This is discussed in detail in our previous work (Glen and Brooks,

2013). Comparable uncertainties are expected for the simulations.

Authors' changes in the manuscript: Added "As reported in Glen and Brooks (2013), the uncertainty in sizing due to differences in the complex refractive indices of oil and water are up to 30% based on a comparison of VOAG oil droplet calibrations of CASPOL to water-based calibrations performed by the manufacturer."

Referee Comment 6: Page 10, line 7: remove "both"

Referee Comment 7: Page 11, line 9 to 12. This sentence is not very clear to me.

Authors' response: We have revised this text.

Authors' changes in manuscript. The text now reads, "Each training dataset contains some particles that are highly backscattering and some particles that are highly depolarizing, but only the ice crystal population contains particles that have both a high depolarization ratio and high backscatter signal."

Referee Comment 8: Referring to figure 1, it seems like the total backscatter signal should have parenthesis in the label of the y axis.

Author Response: This has been changed as suggested by the Referee.

Referee Comment 9: Page 13, line 12, why is 1.75 um an upper limit for the CFDC? Are there some data on this item, or some published values?

Authors' response: The CFDC's standard procedure is to operate with a cyclone impactor installed at the inlet which removes particles larger than 1.75 micron diameter. This was mentioned earlier but not on page 13.

Authors' changes in manuscript. This sentence has been removed because aerosol calculations for larger sizes are included to address a different Referee suggestion.

Referee Comment 10: Page 13, lines 24-26 and related figures: maybe I missed it, but how were the size distributions measured?

Authors' response: The forward scattering detector of the CASPOL detects particles on an individual basis and sorts those particles into a series of size bins ranging from 0.6 to 50 micrometers optical diameter.

Authors' changes in manuscript. Details above are now included on pg 7, ln 4.

5

Referee Comment 11: Page 16, line 24, I think "large" should be "larger".

Authors' response: Changed.

Referee Comment 12: Page 17, line 3, it seems like a "different" is missing when discussing the "statistically significant..."

10

Authors' response: We agreed. Added.

Referee Comment 13: Page 18, line 7, "like" should be "likely"

Authors' response: Corrected.

15

Referee Comment 14: I found the section 3.7 hard to read and to follow. I am not sure what to suggest. Maybe a schematic of the algorithm would help, but as is, for me, it is very difficult to follow.

Authors' response: For clarity, we've structured the text and added details throughout the section to guide the reader. Further, we've added a table that lays out how the training datasets are generated. There were specific points of confusion pointed out by other referees that we addressed here that strengthen the paragraph as well.

20

Anonymous Referee #3 Received and published: 9 August 2017

Review to "Using depolarization to quantify ice nucleating particle concentrations: a new
Method" by Zenker et al. AMTD, 2017   the manuscript by Zenker and coworkers describes the applica

5   tion of a new method to discriminate particle types in continuous flow diffusion
Chamber (CFDC) studies using a depolarization signal obtained from the Aerosol
Spectrometer with POLarization (CASPOL). The work is motivated by the difficulties faced
when particle type discrimination is purely based on particle size ("traditional method"), as particl
es of the same size do not necessarily need to be of the same type. Using a set of

10   training data, where only ice crystals, aerosol particles or (cloud) droplets exist the authors
show how the CASPOL depolarization signal can be used to differentiate these particles types
based on optical signatures.   A linear regression fit model is then used to optimize the
depolarization ratio value considered as (threshold) criterion to differentiate particle types,
concluding with an optimal value of 0.3. The corresponding linear regression is then used

15   to calculate the ice nucleating particle (INP) concentration for an extensive CFDC data
set and the results for the "new" and the "traditional" method are compared. I believe that
the topic of reliable particle type discrimination in CFDC studies (when operating under water
droplet breakthrough (WDBT) conditions) is inherently complex and needs to be addressed in
the future. This manuscript certainly provides motivation to do so and the presented results show

20   evidence that using depolarization ratio can contribute to a more accurate discrimination
of particle type in CFDC studies than is currently done by size discrimination and
ultimately leads to a better quantification of INP concentrations. The manuscript at the current state w
ould benefit from restructuring and major revisions to clarify certain key aspects of
the data analysis and interpretation. Once all concerns given in the following are properly

25   addressed, this manuscript may be suitable for publication in AMT.

Authors' response: Thank you.   We agree that WDBT needs to be addressed for ice nucleation
measurements to be more accurate and performed reliably under a broader range of atmospherically

relevant conditions. Also we agree that depolarization ratio can improve our discrimination between INP and wayward droplets reaching the detector, as our manuscript shows for the laboratory experiments herein.

Authors' changes in the text: We have restructured the introduction, moved the section on particle depolarization, and significantly revised the data analysis and interpretation sections, as well as the modeling section, as discussed in the point by point response and in response below and in response to the other reviewers. We feel that the manuscript has improved greatly in readability and clarity and hope that the referee agrees.

General Comments:

Referee   *Comment:*
Section 1: Please focus more on the core topic of the manuscript and provide background for the particle discrimination in CFDC studies. I also encourage the authors to motivate the need for a better particle type/phase discrimination in order to more clearly indicate the additional value obtained from new methods as presented in this manuscript.

Authors' response: We have restructured the introduction, following the later comment of the reviewer that the benefit of the new methods does become clear on page 4. We have moved that text forward to earlier in the introduction. We do note that current phase discrimination studies available in the literature are cited, and there are not a very large number available, which is further reason that we'd like to see the present study published.

Authors' changes in the manuscript: Please see the revised introduction.

Referee Comment: Section 2: This section requires restructuring and currently misses important technical details for the instruments used (e.g. TAMU CFDC) or appropriate references. Please add mo re instrumental details to the manuscript.

Authors' response: Section 2 has been restructured, with subsections 2.1 and 2.2 reordered (switched), and has been revised according to specific Referee comments here and in the other reviewers. As cited in Section 2, the TAMU CFDC and CASPOL have been discussed in great detail in our previous work (Glen & Brooks, 2013 and 2014, and Glen, 2014.)

5 *Authors' changes in the manuscript:* Please see the revised section 2 in the text.

Referee Comment: In Section 3, the creation of the simulated data sets and implementation of the regression model remains unclear to me. I struggled to follow how the optimal depolarization ratio threshold is identical to the one presented in Section 3.3, which I assumed

10 at this stage to be empirical.

Authors' response: In section 3.3, the training data sets are introduced. In Figure 3B, the population of particles is plotted against depolarization ration. It can be seen from this figure that droplets have depolarization ratios up to 0.3. Therefore, we visually assign 0.3 as the nominal depolarization threshold cut-off. At this point, the caveat remains that a small percentage of aerosols do have depolarizations

15 greater than this threshold. However, in the case of aerosols, there are 2 lines of defense against any aerosols being accidently counted as ice nucleation. In addition to the majority of aerosols having in addition to the depolarization threshold, aerosols with sizes above 1.75 micron diameter are physically removed from the sample upstream of the CFDC chamber.

20   In section 3.7, the linear regression model is introduced and used to optimize the cut-off. The statistically significant results in confirm that 0.3 is an optimal choice of threshold.

Authors' changes in the text: For clarity, section 3.3 now includes the statement. "For each training data set, the frequency distribution of depolarization ratio reported as a percentage of the total particles in the data set is shown in Fig. 3b. It can be seen from this figure that droplets have depolarization ratios up to

25 0.3. Therefore, we visually assign 0.3 as the nominal depolarization threshold cut-off for differentiating between ice crystals and non-ice particles. Unfortunately, it can also be seen that a small percentage of aerosols do have depolarizations greater than this threshold. However, since aerosols with sizes above 1.75 micron diameter are physically removed from the sample upstream of the CFDC chamber, the

combined consideration of size and depolarization may prove a robust strategy for avoiding the miscounting of aerosols as INP as further discussed below."

Secondly, based on referee comments, section 3.7 has largely been rewritten.

5

Referee   Comment: The justification on using a linear regression model and the implicated assumptions on the data
is entirely missing and only legitimated by indicating that other work has used linear regression models. Please add the justification for doing so.

10   *Authors' response:* Linear regressions are commonly used when determining how to use a new technique to determine an atmospheric quantity by relating a measured parameter or parameters to a ground truth measurement.

Authors' changes in the text: To explain to the user that there is a wide array of applications for a linear regression, several more papers that use a linear regression for various purposed (Zimmerman et al. 2017;

15   Brunner et al., 2015; Choi et al., 2016) are now cited.

Referee Comment: Also expand on how the choice of another depolarization ratio threshold does influence your results.

Author response: Please see the rewritten section 3.7

20

Referee   Comment: Lastly, the comparison of the TAMU data to the CSU data stays unclear. As presented in the current manuscript the usage of different cut sizes due to instrumental
differences is irritating and needs clarification.

Authors' response:

25   The TAMU and CSU CFDCs are independent custom-built instruments which operate on the same principles. Most importantly, because the CSU CFDC doesn't experience WDBT until a higher RH, this comparison provides a means to evaluate performance of the new method under conditions which our traditional method is clearly failing. In general, because the two CFDCs differ in dimensions, flow rates,

21

operating conditions (temperature and supersaturation) in the growth and evaporation regions within the instrument, and the choice of detector and size cut-off, an intercomparison is worthwhile.

Most importantly, because the CSU CFDC doesn't experience WDBT until a higher RH, this comparison provides a means to evaluate performance of the new method under conditions which our traditional method is clearly failing. Also, in general, because the two CFDCs are quite different instruments, an intercomparison is worthwhile.

We emphasize that the choice of different size cuts are justifiable, because the two CFDCs are not the same instrument in some key regards. For example, the TAMU CFDC growth chamber is smaller and the residence time is shorter. Therefore ice particles are not expected to grow as large as in the CSU unit. Logically, a small size cut may be more appropriate for the TAMU instrument. However, there are competing parameters, making this a non-straightforward choice, which is why multiple size cuts have been included for consideration in Fig 11. This is an issue that any operator of this type of instrument is concerned with.

Authors' changes in the manuscript. For emphasis we include the following statement on pg 24, ln 20, "Thus, inclusion of the CSU data provides a test of the new method at higher relative humidities under conditions when data obtained through the TAMU CFDC's traditional method is clearly spurious due to water droplet breakthrough."

Also, regarding differences in the 2 CFDCs, on pg 9, ln 14-20, the text now reads, "CFDCs in use today are custom-built instruments which vary in physical dimensions and choice of detector, although all operate under the same basic principles. Due to the combination of different chamber dimensions, flow rates, operating conditions (temperature and supersaturation) in the growth and evaporation regions within the instrument, and the choice of detector and size cut-off, WDBT varies from instrument to instrument."

Referee's comment: A quantification of the (range) extension for the operating conditions of the TAMU CFDC when applying the new method along with the associated error should be included.

Authors' response:

5   The specific conditions of WDBT vary with CFDC temperature, the ambient humidity, the hygroscopicity of sample aerosols, the size of sample aerosols, and the sample flow which determines the residence time in the instrument.

Author's changes in text: This is now stated in the text on page 9, ln 9 as written, "Specific conditions of WDBT vary with CFDC temperature, the ambient humidity, and the hygroscopicity of sample aerosols,

10   the size of sample aerosols, and the sample flow which determines the residence time in the instrument. Typically, in the TAMU CFDC the onset of WDBT occurs at 3 % to 4% SS_w, but has been observed as low as 1 % SS_w and as high as 8 % SS_w."

Specific comments:

15   P. 1-3, Introduction: The authors state the goal of the presented paper to be the development of a new method to quantify INP through a more reliable (phase) discrimination of particles exiting a CFDC, especially when operated under WDBT conditions (cf. p. 1, l. 15-18, p. 4, l. 13-19). In the introduction, the authors carefully describe the importance of ice and mixed-phase clouds and go on to discuss different ice nucleation pathways and INP characteristics (p. 2, l. 3-

20   13 and p. 2, l. 19-20). However, the succinct discussion of ice nucleation mechanism and mixed phase clouds are integral parts of the discussion on the topic of INP so they are not been removed.

After a brief discussion about the hydrometeor discrimination by LIDAR measurements using depolarization signals (p. 2 l. 25 – p. 3 l. 8) the authors give a detailed

25   overview of the CFDC history and the improvements done to CFDCs (p. 3 l. 1625). None of the topics mentioned above adds significant information to the topic discussed in the article, namely the cor rect discrimination of cloud particle type (phase). However, the introduction misses a clear description of the current limitations of particle phase

discrimination in CFDC studies as well as a motivation how such limitations affect past and current INP measurements, using CFDCs.

Authors' response:

5   The introduction has been significantly revised with the section on particle discrimination moved to early in the introduction.

However, given that this is a study on improvements in ice nucleation instrumentation, we feel the historic details lend important context to the issues, especially those related to water droplet breakthrough and the

10   improvements our new methods contributes.

Hence, we keep the majority of the text and we have added additional details specifically on strategies instruments through history have used to differentiate between ice crystals, water droplets, and aerosols. Also, we would be remiss to leave out (or delete) the section defining ice nucleation mechanisms, so that section remains.

15

Traditionally phase discrimination has relied on differences in particle size.   An impactor is used to physically eliminate aerosols larger than a certain point (~ 1.75 micrometer diameter).   Traditional detectors are optical particle counters which detector particles in a range of sizes.

Author's changes in text: Please see the revised and reorganized introduction.

20

Referee   *Comment:*

P. 4 l. 413 give details about how other studies differentiate particle phase, without discussion of the ge neral limitations. Without this discussion it becomes very hard for the reader to correctly

judge the quality of available CFDC data and recognize the need for development of new

25   instrumentation to improve discrimination of hydrometeor type. I suggest to add some references here a s well.

Authors' response: Please see our response to the next comment below. It appears that as the reviewer read further s/he found the answers to his/her questions. To make things clear sooner, we have reordered Sections 1 and 2 of the text, as discussed above.

5 *Referee* *Comment:*

Finally, the benefit of new methods, as described in the presented study becomes clearer.

Authors' response: Thank you. We are glad that this section clarified our motivation for new method development, and have moved that section forward in the text.

10 *Referee* *Comment:*

I recommend major changes to the introduction of the presented paper by considerable

shorten or remove some of the topics mentioned above and focusing on background needed

to understand the (size dependent) discrimination of particle phase and associated limitations, to better p

ut the current study into context.

15 *Authors' response:* Please see above in response to specific changes we have made.

Referee Comment: P. 1, l. 12: Please change "observed" to "measured".

Authors' response: The text is unchanged.

20 *Referee Comment:* P. 1, l. 15: Please change for clarification: "…under which discrimination of

hydrometeor phase and thus determination of INP concentrations based on hydrometeor size

fails."

Authors' response: Okay.

Authors' changes in the manuscript: The text now reads," During WDBT, the standard procedure of

25 counted counting all particle which grow beyond the size cut-off as ice crystals fails, which large droplets

are miscounted as ice."

Referee Comment: P.1, l. 18-19: Please clarify this statement. It is not a challenge

of WDBT that needs to be overcome, as WDBT forms an integral component of any CFDC study if operated at given conditions, but rather the challenge to reliable discriminate particle phase of the particles exiting a CFDC once WDBT conditions are met.

5 *Authors' response:* Okay.

Authors' changes in the manuscript: Revised to read, "To accurately measure INP during WDBT..."

Referee Comment: P. 1, l. 25: Please change "complicated" to "complex".

Authors' response: We prefer the original. The text is unchanged.

10

Referee Comment: P. 1, l. 26: Please clarify whether "precipitation" refers to spatial/temporal distribution of precipitation, precipitation formation or precipitation in general

Authors' response: As written, precipitation in general is implied,.. "Because of their complicated microphysical properties, ice clouds and mixed-phase clouds pose challenges in understanding our global

15 radiative budget and precipitation."

Referee Comment: P. 2, l. 2: Leave out "our".

Authors' response: Done.

20 *Referee Comment:* P. 2, l. 8: Leave out "becomes"

Authors' response: Done.

Referee Comment: P. 2, l. 11: Please insert: "aerosol particle…"

Authors' response: Done.

25

Referee Comment: P. 2, l. 12: Please change to: "aerosol particle collides with a supercooled water droplet and …"

Authors' response: Since, as the next sentence in the text states, *"*While the exact mechanism of contact freezing remains unresolved, it has been shown that the presence of an INP positioned at a droplet surface facilitates freezing at temperatures several degrees warmer than immersion freezing with identical INPs (Fornea et al., 2009; Durant and Shaw, 2005).", we feel the original is more accurate.

5

Referee Comment: P. 2, l. 20 : Delete "Field"
Authors' response: Done.

Referee Comment: P. 2 , l.23: Delete "other"
10   *Authors' response:* Done.

Referee Comment: P. 2, l. 28: Delete "can"
Authors' response: Done.

15   *Referee Comment:* P. 3, l. 4: Please change to: "…components of the LIDAR
signal retrieved from…"

Referee Comment: P. 3, l. 1315: The first argument only applies to field measurements, when
CFDCs are used to characterize ambient INP concentrations. However, the data you present
20   here result from laboratory measurements, where the number of aerosol particles entering
the cloud chamber (and thus the number of INPs) can be varied by the experimentalist, making
this argument irrelevant for this study. Please revise this section by making it clearer, that this
is particularly a limitation of CFDC field studies.
Authors' response: We thank the Referee for pointing out that the first sentence here was our place in this
25   paragraph. It has been moved to the optical section of the introduction.

Referee Comment: P. 3, l. 1022: Shorten this paragraph and to keep the focus on the topic of your
manuscript.

Authors' response: As stated above, the introduction is significantly revised and rearranged. This paragraph no longer exists in its original form.

Referee Comment: P. 3, l. 23: Please change to "… (CLIMET Inc., Model No. CI3100) …"

5   *Authors' response:* Done.

Referee Comment: P. 4, l. 13: Delete "to detect INP"

Authors' response: Revised to, "to determine INP concentration."

10   *Referee Comment:* P. 5, l. 4: Please change to: "… are generated, suspended in dry synthetic air…"

Authors' response: Done.

Referee Comment: P. 5, l. 7: Please specify whether aerosol particles or populations of ice crystals and cloud droplets have been sampled from AIDA.

15   *Authors' response:* Thank you. This is an important distinction.

Authors' changes in the manuscript: Revised to read, "During FIN-02, prior to expansion, aerosols were drawn from the AIDA chamber by the various ice nucleation instruments. Following the aerosol sampling period, an AIDA expansion was performed so that INP concentration determined by AIDA could be compared to results from the various visiting instruments."

20

Referee Comment: P. 5, l. 9: Please add: "… of the TAMU CFDC-CASPOL measurements …"

Authors' response: Done.

Referee Comment: P. 5, l. 25: Please change "limited" to "small".

25   *Authors' response:* Done.

Referee   *Comment:*

P. 6, l. 14: Specify how ice saturation is maintained in the evaporation section of the CFDC

given that you have hydrophobic Teflon walls.   How much are the ice crystals evaporated when passing through the lower most 25 cm of the chamber? Can you show that the ice crystals

remain in the sample flow?

Authors' response: As cited in the text, experimental details and a full description of the development and characterization of the TAMU CFDC are provided in the references below:
Glen, A., and Brooks, S.D.: Single particle measurements of the optical properties of small ice crystals and heterogeneous ice nuclei, Aerosol Science and Technology, 48(11), 1123-1132, 2014.
and
Glen, A.: The development of measurement techniques to identify and characterize dusts and ice nuclei in the atmosphere. Diss. Texas A&M University, 2014.

Referee   *Comment:*

P. 6, l. 4: Please specify why the droplets in some cases only partially evaporate. The

evaporation efficiency is a function of particle residence time in the evaporation section. Your

description of TAMU is missing a statement about the flows and thus residence times used

 within the TAMU CFDC. Such a discussion is only very briefly given on p. 7, l. 7-8

 and should be   moved to the description of the TAMU operation.   Details of the residence

time are also required to understand how the authors are able to grow ice crystals as large as

40 µm in the CFDC, as suggested by Fig. 6.

Authors' response:

By definition, when droplets only partially evaporate, the chamber is under WDBT conditions.

Causes on WDBT have been discussed in detail above and earlier in the text. Ideally, no droplets should

survive the evaporation region of the instrument, but given that WDBT is a problem in this and many

other ice chambers, we see that in practice this is not the case. There are many possible reasons. For

instance, droplets may not come to equilibrium prior to existing the chamber under very moist ambient

conditions.

 CFDC flow conditions were already stated in the original text on page 7. "Two mass flow controllers are

used to set the total flow and recirculating sheath flow through the chamber. The difference between the

total and sheath flows determines the sample flow. For this campaign, the total flow was set to values

ranging from 6 to 9 L min^{-1} and the sheath flow was set to values ranging from 4 to 7 L min^{-1} resulting in a sample flow that was typically ~2 ± 0.5 L min^{-1}."

In Figure 6, direct CFDC measurements are reported. The particles detected (not implied) by the CFDC
5 do include 40 micron diameter particles in size. Ice growth calculations indicate that ice crystals may grow rapidly in size in the chamber (Rogers, 1988; Glen, 2014). Additionally, a known source of large ice crystals are shards that break off the chamber walls occasionally.

Author changes in manuscript: Changes referred to here are all parts of the revision discussed in reference to prior comments.

10

 Referee Comment: P. 6, l. 8-15: This description of cloud chamber preparation does not
add to the topic discussed in the presented paper and should be moved to a supplement.
Authors' response: We respectfully disagree. When a manuscript employs an instrument and experimental procedure which are previously published in detail, there is always a delicate balance between re-reported
15 what has been well documents in previous work or not providing enough basic details for a reader to follow the current manuscript.   In this case, the referee has asked for additions experimental details above and here asks for fewer details. We do not think it wise to remove the details included in the original.

Referee Comment: P. 6, l. 17: Please change to: "… (CLIMET Inc., Model No. CI-3100)…"
20 Authors' response: Done.

Referee Comment: P. 6, l. 26: Please change to: "…backward scatter detector…"
Authors' response: Done. Thanks for pointing this out.

25 *Referee Comment:* P. 6, l. 5: The position of the mass flow controllers should be specified.
I assume these are located downstream of CASPOL?
Authors' response: For clarity, the text has been revised. For a schematic, please see Glen and Brooks, 2014a.

Authors' changes in the text: The text on page 7 ln 14016 now reads "...the CASPOL is installed at the base of the chamber. Two mass flow controllers downstream of CASPOL are used to set the total flow and recirculating sheath flow through the CFDC-CASPOL. The difference between the total and sheath flows determines the sample flow."

5

Referee Comment: P. 7, l. 13: Please change to: "Temperature, …"
Authors' response: Done.

Referee Comment: P. 7, l. 17: Please change "ahead" to "upstream"
10   *Authors' response:* Done.

Referee Comment: P. 7, l. 119: Please specify how the background (BG) signal from the CFDC is taken into account in more detail. Given that the supersaturation at the position of the aerosol lamina is different before and after a RH scan, the background
15   signal is likely to change from before to after the measurement. The statement between lines 16-19 suggest that there is not always a BG measurement before and after each RH scan ("and/or after"). This makes it hard to follow what BG signal is subtracted from your CFDC-CASPOL measurements.

20   *Authors' response:* Okay, the text is now clarified as below. In our experience, RH doesn't appear to cause a large difference in background signal.
Author changes in manuscript: The text now reads "The background period that is closest to a given 1-minute sample period is then applied by subtracting that background concentration from the total concentration measured by the CASPOL at the sample time."

25

Referee   Comment: P. 7, l. 20-
24: This sentence is misleading. I assume you refer to the usage of the optical particle counter and the associated size cutoff used to discriminate between ice crystals and

31

cloud droplets when using the term "traditional analysis". This is in contrast to the p. 6, l.

16- 19, where it is described that TAMU had been used with both, OPC and CASPOL, so in

principle both detectors can be interpreted as the traditional detector technique/analysis

method. I suggest to make a clearer distinction between these two cases (OPC vs. CASPOL as

5   detector) and give a clear statement earlier in the manuscript what the "traditional analysis" refers to. *Authors' response:* Yes, thanks. We see how this could have been confusing in the original text. Actually, we refer to any size-discrimination (by OPC or CASPOL forward scatter detector) as traditional analysis, and the use of the depolarization as a new method.

Author changes in manuscript:

10   p. 4 ln 12: "Particles are sized according to the intensity of light which reaches the CASPOL's forward scatter detector, as in a traditional OPC."

and

p. 8 ln 6: "During FIN-02, data collected by the CASPOL's forward scattering detector was used for the traditional analysis."

15

Referee   Comment:

P. 7, l. 27: This statement is misleading. There are no limitations of the OPC technique (discrimin

ation   purely   based   on   size)   discussed   in   Section   2.3.   Please delete the part in

brackets. The authors start a superficial discussion of the limitations by using and OPC and a

20   size threshold to discriminate the phase of cloud hydrometeors at various points of their manus

cript, e.g. p. 3. l. 15-16, p. 3, l. 23-25. However, a clear statement that under certain

Thermodynamic conditions within the TAMU CFDC, cloud droplets and ice crystals of the same size ca

n be present, thus biasing a pure phase discrimination based on particle size, is missing.

This should be discussed in the introduction.

25

Authors' response: For a detailed discussion of the many causes of WDBT and related instrument details, please see page 8 ln 14-22, which have been expanded and revised. Note, however, that we do not refer

to thermodynamic conditions, however, because WDBT is consistent with failure to remove large supercooled drops which do not reach thermodynamic conditions by the time they reach the chamber.

Referee *Comment:*

5 P. 8, l. 3: The authors mention the limitations of traditional methods, but do not discuss differe nces how the ice crystal size threshold may be chosen. Please give more details.

Authors' response: Ice crystal size thresholds have been chosen empirically based on laboratory results. For further details please see our previous work (Glen, 2014B).

10 *Referee Comment:* P. 8, l. 8: What do the authors mean by positive or negative artifacts?

Authors' response: This was a mistaken choice of words, as noted by 2 referees. In reality only positive artifacts are possible. "Positive artifacts" mean water droplets breaking through are counted as members of the ice crystal population. "Negative artifacts" would mean ice particles not counted because one thinks they are water droplets, but in practice there is no way for that to occur.

15 *Authors' changes in manuscript:* "if the instrument is unintentionally operated at supersaturations above WDBT, droplets will be miscounted as ice crystals."

Referee *Comment:*

P. 8, l. 12: The challenges are not really presented by WDBT, but are rather inherent to any

20 optical method that uses size as a means of phase discrimination.

Authors' response: This is the second time the referee mentions this issue, which is really a word choice issue. We revised the language in the abstract as per his/her recommendation. For clarity, we feel it best to keep the original text here, as this manuscript is addressing a measurement challenge specifically occurring when WDBT occurs.

25

Referee Comment: P. 8, l. 14-21: This section is partly a repetition of the statement made on p. 5, l. 23. Besides, it should be clear to any reader that a particle of any type (aerosol, cloud droplet) larger than the cut size will be misclassified as ice crystal by the OPC

33

when using size thresholds to define an ice phase.

Authors' response: Given the importance of this issue, we keep this section on page 8, but have shortened it.

Authors' changes in manuscript: Pg 8 now reads, "Although operation with an upstream impactor reduced this problem, ~1 to 10% of particles larger than 2 μm (depending on flow) may make it into the chamber to contribute to the apparent INP signal."

Referee Comment: P. 8, l. 19-21: Are the authors trying to say that large aerosols are not counted as ice crystals in their detector and they can be distinguished from an ice crystal of the same size?

Authors' response: At this stage in the manuscript, the text only states that such capabilities would be an improvement, given the limitations of the traditional analysis.

Authors' changes in manuscript: The text now reads, "A new analysis method that differentiates between large aerosols and ice crystals is needed since it would remove the need to limit the size of particles allowed into the instrument in the first place."

Referee Comment:
P. 8, l. 16: The expression "higher supercooled temperatures" is not clear. The authors should indicate more clearly what they compare to and point out reasons why the new analysis method is particularly powerful at higher T. The only indirect hint for this is given by the statement in brackets on p. 8, l. 10.

Authors' response: The statement in question was deleted in response to the Referee's previous comment.

Referee Comment: I recommend moving the discussion of section 2.4 to the Introduction to motivate the development of the new method.

Authors' response: Please see above that we have significantly revised the introduction. Moving this particular section was something the authors previously discussed. We decided that so much detail about challenges specific to our CFDC would be better left in the experimental section.

Referee *Comment:*

P. 8, l. 25: Please be more general in a first statement. The goal, as far as I understand from the present ed study, is to first distinguish more accurately between aerosol particles, ice crystals and cloud droplets and then in a second step quantify the INP, as you clearly write e.g. p. 4, l. 13.

Authors' response: We see the referee's parts 1 and 2 as parts of the same objective. We prefer to keep the original text here.

Referee *Comment:*

P. 9, l. 1: I suggest repeating the meaning of the different parameters again. E.g. "Similar to eq. (1) B$_\perp$,CAS and B$_\parallel$,CAS denote the perpendicular and parallel components of the backscattering signal , respectively, and the subscript CAS refers to the CASPOL signal…."

Authors' response: This is a good suggestion.

Authors' changes in manuscript: Done.

Referee *Comment:*

P. 8, l. 24: Section 2.5 describes CASPOL instrumental details and should be moved to the description of CASPOL in section 2.2.

Authors' response: This is a good suggestion. Due to other suggestions the CASPOL description is now in Section 2.2. and Section 2.5 has been moved to that section.

Referee Comment: P. 9, l. 21: Please explain why the neutralizer prevents particle loss.

Authors' response: Charged particles are attracted to the walls of the tubing.

Authors' changes in manuscript: This statement is now including in the text..."to prevent particle loss since charged particles tend to be attracted to the walls of sample tubing."

Referee Comment: P. 9, l. 22: Please change to: "the" before CASPOL

Authors' response: No. The grammar is correct in the original.

Referee Comment: P. 10, l. 15: I assume you are referring to CFDC-CASPOL measurements,

Authors' response: Yes.

Authors' changes in manuscript: Changed CASPOL to CFDC-CASPOL.

5

Referee Comment: P. 10, l. 20: Please clarify the source of your temperature uncertainty here. How can the temperature uncertainty here be much lower than the value given on p. 7, l. 10?

Authors' response: This is reported instrument uncertainty, whereas on 7, we reported the range of temperatures over which collected experimental data was included in the intercomparisons. Specifically, temperature here is based on experimental temperature, derived from a set of 8 thermocouples calibrated to a reference RTD.

Authors' changes in manuscript: The text on pg 7 has now been clarified to explain that the temperature range on pg 7 was not a report of instrument uncertainty. Instead, it was the range of operating temperatures of measurements included in the FIN-02 intercomparison.

Referee Comment:

P. 10, l. 15: Please change SS to saturation ratio formulation throughout the manuscript. This will avoid confusion as of the negative sign and make your figures more easily readable.

Authors' response: We feel that supersaturation is useful because 0 % demarcates when water droplets may begin to form in the chamber. Also, SS is often used in ice nucleation papers.

Authors' changes in manuscript: None.

Referee Comment:

P. 10, l. 20: Do you suggest that particles smaller than 2 µm are not necessarily frozen?

Authors' response: 2 µm is the nominal size cut for ice. Both calculations and experimental tests have shown that if size nucleation in our chamber, ice will grow to above 2 µm (Glen, 2014.)

Referee Comment: P. 10, l. 23: Insert comma after "datasets"

Authors' response: Done.

Referee Comment: P. 11, l. 4- 5: Please clarify the usage of optical signatures by Hu et al. (2009) and how this relates to your study.

5 *Author's response:* Revised for clarity. Hu et al is a successfully example of using backscatter and depolarization data to determine cloud particle phase.

Authors' changes in the manuscript: "In an analogous method, optical signatures produced from CALIPSO satellite backscatter and depolarization data have been used to identify cloud phase (Hu et al.; 2009)."

10

Referee Comment: P. 11, l. 6: Delete "training"

Author's response: Training has a very specific meaning here, so we choose to keep it.

Referee Comment: P. 11, l. 13: Please clarify whether Dp refers to the optical diameter

15 measured with CASPOL or to another diameter measured with another device.

Author's response: For clarity Dp has been replaced with diameter and revised the text as below:

Authors' changes in manuscript: "As discussed, the ice crystal and droplet training data shown in Fig. 1 only includes particles with optical diameters ≥ 2 μm and ≥ 1 μm, respectively.

20 *Referee*   *Comment:*

P. 11, l. 17: Please extend your interpretation of why almost only ice crystals show high values for B□/ F and what that implies.

Author's response: Here we report a direct observation from data in the figure.

Authors' changes in manuscript: No change has been made.

25

Referee Comment: P. 11, l. 23: Insert point after "et al."

Author's response: Done.

P. 11, l. 24 : Please clarify why this is an empirical tool and how this affects the application to your data.

Author's response: The optical signatures are used to detect patterns in backscattering vs. depolarization

5   plots for different particle types. By definition, these observed differences (if found) are empirical rather than theoretical.

Authors' changes in manuscript: No change has been made.

10   P. 12, l. 4: "It is assumed that the CASPOL emits an incident beam that propagates along the z…" Why is it only assumed? Can you verify this experimentally?

Author's response: The Referee has a good point. This is a reality, not an assumption.

Authors' changes in manuscript: Deleted, "It is assumed that."

15   *Referee Comment:* Which direction is the z direction? A schematic figure defining the different parts of CASPOL along with a coordinate system will definitely improve your description here. Please
 add a figure to your supplement.

Author's response: As clearly stated in the text- z is the direction on propagation of the incident CASPOL laser beam. See page 12, ln 24, "The CASPOL emits an incident beam that propagates along the z

20   direction in the form." Also, schematics of the CASPOL have been previously published in Glen and Brooks 2013 & 2014.)

Authors' changes in manuscript: No change has been made.

Referee Comment: It is not the CASPOL, but the laser diode of the CASPOL that emits the light.

25   *Author's response:* True, "laser" now added.

Referee Comment: P. 12, l. 8: Please change to: "…line linking particle (position) and detection point."

Author's response: We feel that this would not be an improvement.

Referee Comment: P. 12, l. 12: Please insert commas: "… ratio, δModel, can …"

Author's response: Done.

5 *Referee Comment:* P. 12, l. 15-16: Please insert commas: "…matrix, Pij, the amplitude matrix, Sij, and the scattering cross section, Csca, …"

Author's response: Done.

Referee Comment: P. 13, l. 13: Please replace "vs." by "as a function of"

10 *Author's response:* Done.

Referee Comment: P. 13, l. 17: Please delete "the" in front of optical signatures.

Author's response: There is no "the" in the line specified.

15 *Referee Comment:* P. 13, l. 13-21: Please elaborate this discussion and give more details:

Author's response: This section has been rewritten and expanded. Also, the range of particle and ice diameters have been expanded in Figure 2,as discussed in the new text.

Authors' changes in manuscript. Please see the revised section on Pg 14 ln 15 to pg 15, ln 5, and Figure

20 2.

Referee   *Comment:*

Below approx. 2 µm no modeled depolarization ratios are given for any of the ice crystals, making a comparison between aerosol particles and ice crystals as suggested in the text

25 difficult (l. 18-19)

Author's response: This is an excellent point. Calculations for a wider range of ice crystal sizes are now included and discussed. See previous response.

Referee Comment:

The authors discuss the differences in depolarization ratio as a function of ice crystal habit in the range 2- 4 µm. However, there is a clear distinction also above 10 µm for e.g. hexagonal plates and hexagonal columns. This needs to be explained.

5   *Author's response:* Please see our response above. This section has been expanded. The differences at larger diameters are mentioned in the text, although there is not a theoretical explanation for the observed differences.

Referee Comment:

10   What are the uncertainties associated with the modeled results. Errors bars should be included for the individual data points to render a comparison possible at all.

Author's response: Errors bars are not available. This is a tricky question. In the case of the modeling, the model is highly accurate for the chosen inputs. The uncertainty arises from assignments of the correct

15   inputs. In this case, by far the largest uncertainty in the modeled results in the choice of shape.   This is way we include 3 shapes.   Other inputs, including wavelength and particle diameter, refractive index are known with high precision.

Authors' changes in the manuscript: The uncertainty which arises due to particle shape is now explicitly states, "It is not known which of these habits best represents individual ice crystals nucleated and grown

20   in the CFDC. Fortunately, if it is assumed that only particles of 2 µm diameter or larger are ice crystals in the CFDC, these theoretical results shown that all water and ice particles on any of the three habits will be accurately identified."

Referee Comment: P. 14, l. 1: Please insert: "aerosol particles"

25   *Author's response:* Since "aerosols" is acceptable grammar, we prefer to keep it. This is unchanged.

Referee Comment: P. 14, l. 2: Please insert: "… shown in Fig. 1 …"

Author's response: Done.

Referee   *Comment:*

P. 14, l. 4: Please change to: "Each nominal droplet size produced by the VOAG is treated as a
separate population in the training data set and …"

5   *Author's response:* We consider the original text to be more succinct in this case.

Referee Comment: P. 14, l. 5: Please change to: "… in Fig. 1a …"
Author's response: Done.

10   *Referee*   *Comment:*

P. 14, l. 10: Please clarify how the selection criterion for ice crystals (depolarization ratio > 0.3) is derived and how it is connected to the values discussed in Fig. 1 (cf. p. 11, l. 15).

Author's response: It can be seen qualitative in the figure that droplets have depolarization ratios up to 0.3. At this point in the manuscript, this is only a simple choice based on visual observation. However, in
15   Section 3.7, optimization of the depolarization threshold is performed using linear regression analysis, and the results come to the same conclusion, that 0.3 is the preferred choice of nominal threshold.

Author's changes in manuscript: We have added text (pg 15 ln 20), that states "It can be seen from this figure that droplets have depolarization ratios up to 0.3. Therefore, we visually assign 0.3 as the nominal depolarization threshold cut-off for differentiating between ice crystals and non-ice particles. The choice
20   on 0.3 is further evaluated in Section 3.7 below."

Referee   *Comment:*   P. 14, l. 15-
16: Why do the aerosol particles in Fig. 1c show a mode only in the constrained size
range between 5 to 10 µm and not above 5 µm in general?

25   *Author's response:* Fig. 1c is not discussed at this point in the manuscript, so we are unsure of the Referee's intended question.

Referee *Comment:*

P. 15, l. 12: Please specify what you mean by "the size mode". I think you are referring to the smaller mode of the bimodal size distribution described above.

Author's response: Yes, that's correct.

5   *Authors' changes in manuscript:* Changed "the size mode" to "aerosol size distribution."

Referee Comment: P. 15, l. 13- 19: In section 3.3 you discuss the usage of a depolarization Threshold of 0.3 to discriminate between different particles types ("nominal selection criteria for depolarizing ice crystals"). In Fig. 4b all of your particles have significantly lower

10 depolarization values, even at times when you are supersaturated. Please clearly state, that water droplets cannot be present during the time period before 11:55 due to the fact of being sub saturated, to avoid any confusion with your threshold of 0.3 discussed earlier.

Author's response: Actually, the value here is the mean depolarization reported and it is consistent with the mean depolarization of training data ice crystals. As indicated on the y axis label, Figure 4b shows

15 the mean depolarization ratio of all particles above 2 microns at that time. Because we only consider those particles larger than 2 microns and we are not in WDBT conditions until 11:55, these particles are ice crystals.

Authors' changes in manuscript: We have expanded the previous section that discusses mean depolarization ratio of the training datasets to reduce confusion.

20

Referee *Comment:* P. 15, l. 16-

18: This is not correct. It is not the mean depolarization ratio, which has a strong dependence on whether WDBT is occurring in the CFDC, or not. Analyzing the depolarization ratio, you can observe the moment when WDBT occurs in the CFDC. Please phrase that more

25 carefully.

Author's response: See previous comment.

P. 16, l. 17: The statement "… at colder temperatures of these runs" is misleading, as the center

 temperature in your CFDC stays constant for each of the two runs. Further, the two Snomax®

Cases presented are not labeled in the figure, such that the reader cannot assign a CFDC c

5 enter temperature difference between the runs from the lines in Fig. 5.

Author's response: We agree this should be clearer.

Authors' changes in manuscript: The text is now modified. In addition, we have added labeled,

"Snowmax 21 °C, and Snowmax 33 °C to figure 5.

10 *Referee* Comment: P. 16, l. 26-

27: How does the error shown for the observed values compare to the instrumental

uncertainty from CASPOL to determine the right depolarization ratio? Please add

error bars associated with the modeled results. Consider using standard error of the

 mean for normalization to number of observed particles at the different sizes.

15 *Author's response:* Please see our responses above regarding the challenges of reporting error for the

modeling results.

 Referee Comment:

P. 16, l. 28: Please add for clarification: "… from all FIN02 experiments and not only

20 the Snomax® experiments discussed in Section 3.5."

Author's response: Done.

Referee Comment: P. 17, l. 1: Remove "u" after 2.

Author's response: Done.

25

 Referee Comment: P. 17, l. 1-

4: Consider deletion as you already reference to the description given in section 3.5.

Author's response: Although this is somewhat redundant, we feel it best to restate these rules to avoid any confusion.

Referee Comment: P. 17, l. 510: Do the authors have any idea what type of ice crystal is formed in the CFDC? Is this dependent on the aerosol type/experiment? Which of the modeled ice crystals is closest to the "CFDC ice crystals"?

Author's response: Unfortunately, no. We see a wide variety in backscatter and depolarization ratios and don't have any way to answer assess this. As an aside, we have tried collecting ice crystals exiting the CFDC in plastic casts (made from dissolving plastic in dichloroethane), but our attempts so far data were not of high enough quality to determine ice crystal habit.

Referee Comment: P. 17, l. 14: Please replace "region" by "population".

Author's response: Done.

Referee Comment: P. 17, l. 19: Why do the "CFDC ice crystals" show depolarization ratios < 0.35 for all sizes shown? It is unclear to me how this relates to the data shown in Fig. 5, where the majority other ice crystals show larger depolarization ratios. In addition, none of your "CFDC ice crystals" would meet the 0.3 threshold in depolarization ratio discussed on p. 14. Please explain. Is this due to averaging over all FIN-02 experiments?

Author's response: Please look again at the figure 5 and the related discussion. The manuscript states the opposite of what the referee has said. As stated "13.5 % of ice crystals in the CFDC achieve a depolarization ratio > 0.3, compared to 1.5 % percent of water droplets and 0.3 % of aerosols. Additionally, please note the figure 6 is showing mean values depolarization ratio. Since many of the particles detected have relatively low depolarization ratios (see figure 5 and figure 3b), this value will be low. We've added the mean throughout the discussion of figure 6 to clarify this.

Author's changes in the manuscript: "In this section, modeled and observed particles discussed in the preceding results section are compared. Fig. 6 shows modeled and observed mean depolarization ratios

of particles…" "In Fig. 6, both the model calculations and the observed results indicate that ice crystals have higher mean depolarization ratios…"

Referee Comment: P. 17, l. 23-26: More details about the "underestimation of the depolarization by CASPOL and the detection limit" along with an appropriate reference should be given. Should the under estimation of depolarization by CASPOL not preliminary affect smaller sized particles (that scatter in relatively less light)? Thus the discrepancies between modeled and observed results should decrease as a function of size, as the detection by CASPOL becomes more reliable?

Author's response: In general, particles scatter relatively little perpendicularly polarized light in the backward 1 raw count which translates roughly a scattering cross section of ~1 x10^{-13} cm^2. This limit results in the CASPOL registering a perpendicular signal below the CASPOL's detection limit for 45 % of training ice crystals, 76 % of training aerosols, and 57 % of training droplets. In the training data sets, all particles with undetected perpendicularly polarized detector were assigned depolarization ratio of zero.

Author's change in the manuscript: The full explanation above, "In general, particles scatter relatively little perpendicularly polarized light in the backward direction, …" is now added to the text on pg 20 ln 12.

Referee Comment: P. 18, l. 22-24: How does this statement fit to your data shown in Fig. 6 (cf. "CFDC ice crystals")?

Authors' response: This statement cannot be directly applied to figure 6 since the figure shows a mean and error bars that report the standard deviation. Since only 13.5 % of ice crystals achieve a depolarization ratio of 0.3 or greater, the error bars here will not show this range of particles. Since we have focused heavily on this point in the depolarization ratio distributions previously in the manuscript, we do not wish to expand anymore here. Rather, the point of this figure is to compare the mean observed depolarization ratios to modeled depolarization ratios. No change has been made.

Referee Comment: P. 18, l. 25: This is contradictory to the values you state on p. 16, l. 8-9. Please clarify.
Authors' response: The referee is right. This was a typo in the original statement here.

Author's change in the manuscript: The text (pg 21, ln 1) now reads, "A depolarization ratio threshold of 0.3 is a favorable criterion to detect ice crystals because < 2% water droplets and aerosols achieve this depolarization ratio."

5 *Referee Comment:* P. 18, l. 27: Please clarify what signal to noise ratio you refer to.

Authors' response: The signal is ice crystals, the noise is water droplets with a depolarization ratio of 0.3 or greater.

Author's change in the manuscript: Pg 21, ln 5: "…effectively reducing the signal (ice crystals) to noise (water droplets with $\delta \geq 0.3$) ratio ~1:1 or worse."

10

Referee Comment: P. 19, l. 7: I suggest giving more details here, as referring to an "optimal threshold" at this point is confusing. This threshold comes out of your training data sets (Fig. 3). However, in Fig. 6 you show that application of this threshold is not sufficient to discriminate droplets and ice crystals for WDBT conditions anymore. There, using the term "optimal threshold" should be avoided.

15 *Authors' response:* Agreed.

Author's change in the manuscript: The text has been modified and the depolarization ratio threshold is not referred to as optimal until after the linear regression fit has been introduced on pg. 22 ln 20. "Figure 7 shows that the 0.35 threshold out performs all other thresholds when $M > 20$. The mean R^2 value for the 0.35 threshold is 0.46. The next best performing threshold is 0.3 with a mean R^2 value of 0.44.

20 However, aerosol and water droplet concentrations in CFDC experiments are typically in the range $1 < M < 20$ so it is appropriate to give more weight to the performance of the fit at these values. The mean R^2 value in this range of M for the 0.3 and 0.35 thresholds 0.71 and 0.7 respectively. While the performance of these thresholds perform comparably over this range, we selected the 0.3 threshold because it will slightly outperform the 0.35 threshold, especially when detecting lower INP concentrations."

25

P. 19, l. 24-28: Please specify why the linear fit was done for the case of $M = 1$. It is not clear, why the fit derived from the $M = 1$ case, is applied to all the other data sets $M = 2$ to $M = 50$.

Authors' response: The concentration of aerosols and droplets can change in the CFDC. This purpose of this exercise is to understand how that fit will perform over all ranges of *M*. This is stated in the manuscript where we say, "Only one fit is determined for each threshold because we cannot feasibly design a model that adapts to water droplet and aerosol concentration in the CFDC."

5   *Author's changes in the manuscript:* pg 21, ln 26: 1) "The upper range of *M* values here represents an extreme sampling condition where there are many aerosols and many CCN that will form cloud droplets, but not many INP that will form ice crystals. Given the relatively high number of aerosols and droplets, this would represent the most challenging sampling scenario for proposed new method."

10 *Referee Comment:* P. 20, l. 4: Please replace "The Fig." by "It".
Authors' response: This sentence was removed during revision of the section.

Referee Comment: P. 20 l. 9: Given that you describe an optimization problem, there should be one optimum and a range of acceptable values. Please justify your statement on p. 9, l.2

15 *Authors' response:* This is a good point. Please see our response above. We have added additional values and discussion.

Referee Comment: P. 20, l. 5-8: You describe a threshold used to distinguish between ice crystals, droplets and aerosols, to then derive Eq. (9), which yields the number of ice nucleating particles. However, the

20 number of ice crystals is usually way larger than the number of INP. Please explain in more detail, how you derive a "parameterization" for INP at this stage.
Authors' response: In the CFDC, we assume a one to one relationship between ice crystals and INP. There is no shattering or multiplication, so this is an accurate assumption. We believe the reviewer is alluding to field observations of ice crystals which have been larger than concurrent INP concentrations.

25 It is far beyond the scope of this manuscript to deal with disagreements between instruments in the literature, and most importantly, that question is not applicable to the internal chamber of the CFDC.

Referee Comment: P. 20, l. 22: Please add: "Each relative humidity scan..."

Authors' response: Done.

Referee Comment: P. 20, l. 23: Please replace: "Supersaturation" by "Saturation ratio"

Authors' response: Please see above. We have chosen to keep "supersaturation" as the metric of interest throughout this manuscript.

Referee Comment: P. 20, l. 25: Before this statement the meaning of the circles and the asterisks needs to be introduced in the text.

Authors' response: Done.

Author's change in the manuscript: In section 3.8, we've modified to, "The reported concentrations reveal that the traditional (circles) and depolarization ratio (*) methods generally agree during "ice only" periods (blue symbols in Fig. 8)."

Referee Comment: P. 21, l. 11: Please specify what the value of the CASPOL uncertainty refers to. Is this the depolarization ratio signal?

Authors' response: This is the CFDC-CASPOL uncertainty in INP concentration, based on combined instrumental uncertainties.

Authors' changes in the manuscript: This statement is now included.

Referee Comment: P. 21, l. 23: Please quantify the detection limit of CASPOL or give an appropriate reference.

Authors' response: As discussed in the experimental section in considerable detail, the CASPOL is a single particle 60 Hz instrument. Please see Glen and Brooks 2013 and 2014 for characterization of instrument performance.

Referee Comment: P. 21, l. 22: Please replace "polluting" to "biasing"

Authors' response: Revised to " large water droplets being miscounted as INP"

Referee Comment: P. 22, l. 2: Please add: "...mean percent error (MPE)..."

Authors' response: Done.

Referee Comment: P. 22, l. 11-12: Please quantify the concentration rate, where the new method is applicable rather than stating "high concentrations" and quantify the "accuracy" indicated.

Authors' response: Since accuracy as a function of concentration was just discussed in detail in the previous paragraph of the manuscript, we do not wish to repeat those details here.

Referee Comment: P. 22, l. 16: The benefit from this last paragraph and the additional comparison to the CSU CFDC, along with different cut-sizes shown in Fig. 11, does not become clear. Please explain in more detail.

Authors' response: Please see the experimental section in which a detailed description of the differences between the two CFDC are discussed. Most importantly, because the CSU CFDC doesn't experience WDBT until a higher RH, this comparison provides a means to evaluate performance of the new method under conditions which our traditional method is clearly failing.

Also, in general, because the two CFDCs are quite different instruments, an intercomparison is worthwhile.

Authors' changes in the manuscript. For emphasis we include the following statement on page 24, ln 20 Thus, inclusion of the CSU data provides a test of the new method at higher relative humidities under conditions when data obtained through the TAMU CFDC's traditional method is clearly spurious due to water droplet breakthrough."

Referee Comment: P. 22, l. 16 – P. 23, l. 14: Is your new method not applicable to other CFDCs operated along with CASPOL at all?

Authors' response: In theory the method is application. No one has tried that yet, to the best of our knowledge.

49

As the comparison to the modeled results indicates, having the CASPOL's unique particle-by-particle measurements of both depolarization and size is a clear advantage for reliable particle discrimination. Depolarization alone can be used to differentiate between droplets and ice crystals. However, to differentiate between dust aerosol and ice crystals are both depolarizing, so the size information provided

5   by the forward scattering detector is needed as well as depolarization.

Figures:

Referee Comment: Figure 1: Please locate the axis ticks also outside of the subpanel boxes to increase readability. Please be consistent with the terminology defined in Eq. (2) and include the subscript "CAS"

10   in the axis labels (also on the y-axis). "CAS" subscript should be included in terminology used in figure caption.

Authors' response: Done.

Referee Comment: Subpanels (a/d), (b/e) and (c/f) are plotted for the same datasets. However, the color

15   bars for the upper row of subpanels and the lower row of subpanels use different colorcoding, which renders a comparison difficult. I suggest to change this using the same range for the color scale.

Authors' response: The color scales for the plots have been carefully selected for readability of the plots. The objective of the plot is to reports patterns in the optical signatures and not to compare them, so it's appropriate that the scales are different in this case. No change has been made.

20

Referee Comment: Figure 2: X-axis (labels) should be read as log-scale.

 Please include model calculations for larger aerosol sizes, such that there is a size overlap for the different particle types. This is needed to justify your statement on p. 13, l. 18.

 Please delete the term "Model" in your legend, as this is redundant information from the y-

25   axis label and the figure caption. Caption: Please insert comma after droplets.

Authors' response: The x-axis is already plotted as a log scale. Larger aerosols and smaller ice crystals have now been incorporated into the figure, and "model" has been removed from the legend. The comma has been added to the caption.

Referee Comment: Figure 3: Please add symbol for depolarization ratio in x-axis label of panel (b), for consistency. These are all size distributions measured with CASPOL, right? Was there any additional instrument used, e.g. an Aerodynamic Particle Sizer, to verify the size of the produced particles? If so,

5   please add these information and graphs to a supplement.

Authors' response: No other instrument was used to size particles here.

Authors' changes in the manuscript: To figure 3, we have added "as detected by CASPOL" in the caption, and added d.r. symbol to x-axis of (b).

10   *Referee Comment:* Figure 4:

   What are these large particles prior to 10:45 CET? The authors mention (p. 5, l. 24) that no

   impactor was used during the FIN-02 campaign and that the number of large particles was

   limited. I suggest to add a number size distribution of the Snomax® sample shown in Fig. 4 to the

   appendix for clarification. How do these large particles in the range 5- 10 μm influence the depolarization

15   ratio shown in Fig. 4b (see also your Fig. 3)? Please add a description to the discussion in the manuscript.

Authors' response: The large particles here are ice crystals. We've added a size distribution to the supplemental section that shows that there are no Snomax aerosols that are larger than 2-micron diameter.

Author's changes to the manuscript: The text now includes the supplement figure, Fig S1. and a statement referring to it (pg 17, ln 6.)

20

Referee Comment: I suggest showing Panels (a) and (b) as a function of saturation ratio w.r.t. water instead of time. Saturation ratio w.r.t. ice can then be given as a second/top x-axis for instance. There is no additional information given by time. By using saturation ratio w.r.t. water it will be easier for the reader to put the discussed WDBT into context. Indicating ice saturation ratio will help to identify the

25   formation of ice crystals.

Authors' response: This is a good advice. However, there are several challenges presented by the data that inhibit us from displaying the data in this manner. Because the data is not collected at regular intervals

of super saturation, there would be breaks in the data that make the plots hard to decipher and likely confusing to the reader. After attempting to plot the data this way, we decided that it would be better to display the data as we have here.

5   *Referee Comment:* The text on p. 15 should be changed accordingly and can make more clear what is meant with "normal operating conditions" (p. 15, l.8). Further, labels for "normal" and "WDBT" conditions in Fig. 4 could help.

Authors' response: In the original version of figure 4, there was already a label to describe when WDBT happens.

10   Authors' response: We have added a label for "Normal Operating Conditions" to Fig. 4.

Referee Comment: Please make axis ticks more visible (e.g. reduce thickness of axes) and add ticks to x-axes in Fig 4a/b.

Authors' response: Done.

15

Referee Comment: Add explanation for the horizontal dashed lines in the figure caption (see p. 7, l.20).

Authors' response: Done.

Referee Comment: Caption for panel c should include the case number and a reference to Table 1.

20   *Authors' response:* Done.

Referee Comment: Figure 6: I suggest using log-scale for the x-axis.
 Even though you state that the error bars show standard deviations from the mean, they seem
to be on the same order of magnitude. Please add error bars (e.g. for some of the data)

25   *Authors' response:* The author's are confused about what this comment is requesting since all standard deviations are reported. Additionally, we have confirmed that the standard deviations reported are correct. The x-axis is already reported as a log-scale.

Referee Comment Please change the label of the y-axis as the data is a mixture of modeled and observed depolarization ratios.

Authors' response: Done.

5 *Referee Comment:* Figure 10:

The x-axis label should read "traditional concentration".

Authors' response: Done.

Anonymous Referee #4 Received and published: 9 August 2017

10

This manuscript (Using depolarization to quantify ice nucleating particle concentrations: a new method by Zenker et al.) capitalizes on the ability of the CASPOL detection method to capture the depolarization information from particles, droplets and ice particles in the TAMU CFDC and identify them under different operating conditions. The method may be applicable to other systems but each CFDC is unique.

15 The manuscript includes the development of a new empirical analysis method, to quantify ice nucleating particle concentrations and presents a way to deal with especially the data obtained during water droplet breakthrough, which is difficult to interpret. I believe that the manuscript topic does fall into the scope of AMT. Generally, the paper is readable, the analysis is carefully done and discussion points seem to be well supported by data. There is a limitation for this method in that higher concentrations only obtainable

20 in a laboratory are applicable; the authors are upfront about this limitation.

Referee Comment: There are some major considerations that, if addressed, could strengthen the paper: The authors may want to consider strengthening the end of their introduction to describe in more details the trajectory of work presented in the paper. Such a road map is limited here and more details could be

25 helpful. In the body, there is little text regarding the comparison but there is a lot of text with many details regarding the development of the empirical analysis, yet these seem equally weighted in the introduction.

Authors' response: As per this Referee's comment as well as those of another, the introduction has been significantly restructured, including a "road map" in the final paragraph of the section, as suggested here.

Authors' changes in the manuscript. Please see the new introduction as a whole.

Referee Comment: In terms of the training data, the text notes that no droplets below 2 µm were studied and this is reflected in figure 3. However, figure 6 shows training droplets at 0.7 µm. This is confusing.

5 Further, since this size is a cut-off point for the analysis, it might be helpful to include smaller particles generation or to explain how the data in figure 6 was observed.

Authors' response: I would ask the referee to revisit the figure. No training droplets below 1 micron are plotted. The training droplets are cut at 1 micron to eliminate residual 2-propanol droplets that form in the generation of the olive oil droplets.

10 *Authors' changes in the manuscript:* To avoid confusion, Figure 6 has now been revised and does not show training droplets below 1 micron. The elimination of <1 micron diameter residual 2-propanol droplets is also stated in the text.

Referee Comment: There may be minor scientific issues associated with the depolarization theory (that

15 section of the paper was difficult to follow and there seemed to me to be some confusion or missing information associated with representations of matrices, matrix elements and values and/or units). In particular, the section on page 12 surrounding equations 6-7 is especially confusing. The authors note that these equations deal with the amplitude matrix, but then their inclusion in the equation appears to be an element with only one index. Further, it would be helpful to explain this part of the model further. What

20 do these relationships (eqn 6-7) represent? I see how they combine to create eqn 8 but why?

Authors' response: The text has been revised to indicate that not only one index is included. Also, equation 8 is required in the form presented here for direct comparison to the CASPOL which detects light over single band of back scattering angles. 168° to 176°. This was mentioned in the experimental section, but we now include it here as well.

25

Authors' changes in the manuscript: The text on page 13 now reads, "Using the following relations between the elements of scattering phase matrix, P_{ij}(i,j=1,2,3,4), and the elements of amplitude matrix, S_i (i=1,2,3,4), below,

54

$$|S_4(\theta)|^2 + |S_2(\theta)|^2 = (P_{11}(\theta) + P_{12}(\theta)) \times C_{sca}, \tag{6}$$

$$|S_4(\theta)|^2 - |S_2(\theta)|^2 = (P_{21}(\theta) + P_{22}(\theta)) \times C_{sca}, \tag{7}$$

where C_{sca} is the scattering cross-section of a particle. As described above, the CASPOL detects light over single band of back scattering angles. 168º to 176º. To compare to the CASPOL measurements, we define the mean modeled depolarization ratio over the angular range of 168° to 176° and is expressed

5 below in Eq. (8).

$$\bar{\delta}_{Model}(168°\text{:}176°) = \frac{\int_{168°}^{176°}(P_{11}(\theta) + P_{12}(\theta) - P_{21}(\theta) - P_{22}(\theta))\ \sin(\theta)\ d\theta}{2\int_{168°}^{176°}(P_{11}(\theta) + P_{12}(\theta))\ \sin(\theta)\ d\theta} \tag{8''}$$

Referee Comment:

It would also potentially be helpful for the authors to further discuss the use of the T matrix model for
10 dust (and ice)? A recent technical note (Koepke et al., ACP, 2015, 5947) may be helpful. Generally, the paper would be enhanced with some additional details, clarity or references (and/or possibly even information in the experimental section) associated with the model calculations.

Authors' response: To clarify, the ice crystal calculations were performed using improved geometric optics methods, while the dust calculations were performed using t-matrix. We have now added additional
15 details regarding each of these methods, and have added more additional references.

Authors' changes in the manuscript: The text on pg. 14 ln 4-13 now reads, "To compute the scattering phase matrices of these models with specific sizes at CASPOL wavelength, we apply so-called improved geometric optics method (IGOM) for particle with relatively large size and the invariant imbedding T-matrix method (II-TM) for particles with relatively small sizes (Yang et al., 1996; Bi et al., 2013; Bi and
20 Yang, 2014; Johnson, 1988). The combination of these two methods is chosen because of the different size parameters of the aerosol and ice crystal populations. The T-matrix method is a highly accurate

method for calculating scattering properties of atmospheric particles (Koepke et al., 2015; Brooks et al., 2004). However, it becomes impractical for large particles due to its excessive demands on the computational power. In contrast, the IGOM is accurate over the range of particle sizes over which the particle size to be much larger than the incident wavelength (Xu et al, 2017)."

5

Added references:

Brooks, S. D., O. B. Toon, M. A. Tolbert, D. Baumgardner, B. W. Gandrud, E. V. Browell, H. Flentje, and J. C. Wilson (2004), Polar stratospheric clouds during SOLVE/THESEO: Comparison of lidar observations with in situ measurements, *Journal of Geophysical Research-Atmospheres*, *109*(D2).10.1029/2003jd003463.

Koepke, P., J. Gasteiger, and M. Hess (2015), Technical Note: Optical properties of desert aerosol with non-spherical mineral particles: data incorporated to OPAC, *Atmospheric Chemistry and Physics*, *15*(10), 5947-5956.10.5194/acp-15-5947-2015.

Xu, G., B. Sun, S. D. Brooks, P. Yang, G. W. Kattawar, and X. Zhang (2017), Modeling the inherent optical properties of aquatic particles using an irregular hexahedral ensemble, *Journal of Quantitative Spectroscopy & Radiative Transfer*, *191*, 30-39.10.1016/j.jqsrt.2017.01.020.

20 *Referee Comment:*
Overall, there is a lack of consistency within the text and figures where attention to detail would help. This is true, especially with the ordering of the types of particles within the different sections and also within the figures and captions. Further axis labels should include units where possible. A specific example is that in Fig. 6, there are both model and experimental results displayed but the y-axis includes

25 the model label and the x-axis is missing units. Some additional specifics are included below.
Authors' response: Thank you for addressing these specific inconsistencies. We have edited many of the figures in response to this comment and others.

56

Authors' changes in the manuscript: Please see the manuscript for revised figures. Labels and captions are now be consistent.

Specific comments:

5 *Referee Comment:* Pg 9, line 24: e is missing from the

Authors' response: Added.

Referee Comment: Pg 10, line 11: "both" is unnecessary and confusing.

Authors' response: Deleted.

10

Referee Comment: Pg 10, line 19-20: In final copy, watch for placement of the minus sign

Pg 11, line 6-7: placement of training

Authors' response: This has now been fixed.

15

Referee Comment: Pg 11, line 8: based on the figure, the authors mean total backscatter vs. depolarization ratio. I'd also suggest reversing the order in the follow up sentence on lines 8-10.

Authors' response: The text in this section (now pg 12, ln 14-17) has been revised has been revised for clarity.

20

Referee Comment: Pg 12, line 7: k is in eqn 3, but omega and t are not present. Is the equation missing time dependence? Also, r is not defined until line 11. Pg 12, equation 4: related to above, are both matrices and matrix elements included? Pg 12, missing comma after Pij

Authors' response:

25 Yes, indeed Equation, 3 should be written as

$$\boldsymbol{E}_i = \begin{pmatrix} E_{\parallel i} \\ E_{\perp i} \end{pmatrix} e^{i(kz-\omega t)} = \begin{pmatrix} E_{\parallel i} \\ 0 \end{pmatrix} e^{i(kz-\omega t)},$$

but note that $e^{i(\omega t)}$ is later omitted when express the relation between incident and scattered field in Eq(4) , because the scattering is assumed to be elastic. As in the original, r is introduced when it first used. *Authors' changes in manuscript.* Equation 3 has been corrected and "…scattering is assumed to be elastic." is now included. The elements of the amplitude matrix in Equation 4 are now defined: S_i (i=1,2,3,4) in Eq(4). Also, the text as been added: "Note that $e^{i(\omega t)}$ term is omitted since the scattering is assumed to be elastic."

Referee Comment: Pg 12, missing comma after Pij
Authors' response: Added. Thank you.

Referee Comment: Pg 14, line 5: I think you mean Fig. 3a here.
Authors' response: Corrected. Thank you.

Referee Comment: Pg 14, lines 14-17: This is confusing, please clarify. In figure 3b, it seems the % of total population of all particles having a depolarization ratio of 0.2 is close to 100%. How do other ratios exist for the population? This also makes interpretation of values in the text confusing.
Authors' response: Please note that the log y-scale is percent, not fraction. At a depolarization of 0.2 the percent of particles is ~1 %, not 100 %. Note that the log y-scale is percent, not fraction.
Authors' changes in the manuscript: None.

Referee Comment: Fig 6: Does it make sense to include the error bar information in the caption to make the figure less busy? Or at least remove and caption some of it?
Authors' response: We agree that the figure is busy, but the error bars reported are a big part of our discussion so it's important to retain these in the figure.
Authors' changes in the manuscript: No change has been made.

Referee Comment: Pg 17, line 1: typo of added "u". Also here you switch from >< notation to larger than and smaller than.

58

Authors' response: The text has been modified as suggested. "Larger than" and "smaller than" are now used throughout the text.

Referee Comment: Pg 18, line 12: typo likely

5 *Authors' response:* Corrected.

Referee Comment: Pg 20, line 4: double check wording for how this figure is introduced and also in the caption to be consistent and correct

Authors' response: The figure has been modified and now labels M as the "multiplication factor" as stated

10 in the text and caption.

Referee Comment: Pg 20, line 5: suggest figure or Fig. 7

Authors' response: Corrected to "Figure"

15 *Referee Comment:* Fig 8: Caption could be improved, especially repetition in description of panel c.

Authors' response: Agreed and corrected.

Authors' changes in manuscript: The caption now reads "Figure 8: Application of depolarization ratio method on three CFDC runs. Aerosol composition and temperature are labeled in the title. (a) Time series of supersaturation with respect to water. (b) INP Concentrations under normal (blue) and WDBT (red)

20 conditions are shown for the traditional (circles) and new (asterisks) analysis methods. (c) The normalized number distributions of all particles detected by the CASPOL. Time is reported in local time (CET)."

Referee Comment: Pg 20, line 26, suggest: In 2 out of 3 cases shown. Alternatively, you may want to clearly state (as you do later) that 27 cases/periods were evaluated (see Fig 9).

25 *Authors' response:* This is a good suggestion. Done.

Referee Comment: Pg 21, line 7: center panel of Fig. 8c?

Authors' response: Changed to "middle" panel.

Referee Comment: Pg 21, line 12: is data missing from fig 9 or is it just hard to see?

Authors' response: We have confirmed that no data is missing here. There are cases where no WDBT conditions occur in a run so there is no data to report.

5 *Authors' changes in the manuscript:* On page 22 ln 5, this is now noted in the manuscript, "In cases 24, 25, and 26 WDBT did not occur, so no data is reported.

Referee Comment: Fig 10: Which axis contains the data for the new method? I suspect the x, but am unsure due to confusion noted above. Please clarify and update axes. Would it make sense to fit this data 10 to observe is there is a small bias in the new data?

Authors' response: The figure has now been correctly labeled with the traditional concentration on the x-axis and the new concentration on the y-axis. Though a fit could be used to describe the bias, the authors felt that a new discussion about a completely different application of a linear regression would be confusing to readers. The object of the plot is achieved by discussing the biases of the new method.

15

Referee Comment: Pg 22, paragraph beginning on line 5: I am confused about how the errors in two regions can be 500 and 50% but overall it's 32%. I believe this is averaged values for each region considered. Is this the best way to present the uncertainty? Also as a minor detail, spacing when reporting numbers is inconsistent here and somewhat throughout the document, which would probably be fixed 20 upon typesetting.

Authors' response: Fit to the results of the linear regression (Eq. 9), which has a very large y-intercept contribute to this variable performance. The 500% represents the lowest range of concentration detected and represents just a small portion of the large range of INP concentrations measured during the FIN-02 campaign. Above the 50,000 L^{-1}, the new method's performance improves greatly with measurements are 25 within 50 % of the traditional concentration. No measurements here have error larger than 50%. The mean error for all measurements is 32.1 %.

Authors' changes in the manuscript: We've reordered and modified the text slightly to make this clearer.

Referee Comment: Figure 11: Consistency with previous figures and also double check captioning.

Authors' response: Thank you. The caption is now consistent with other figures.

Referee Comment: Pg 23, line 9: Does Fig 11b warrant more of a discussion? Can a literature comparison

5   be included?

Authors' response: This case was discussed earlier in the text, and does deserve an additional brief discussion here. Since a detailed FIN-02 intercomparison is forthcoming in the literature in the near future (DeMott, et al, 2017), we limit the discussion here.

Authors' changes in the manuscript: This text (p. 26 ln 6) now reads, "Fig. 11b shows the special case of

10 high activation of INP discussed above and in Figure 8b. This case involves a highly active INP, Snomax$^®$ at -20 $^°$C, a significantly colder temperature than required for the Snomax$^®$ to activate as INP. Since most particles activated prior to the onset of WDBT, there is negligible difference in the concentrations reported during "ice only" and WDBT periods."

15

20

Using depolarization to quantify ice nucleating particle concentrations: a new method

Jake Zenker[1], Kristen N. Collier[1], Guanglang Xu[1], Ping Yang[1], Ezra J. T. Levin[2], Kaitlyn J. Suski[2,3], Paul J. DeMott[2], Sarah D. Brooks[1]

[1]Department of Atmospheric Science, Texas A&M University, College Station, TX 77843
[2]Department of Atmospheric Science, Colorado State University, Fort Collins, CO 80526
[3]Now at Pacific Northwest National Laboratory, Richland, WA 99352

Correspondence to: S.D. Brooks (sbrooks@tamu.edu)

Abstract. We have developed a new method to determine ice nucleating particle (INP) concentrations observed by a Continuous Flow Diffusion Chamber (CFDC) under a wide range of operating conditions. In this study, we evaluate differences in particle optical properties detected by the Cloud and Aerosol Spectrometer with POLarization (CASPOL) to differentiate between ice crystals, droplets, and aerosols. The depolarization signal from the CASPOL instrument is used to determine the occurrence of water droplet breakthrough (WDBT) conditions in the CFDC. The standard procedure for determining INP concentration is to count all particles that have grown beyond a nominal size cut-off as ice crystals. During WDBT this procedure overestimated INP concentration, because large droplets are miscounted as ice crystals. Here we design a new analysis method based on depolarization ratio that can extend the range of operating conditions of the CFDC. The method agrees reasonably well with the traditional method under non-WDBT conditions with a mean percent error of ± 32.1%. Additionally, a comparison with the Colorado State University (CSU) CFDC shows that the new analysis method can be used reliably during WDBT conditions.

1 Introduction

Ice clouds cover approximately 40% of the Earth's atmosphere (Wylie and Menzel, 1999). Because of their complicated microphysical properties, ice and mixed-phase clouds pose challenges in understanding our global radiative budget and precipitation (Wendisch et al., 2005; Pinto et al., 1998; Yang et al., 2015;

Korolev, 2007). Despite ~~a significant amount of effort by the atmospheric research community in the last~~ several decades of effort by the atmospheric community to study ice clouds, there are still large gaps in our understanding of the impacts they have on our climate (Boucher et al., 2013). While experimental chambers have been used to study ice nucleation processes and INP concentrations for more than 30 years, INP measurement techniques are still under development.

Ice nucleation measurements are challenging for several reasons. The concentration of effective INPs is typically 0.1 to 1000 L^{-1} or ~10^{-6} to 10^{-4} of the total aerosol concentration (DeMott et al., 2003; DeMott et al., 2015; Jiang et al., 2014; Mason et al., 2016; Cziczo et al., 2017). Secondly, differentiating between ice crystals and droplets using particle discrimination methods is experimentally challenging. Thirdly, i~~I~~ce crystals can nucleate via several mechanisms (Vali, 1985; Vali et al., 2015), and accurate measurements mus~~eth~~t account for ice crystals initiated by each of these mechanisms. ~~.~~

At temperatures below ~ -36 °C, ice crystals can nucleate homogen~~e~~ously from water droplets. At higher temperatures, an aerosol particle is needed to act as an ice nucleating particle (INP) which facilitates the formation of an ice crystal via heterogeneous nucleation. Heterogeneous nucleation pathways include depositional nucleation,~~freezing~~ which occur through the direct deposition of water vapor on an INP surface. Immersion freezing occurs when an INP ~~becomes~~ embedded within a water droplet enters a cooler environment and nucleates an ice crystal. Evidence suggests that immersion freezing provides the largest contribution to ice crystal nucleation in clouds (De Boer et al., 2011; Murray et al., 2012). In addition, when an aerosol forms a solution droplet below the melting point, condensational freezing may occur. Finally, contact freezing occurs when an aerosol in contact with ~~a~~ a water droplet surface ~~and~~ initiates freez~~ing~~es. While the exact mechanism of contact freezing remains unresolved, it has been shown that the presence of an INP positioned at a droplet surface facilitates freezing at temperatures several degrees warmer than immersion freezing with identical INPs (Fornea et al., 2009; Brooks et al, 2014; Durant and Shaw, 2005). Knowledge of each of these mechanisms is important for understanding the formation of ice in mixed-phase clouds (containing droplets and ice crystals) and for developing robust parameterizations for global climate model (GCMs) (Tan et al., 2016; Pithan et al., 2014).

Composition, surface structure, and size are important factors in determining the ice nucleating ability

of an aerosol particle (Zolles et al., 2015; Niemand et al., 2012, Hoose and ~~Mohler~~Möhler, 2012). ~~Field Mm~~easurements suggest that K-feldspar, a common component of soil dust aerosol, may account for a large fraction of Earth's INPs (Atkinson et al., 2013; Yakobi-Hancock et al., 2013). Recent investigations of other aerosols have identified aromatic pollutant aerosols, secondary organic aerosols (SOA), ~~other~~ marine aerosols, and aerosols produced from biomass burning as effective INPs (Brooks et al, 2014; DeMott et al., 2016; McCluskey et al., 2016; Levin et al., 2016; McCluskey et al., 2014; Collier and Brooks, 2016).

Optical techniques have been used to detect and characterize ambient ice crystals (Mishchenko and Sassen, 1998; Yoshida et al., 2010; Noel and Sassen, 2005). For example, Light Detection and Ranging (LIDAR) observations ~~can~~ use the depolarization ratio to distinguish cloud particle type (i.e., ice crystals or water droplets). In traditional LIDAR applications, the depolarization ratio is calculated using Eq. (1),

$$\delta_{LIDAR} = \frac{B_\perp}{B_\parallel} \qquad (1)$$

where $B_\perp$ and $B_\parallel$ are the perpendicular and parallel components of the LIDAR signal retrieved from the ambient atmosphere or clouds. Under single scattering conditions, the depolarization ratio associated with an ensemble of water droplets is essentially zero while the counterpart for ice crystals is nonzero with a specific value depending on particle habit and orientation. Ice crystal depolarization ability is attributed to the high irregularities in the shapes and surfaces of ice crystals (Bohren and Huffman, 1983).

The number of INPs present in a cloud can dictate its optical properties throughout the ice nucleation process (Hoose and Möhler, 2012; Murray et al., 2012). ~~Cloud cChambers that reproduce ice nucleation conditions have been used for the last 30 years to make INP measurements. Techniques used to detect and measure nucleated ice crystals in these devices are still under development~~

~~for several reasons. First, it is difficult to measure INPs with ice nucleation chambers because the concentration of effective INPs is typically 0.1 to 1000 L^{-1} or ~10^{-6} to 10^{-4} of the total aerosol concentration (DeMott et al., 2003; DeMott et al., 2015; Jiang et al., 2014; Mason et al., 2016; Cziczo). Secondly, differentiating between ice crystals and droplets that form in the chamber is essential and can~~

be difficult to account for. ~~The Continuous Flow Diffusion Chamber (CFDC) was originally developed by Rogers (1988) at the University of Wyoming and was later modified and rebuilt at Colorado State University (CSU). The CSU CFDC has been operated in multiple field projects each year for the past 15 years (e.g. Creamean et al., 2016; DeMott et al., 2015; Prenni et al., 2013). Several other ice nucleation~~

5 ~~chambers have been developed since then including the CFDC at Texas A&M University (TAMU) that is used in this study. Many enhancements have been made to CFDCs (e.g. Rogers et al., 2001~~Creamean et al., 2016; DeMott et al., 2015; Prenni et al., 2013~~), including replacement of the TAMU CFDC's traditional aerosol spectrometer (CLIMET, Model No. CI-3100), which uses particle size to distinguish ice crystals from water droplets and aerosols, with the Cloud and Aerosol Spectrometer with POLarization~~

10 ~~(CASPOL, Droplet Measurement Technologies, Inc.). The CASPOL detects forward scattering, backward scattering and depolarization on a single particle basis. The instrument has previously been used to differentiate between ice crystals and various types of dust and soil particles (Glen et al., 2013, 2014).~~

~~—~~Several previous studies have designed new analysis methods for ice chambers that utilize the

15 depolarization ratio measured by optical particle counters (OPCs) ~~that operate similarly to the CASPOL~~ (Glen and Brooks, 2014; Nicolet et al., 2010; Clauss et al., 2013; Garimella et al., 2016). Nicolet et al. (2010) accurately quantified ice crystals in the presence of water droplets in a chamber by using the peak intensity of the depolarization ratio to discriminate between ice crystals and droplets with the Ice Optical DEtector (IODE). Rather than using the peak intensity of the depolarization signal, Clauss et al. (2013)

20 used the width of the pulse detected in the depolarization channel of the Thermo-stabilized Optical Particle Spectrometer for the detection of Ice (TOPS-ice) for phase discrimination. Alternatively, Garimella et al. (2016) used a machine learning technique with scattering signals, including linear depolarization signals detected by an OPC installed in the SPectrometer for Ice Nuclei (SPIN, Droplet Measurement Technologies, Inc.) to determine~~tect~~ INP concentration.

25 A Continuous Flow Diffusion Chamber (CFDC) designed to measure ice nucleation was originally developed by Rogers (1988) at the University of Wyoming and was later modified and rebuilt at Colorado State University (CSU). Several other ice nucleation chambers have been developed since then including the CFDC at Texas A&M University (TAMU) used in this study. Many enhancements have been made

65

to ice nucleation chambers (e.g. Rogers et al., 2001; Creamean et al., 2013; DeMott et al., 2015; Prenni et al., 2013; Coluzza, et al., 2017); Zanji et al., (2017)), including replacement of the TAMU CFDC's standard optical detector (CLIMET, Model No. CI-3100), which uses particle size to distinguish ice crystals from water droplets and aerosols, with the Cloud and Aerosol Spectrometer with POLarization

5 (CASPOL, Droplet Measurement Technologies, Inc.). The CASPOL detects forward scattering, backward scattering and depolarization on a single particle basis. In addition, the CASPOL has been used to differentiate between ice crystals and various types of dust and soil particles based on backward scattering and depolarization signals (Glen et al., 2013, 2014).

In this study, we demonstrate how differences in particle optical properties can be used to differentiate

10 between ice crystals, droplets, and aerosols detected by the CASPOL. In addition, we present a new method to quantify INP concentrations detected by the TAMU CFDC using depolarization ratio. ~~, and determine the accuracy of that method in comparison to the traditional analysis method that primarily uses particle size to identify aerosol particles that have nucleated ice crystalsactivated ice crystals as INPs.~~ Finally, INP concentrations obtained using the new method are compared with results obtained through

15 the traditional analysis method that primarily uses particle size to identify INP. as well as to INP concentrations reported by another ice nucleation chamber, the CSU CFDC.

2 Experimental

2.1 The TAMU Continuous Flow Diffusion Chamber (CFDC) and Cloud and Aerosol Spectrometer

20 with POLarization (CASPOL)

The TAMU CFDC was custom built in our laboratory at Texas A&M University and has been operated in previous laboratory and field campaigns to take temperature and supersaturation resolved INP concentration measurements (Glen and Brooks, 2014; McFarquhar et al., 2011). Additional details on

25 CFDC and CFDC-CASPOL instrument design and operation are provided in our previous work (Glen and Brooks, 2013 and 2014; Glen, 2014.) Hereafter, CFDC refers to the TAMU CFDC unless otherwise stated.

During operation, sample aerosols pass through a diffusion dryer to remove moisture from the air and

66

before they enter the CFDC. Typically, aerosol flow is directed through a BGI Sharp Cut Cyclone impactor (Model 0.732) prior to entering the CFDC, in order to remove aerosols with a diameter greater than ~1.75 μm from the sample flow. However, the data presented here was collected by the TAMU CFDC-CASPOL during ~~The data presented here were collected during~~ the second phase of the Fifth International Ice Nucleation Workshop campaign (FIN-02) and no impactor was used during the campaign. Reasons for this choice were that the objective of FIN-02 was intercomparison with other instruments that~~which~~ did not have impactors available, and also aerosol size distributions were well characterized and supermicron particle numbers were small.

Next, aerosols enter the CFDC processing chamber where temperature and supersaturation are controlled. The processing chamber consists of two concentric cylindrical walls coated with ice. Separate refrigeration units on each wall can be controlled to create a temperature gradient in the chamber that imposes a region of supersaturation with respect to ice (SS_i) in the CFDC. The CFDC chamber is 75 cm long. The bottom 25 cm of the walls are coated with hydrophobic Teflon to prevent water from freezing to the wall in this region. This section of the chamber is referred to as the evaporation region because it remains subsaturated with respect to water and partially or completely evaporates any water droplets that nucleate in the CFDC. The separate wall temperatures are manually controlled and monitored through a Labview program. The temperature and supersaturation conditions at the position of the sheath air surrounded aerosol lamina are calculated using analytical equations reported in Rogers (1988).

Before measurements can be taken with the CFDC, the processing chamber must be prepared. First, a vacuum pump is used to evacuate the chamber for approximately 30 minutes in order to eliminate ambient aerosols that may have infiltrated the chamber and to remove moisture that may cause the walls to accumulate an uneven coating of ice or allow ice to accumulate in other sensitive regions. The walls are then cooled to a temperature of -25 °C and the CFDC walls are iced by pumping Nanopure water into the chamber from the base. Excess water is drained out of the instrument for approximately a minute after icing is complete. Then, the chamber is evacuated and refilled with N_2 gas once more before sampling is initiated.

At the base of the processing chamber, particles pass through a detector to determine INP concentration. In previous TAMU CFDC studies, either an optical particle counter (Climet, Inc.) or the

Cloud and Aerosol Spectrometer with Polarization (CASPOL) were employed (Glen et al., 2014, McFarquhar et al.,., 2011). During FIN-02, the CASPOL was the chosen detector. Two mass flow controllers downstream of the CASPOL are used to set the total flow and recirculating sheath flow through the CFDC-CASPOL. The difference between the total and sheath flows determines the sample

5 flow. For this campaign, the total flow was set to values ranging from 6 to 9 L min^{-1} and the sheath flow was set to values ranging from 4 to 7 L min^{-1} resulting in a sample flow that was typically ~2 ± 0.5 L min^{-1}. During operation, the CFDC made scans from low to high supersaturation at a constant aerosol lamina temperature (± 1.5 °C). This is accomplished by increasing wall temperature difference in a manner that retains the desired temperature at the position of the aerosol lamina.

10   The CASPOL (Droplet Measurement Technologies, Inc.) is a prototype particle-by-particle counter. Laser light (680 nm) is scattered by single particles entering the CASPOL and detected by three detectors that give information about the optical properties: A forward scatter detector, a backward scatter detector with a parallel polarized filter, and a backward scatter detector with a perpendicular polarized filter. Particles are sized according to the intensity of light, which reaches the CASPOL's forward scatter

15 detector, as in a traditional OPC. The forward scattering detector of the CASPOL registers particles on an individual basis and sorts those particles into a series of size bins ranging from 0.6 to 50 micrometers optical diameter. In addition, the instrument has a fourth detector that determines if a particle is properly aligned in the laser beam and should thus be recorded.

   The depolarization ratio derived from CASPOL measurements is defined as follows (Glen et al., 2014).

20

$$\delta_{CAS} = \frac{B_{\perp,CAS}}{B_{\perp,CAS} + B_{\parallel,CAS}} \tag{2}$$

where $B_{\perp,CAS}$ and $B_{\parallel,CAS}$ denote the signals from the CASPOL's perpendicular and parallel backward scattering detector, respectively. This definition differs somewhat from the conventional depolarization ratio used in remote sensing based on LIDAR observations. The main difference is that the CASPOL detects light at the back scattering angles of 168° to 176°, rather than precisely 180° in the case of LIDAR.

25 Also, the CASPOL occasionally detects a particle for which the parallel backscatter signal is below the limit of detection and thus is registered as zero, while the same particle has a nonzero perpendicular signal.

In such cases, the calculated LIDAR depolarization ratio of such particles is of spurious singularity. In contrast, the value of depolarization ratio calculated by Eq. 2 in the aforementioned case yields a value of unity, making the depolarization ratio of these particles quantitatively meaningful. Likewise, in cases where the perpendicular backscatter is below the limit of detection, the reported depolarization ratio is
5 also unity.

2.2 Data cCollection dDuring the Fifth International Ice Nucleation Workshop campaign (FIN-02)

~~The data presented here were collected during~~ The second phase of FIN-02 took place at the Institute
10 of Meteorology and Climate Research: Atmospheric Aerosol Research (IMK-AAF) facility at the Karlsruhe Institute of Technology (KIT) in Karlsruhe, Germany (DeMott et al., 2017). Two specialized chambers at KIT were used in this campaign: the Aerosols Interaction and Dynamics in the Atmosphere (AIDA) chamber and the Aerosol Preparation and Characterization (APC) chamber. The AIDA chamber can be used to simulate atmospheric conditions that give rise to cloud particle formation~~nucleation~~ and
15 growth, and has been used in many previous campaigns and instrument intercomparisons to examine the ice nucleating ability of various aerosols (Amato et al., 2015; Schnaiter et al., 2016; Wagner et al., 2015; DeMott et al., 2011). The AIDA chamber is a three-story, 84 m^3 volume that uses adiabatic expansion to simulate the atmospheric conditions required for ice nucleation to occur. During FIN-02, aerosols were drawn from the AIDA chamber by the various ice nucleation instruments prior to expansion. Following
20 the aerosol sampling period, an AIDA expansion was performed so that INP concentration determined by AIDA could be compared to results from the various visiting instruments. The ~~The~~ second chamber, the APC, is a 3.7 m^3 volume in which ~~controlled and homogenous conditions~~ aerosols of a selected composition are produced by atomization and solid aerosol generation methods, d suspended in ~~with~~ dry synthetic air, uniformly distributed with a mixing fan and maintained at constant temperature and pressure
25 (Linke et al., 2006). While the APC lacks the adiabatic expansion capabilities of AIDA, the APC was used during FIN02 to provide a uniform high concentration of aerosols of various compositions. Samples were subsequently distributed to the participating ~~It was used during FIN-02 to provide aerosol populations of varied compositions for sampling by~~ ice nucleation instruments.

During the ~~FIN-02~~ campaign groups from 22 institutions sampled both the AIDA and APC chambers using a variety of online and offline ice nucleation measurement techniques~~methods~~. For verification of the TAMU CFDC-CASPOL measurements and new analysis method, we compare our results to the measurements of the CSU CFDC. In order to test the CASPOL detector response to ice and non-ice particles, auxiliary measurements of olive oil droplets, ambient aerosols, and homogeneously frozen ice crystals are also evaluated and compared to the TAMU CFDC-CASPOL heterogeneous nucleation data collected during FIN-02.

2.1 The TAMU Continuous Flow Diffusion Chamber (CFDC)

The TAMU CFDC was custom built in our laboratory at Texas A&M University and has been operated in previous laboratory and field campaigns to take temperature and supersaturation resolved INP concentration measurements (Glen, 2014; Glen and Brooks, 2014; McFarquhar et al., 2011). Hereafter, CFDC refers to the TAMU CFDC unless otherwise stated. Sample aerosols pass through a diffusion dryer to remove moisture from the air and aerosols before they enter the CFDC. Typically, aerosol flow is directed through a BGI Sharp Cut Cyclone impactor (Model 0.732) prior to entering the CFDC, in order to remove aerosols with a diameter greater than ~1.3 µm from the sample flow. However, no impactor was used during the FIN-02 campaign since aerosol size distributions were well characterized and supermicron particle numbers were limited. The aerosols then enter the CFDC where temperature and supersaturation are controlled. The CFDC consists of two concentric cylindrical walls coated with ice. Separate refrigeration units on each wall can be controlled to create a temperature gradient in the chamber that imposes a region of supersaturation with respect to ice (SS_i) in the CFDC. The CFDC chamber is 75 cm long. The bottom 25 cm of the walls are coated with hydrophobic Teflon to prevent water from freezing to the wall in this region. This section of the chamber is referred to as the evaporation region because it remains subsaturated with respect to water and partially or completely evaporates water droplets that nucleate in the CFDC. The separate wall temperatures are manually controlled and monitored through a Labview program. The temperature and supersaturation conditions at the position of the sheath air surrounded aerosol lamina are calculated using analytical

70

equations reported in Rogers (1988).

Before measurements can be taken with the CFDC, the chamber must be prepared. First, a vacuum pump is used to evacuate the chamber for approximately 30 minutes in order to eliminate ambient aerosols that may have infiltrated the chamber and to remove moisture that may cause the walls to accumulate an uneven coating of ice or allow ice to accumulate in other sensitive regions. The walls are then cooled to a temperature of -25 °C and the CFDC walls are iced by pumping Nanopure water into the chamber from the base. Excess water is drained out of the instrument for approximately a minute after icing is complete. Then, the chamber is evacuated and refilled with N_2 gas once more before sampling is initiated.

At the base of the processing chamber, particles pass through a detector to determine INP concentration. In previous TAMU CFDC studies, either an optical particle counter (Climet, Inc.) or the Cloud and Aerosol Spectrometer with Polarization (CASPOL) were employed.

2.2 The Cloud and Aerosol Spectrometer with POLarization (CASPOL)

The CASPOL (Droplet Measurement Technologies, Inc.) is a prototype particle-by-particle counter used in previous studies to detect and distinguish between dust and ice particles and even between various types of dust (Glen et al., 2013, 2014). The CASPOL instrument has three detectors that give information about the optical properties: A forward scatter detector, a backward scatter detector with a parallel polarized filter, and a backwards scatter detector with a perpendicular polarized filter. In addition, the instrument has a fourth detector that determines if a particle is properly aligned in the laser beam and should thus be recorded.

2.3 CFDC-CASPOL data analysis

CFDC-CASPOL data is sorted into 1-minute segments in order to achieve a sufficient sample volume detected by the CASPOL. The temperature, pressure, sample and sheath flows are used to determine a STP (standard temperature and pressure; 273 K, 1013.5 mb) sample volume, which is used to convert the

raw count of particles in each 1-minute segment to a concentration. Occasionally ice particles may detach from the ice-coated ~~chamber~~ walls. To account for this, ~~before and/or after each supersaturation scan is taken,~~ a ~~high efficiency aerosol~~ filter is placed upstream ~~ahead~~ of the sample inlet in order to determine background signal of the CFDC chamber. The background period that is closest to a given 1-minute

5 sample period is applied ~~The~~ by subtracting that background concentration from the total ~~concentration of particles measured while the filter is in place is subtracted from the total~~ concentration measured by the CASPOL at the sample time.

The traditional analysis method counts INPs based on a nominal size cut of 2 μm in diameter in order to discriminate between unactivated aerosols and ice crystals. The approximate size cuts has been

10 determined by modeling calculations indicate that ice nucleating in the CFDC will grow beyond this size diameter (Rogers, 1988). During FIN-02, data collected by the CASPOL's forward scattering detector was used for the traditional analysis. The CASPOL forward scattering signal is accurately calibrated for spherical particles. For non-spherical ice crystals, the particle size-scattering relationship is less certain.

15 **2.4 Limitations of the traditional analysis method**

There are several limitations to the traditional analysis method used to process CFDC data, which relies on size alone to differentiate ice from water particles (as described in Section 2.3). As previously mentioned, supercooled water droplets may form in the chamber in conditions supersaturated with respect

20 to water (SS_w). At high SS_w, water droplets may pass through the evaporation region without fully evaporating. Any droplets that remain larger than the nominal size cut and reach the detector ~~downstream of the evaporation region~~ will be miscounted as ice crystals. This phenomenon is referred to as water droplet breakthrough (WDBT).

25 WDBT is a common issue in continuous flow ice nucleation instruments, although the point at which WDBT occurs varies between instruments of differing dimensions and even as a function of operating conditions (especially temperature) within a single instrument (Rogers et al., 2001, DeMott et al, 2015, Garimella et al., 2016). CFDCs in use today are custom-built instruments which vary in physical

dimensions and choice of detector, although all operate under the same basic principles. Due to the combination of different chamber dimensions, flow rates, operating conditions (temperature and supersaturation) in the growth and evaporation regions within the instrument, and the choice of detector and size cut-off, WDBT varies from instrument to instrument. In some cases, it can be difficult to determine when WDBT is occurring, and if the instrument is unintentionally operated at supersaturations above WDBT, droplets will be miscounted as ice crystals. Even within a single instrument, specific conditions of WDBT vary with operating temperature, the ambient humidity, the hygroscopicity and the size of sample aerosols, and the sample flow which determines the residence time in the instrument. Typically, in the TAMU CFDC the onset of WDBT occurs at 3 % to 4% SS_w, but has been observed as low as 1 % SS_w and as high as 8 % SS_w. In some cases, it can be difficult to determine when WDBT occurs, and if the instrument is unintentionally operated at supersaturations above WDBT, droplets may be miscounted as ice crystals. A new analysis method would be valuable for overcoming the challenges presented by WDBT.

In the traditional analysis, any aerosols larger than the nominal size cut are miscounted as INPs. OWhile peration with an upstream the use of the impactor reduces this problem. However, depending on the flow, 1 to 10% of particles larger than 2 μm may still make it through the impactor and into the chamber to contribute to the apparent INP signal. A new analysis method that differentiates between large aerosols and ice crystals is needed since it would remove the need to limit the size of particles allowed into the instrument in the first place. that allows for the inclusion of larger aerosols could improve our measurements of INPs, especially in CFDC conditions withat low SS$_w$ and higher supercooled temperatures in which few aerosol particles nucleate ice crystals. Larger aerosols may contribute more to the INP concentration than small aerosols in these conditions, but the CFDC operating procedures and analysis method are not equipped to investigate this phenomenon.

2.5 CASPOL depolarization ratio definition

The goal of this study is to developsign an improved analysis method that uses single-particle depolarization ratio to identify ice crystals in order to quantify INP. In this study, the depolarization ratio

$$\delta_{CAS} = \frac{B_{\perp,CAS}}{B_{\perp,CAS} + B_{\parallel,CAS}}$$

(2)

This definition differs somewhat from the conventional depolarization ratio used in remote sensing based on LIDAR observations. The main difference is that the CASPOL detects light at the back scattering angles of 168° to 176°, rather than precisely 180° in the case of LIDAR. Secondly, the CASPOL occasionally detects a particle for which the parallel backscatter signal is below the limit of detection and thus is registered as zero, while the same particle has a nonzero perpendicular signal. In such cases, the calculated LIDAR depolarization ratio of such particles is infinite. In contrast, the value of depolarization ratio calculated by Eq. 2 yields a value of unity, making Eq. (2) is 1 making the depolarization ratio of these particles quantitatively meaningful.

2.56 Auxiliary CASPOL measurements

Measurements were taken with the CASPOL independent of the CFDC to provide instrument response to various types of particles, which may coincidently reach the detector during CFDC-CASPOL operation.

One population of interest is water droplets. Using aA Vibrating Orifice Aerosol Generator (VOAG) (TSI, Inc., Model 3450) was used along with olive oil solutions is a standard method used to produce monodisperse spherical droplets of chosen sizes as a proxy for water droplets that form in the CFDC. Though the index of refraction of olive oil (1.44 to 1.47) is slightly higher than water (1.33) (Hecht and ZajacZajak and Hecht, 20023), these droplets are a reasonablesuitable approximation for the depolarization ratio signal of water droplets because they are uniform spheres. As reported in Glen and Brooks (2013), the uncertainty in sizing due to differences in the complex refractive indices of oil and water are up to 30% based on a comparison of VOAG oil droplet calibrations of CASPOL to water-based calibrations performed by the manufacturer. For this project, droplets were generated with the diameters of 2 ± 0.6 µm, 6 ± 1.8 µm, 8 ± 2.4 µm, and 10 ± 1.5 µm.

For VOAG droplet generation,For this project 2, 6, 8 and 10 µm droplets were generate a separate

olive oil and 2-propanol solution is prepared for each desired size. The VOAG's vibration frequency, and dispersion and dilution flows are set according to computed specifications as detailed in the VOAG manual and as previously performed (Glen and Brooks, 2013&2014). Downstream of the VOAG, the sample droplets travels through a charge neutralizer (TSI Inc., Aerosol Neutralizer 3054A) to prevent

5   particle loss since charged particles tend to be attracted to the walls of sample tubing. Following the neutralizer, sample flow is split between flow to the CASPOL, controlled by a mass flow controller and a Gast air pump on the downstream side, and a dump line which allows for excess flow generated from the VOAG to be expelled from the system. For each size, data is collected for roughly 15 minutes during which approximately 10,000 droplets are sampled. It was observed that a mode of small (submicron

10   diameter) residual 2-propanol do not evaporate but remain in the sample flow and are detected by the CASPOL. For this reason, all particles less than 1 μm are removed from the dataset during processing.

The CASPOL's response to a second population of interest, ambient aerosol, was also evaluated for the new analysis method. Aerosol was sampled at the Storm Peak Laboratory (SPL) in Steamboat Springs, CO during the third phase of the Fifth International Ice Nucleation Workshop campaign (FIN-03) in

15   September 2015.   The use of a diverse aerosol population is necessary to ensure that the new analysis method be successful at discriminating ice crystals in the CFDC from a wide range ofin aerosols. SPL is an ideal sampling location because the aerosol population comes from many sources including mineral dust, organics from deciduous and coniferous forests, biomass burning aerosols that have been transported from forest fires in the western United States, and sulfates that are produced by two coal burning power

20   plants that are both located approximately 50 km and 100 km from the laboratory. Ambient aerosol sampling at SPL was accomplished by connecting the CASPOL directly to an ambient sample inlet in the laboratory for a total time of ninety-two92 hours over a seven day period.

Thirdly, a population of ice crystals was needed for the new method. CFDC-CASPOL measurements were taken under conditions that approached those needed for homogeneous freezing, thus generating

25   higher concentrations of ice crystals in the absence of activated liquid droplets. These measurements are detailed in Glen et al. (2014). For these measurements, the sample flow was conditioned with a pre-cooler, which was set to -10 °C to remove excess moisture and the CFDC was operated at -55 ± 0.2 °C and 51 ± 2.3 % SS_i.(-11 $\pm$ 1.5 % SS_w). Under these conditions, we can ensure that all particles larger than the 2 μm

size cut were frozen, which is the goal of this experiment.

For clarity, the CASPOL measurements of the VOAG droplets, ambient aerosols collected at SPL, and ice crystals generated in homogeneous conditions are referred to as droplet, aerosol, and ice crystal training datasets, respectively.

5

3 Results

3.1 Discriminating water droplets, aerosols, and ice crystals with optical signatures

10

This analysis used optical differences between ice crystals, droplets, and aerosols in order to identify and quantify ice crystals that form in the ~~TAMU~~ CFDC. The CASPOL has been used previously to discriminate between different aerosol populations using an empirical tool known as an optical signature (Glen et al., 2013). In an analogous method, optical signatures produced from CALIPSO satellite backscatter and depolarization data have been used to identify cloud phase ~~of various types of clouds have been reported by~~ (Hu et al., ~~(~~2009).

In Fig. 1-a-c, CASPOL optical signatures for ice training, droplet and aerosol training data are shown, respectively. The signatures show depolarization ratio (as defined in Eq. (2~~)~~) versus total backscatter. The signatures are generated by defining a 50 x 50 Cartesian grid with depolarization ratio on the x-axis and total backscatter (calculated as the sum of the CASPOL's parallel and perpendicular signal intensities) on the y-axis. Each particle detected by the CASPOL is placed in the appropriate grid cell. The color scale in Fig 1. reports the fraction of particles in a dataset that populate that grid cell. ~~The optical signatures are generated by defining a 50 x 50 Cartesian grid with depolarization ratio on the x-axis and total backscatter (calculated as the sum of the CASPOL's parallel and perpendicular signal intensities) on the y-axis. Each particle detected by the CASPOL is placed in the appropriate grid cell. The color scale displays the fraction of particles in a dataset that populate that grid cell. As discussed, the ice crystal and droplet training data shown in Fig. 1 only includes particles with diameters ≥ 2 μm and ≥ 1 μm, respectively.~~ Each training dataset contains some ~~members~~ particles that are highly backscattering ~~(> 75,)~~ and some

76

particles members that are highly or highly depolarizing, (> 0.1), but only the ice crystal population contains particles that have both a high depolarization ratio and high backscatter signal.

In Fig. 1 d-f, optical signatures normalized with respect to forward scatter, F, are displayed. Here the total backscatter signal to forward scatter signal ratio is plotted against the back perpendicular signal to forward signal ratio. The back perpendicular to forward ratio is a measure of depolarizing ability normalized by size (which is determined by the forward signal, F). In Fig.s 1 d-f, we see that very few aerosols and droplets achieve a back perpendicular to forward ratio larger than> 0.05. In contrast, many of the ice crystal training dataset particles exceed that value.

Consistent with the findings of Glen et al. (2013), CASPOL optical signatures can be used as an empirical tool to detect differences in the bulk optical properties of different particle populations. However, in order to design a new analysis method, it is necessary to gain a quantitative understanding of how the CASPOL detects single particles as opposed to bulk populations of particles.

CFDC CASPOL data is sorted into 1-minute segments in order to achieve a sufficient sample volume detected by the CASPOL. The temperature, pressure, sample and sheath flows are used to determine a STP (standard temperature and pressure; 273 K, 1013.5 mb) sample volume, which is used to convert the raw count of particles in each 1-minute segment to a concentration. Occasionally ice particles may detach from the ice-coated chamber walls. To account for this, before and/or after each supersaturation scan is taken, a high efficiency aerosol filter is placed ahead of the sample inlet in order to determine background signal of the CFDC chamber. The background period that is closest to a given 1-minute sample period is then applied The by subtracting that background concentration from the total concentration of particles measured while the filter is in place is subtracted from the total concentration measured by the CASPOL at the sample time.

The traditional analysis method counts INPs based on a nominal size cut of 2 or 5 μm in diameter in order to discriminate between unactivated aerosols and ice crystals. The CASPOL signal is accurately calibrated for spherical particles. For non-spherical ice crystals, the particle size-scattering relationship is less certain. Thus, the 2 and 5 μm size cuts are only approximate.

2.4 Limitations of the traditional analysis method

There are several limitations to the traditional analysis method used to process CFDC data, which relies on size alone to differentiate ice from water particles (as described in Section 2.3). As previously mentioned, in supersaturated conditions with respect to water (SS_w), supercooled water droplets form in the chamber. At high supersaturations, water droplets may pass through the evaporation region without fully evaporating. Any droplets that remain larger than the 2 μm size cut downstream of the evaporation region will be miscounted as ice crystals. This phenomenon is referred to as water droplet breakthrough (WDBT). ,WDBT is a common issue in continuous flow ice nucleation instruments, although the point at which WDBT occurs varies between instruments of differing dimensions and also depends on operating conditions (especially temperature) within a single instrument (Rogers et al., 2001, DeMott et al, 2015, Garimella et al., 2016). CFDCs in use today are custom-built instruments, which vary in physical dimensions and choice of detector, although all operate under the same basic principles. Due to the combination of chamber dimensions, flow rates, operating conditions (temperature and supersaturation) in the growth and evaporation regions within the instrument, and the choice of detector and size cut off, WDBT varies from instrument to instrument. In some cases, it can be difficult to determine when WDBT occurs, and if the instrument is unintentionally operated at supersaturations above WDBT, droplets may be miscounted as ice crystals. A new analysis method would be valuable for overcoming the challenges presented by WDBT.

 areisWhile the use of the impactor reducesd this problem;, depending on the sample flow of the CFDC ~1 to 10% of particles larger than 2 μm may still make it through the impactor and into the chamber to contribute to the apparent INP signal. A new analysis method that allows for the inclusion of larger aerosols could improve our measurements of INPs, especially in CFDC conditions withat low SS_w and higher supercooled temperatures in which few aerosol particles nucleate ice crystals. Larger aerosols may contribute more to the INP concentration than small aerosols in these conditions, but the CFDC operating procedures and analysis method are not equipped to investigate this phenomenon..

2.5 CASPOL depolarization ratio definition

The goal of this study is to ~~develop~~sign an improved analysis method that uses single-particle depolarization ratio to identify ice crystals in order to quantify INP. In this study, the depolarization ratio is defined as follows (Glen et al., 2014).

$$\delta_{CAS} = \frac{B_{\perp,CAS}}{B_{\perp,CAS} + B_{\parallel,CAS}}$$

(2)

This definition differs somewhat from the conventional depolarization ratio used in remote sensing based on LIDAR observations. The main difference is that the CASPOL detects light at the back scattering angles of 168° to 176°, rather than precisely 180° in the case of LIDAR. Secondly, the CASPOL occasionally detects a particle for which the parallel backscatter signal is below the limit of detection and thus is registered as zero, while the same particle has a nonzero perpendicular signal. In such cases, the calculated LIDAR depolarization ratio of such particles is infinite. In contrast, the value of depolarization ratio calculated by Eq. 2 yields a value of unity, making Eq. (2) is 1 making the depolarization ratio of these particles quantitatively meaningful.

2.6 Auxiliary CASPOL measurements

Measurements were taken with the CASPOL independent of the CFDC to provide instrument response to various types of particles, which may coincidently reach the detector during CFDC CASPOL operation.

One population of interest is water droplets. Using ~~a~~A Vibrating Orifice Aerosol Generator (VOAG) (TSI, Inc., Model 3450) was used along with olive oil solutions is a standard method used to produce monodisperse spherical droplets of chosen sizes as a proxy for water droplets that form in the CFDC. Though the index of refraction of olive oil (1.44 to 1.47) is slightly higher than water (1.33)Hecht and Zajac2, these droplets are a suitable approximation for the depolarization ratio signal of water droplets because they are uniform spheres. 0.61.82.41.5For this project 2, 6, 8 and 10 μm droplets were generated. A separate olive oil and 2-propanol solution is prepared for each desired size and the vibration frequency, and dispersion and dilution flows are set according to computed specifications as detailed in the VOAG

manual and as previously performed (Glen and Brooks, 2013&2014).

During VOAG CASPOL sampling, the olive oil aerosol stream first travels through a charge neutralizer (TSI Inc., Aerosol Neutralizer 3054A) to prevent particle loss. Following the neutralizer, sample flow is split between flow to the CASPOL, controlled by a mass flow controller and a Gast air pump on the downstream side, and a dump line which allows for excess flow generated from the VOAG to be expelled from the system. Small residual droplets of 2-propanol that do not evaporate remain in the sample flow and are detected by the CASPOL. Aerosols are sampled for roughly 15 minutes during which approximately 10,000 droplets are sampled. Small residual droplets of 2-propanol that do not evaporate remain in the sample flow and are detected by the CASPOL. For this reason, all particles less than 1 µm are removed from the dataset during processing.

A second population of interest is ambient aerosol. Aerosol was sampled at the Storm Peak Laboratory (SPL) in Steamboat Springs, CO during the third phase of the Fifth International Ice Nucleation Workshop campaign (FIN-03) in September 2015. The use of a diverse aerosol population is necessary to ensure that the new analysis method be successful at discriminating ice crystals in the CFDC from a wide range in aerosols. SPL is an ideal sampling location because the aerosol population comes from many sources including mineral dust, organics from deciduous and coniferous forests, biomass burning aerosols that have been transported from forest fires in the western United States, and sulfates that are produced by two coal burning power plants that are both located approximately 50 km and 100 km from the laboratory. Ambient aerosol sampling at SPL was accomplished by connecting the CASPOL directly to an ambient sample inlet in the laboratory for a total time of ninety two92 hours over a seven day period.

Thirdly, CFDC measurements were taken under conditions that approached those needed for homogeneous freezing, thus generating higher concentrations of ice crystals in the absence of activated liquid droplets. These measurements are detailed in Glen et al. (2014). For these measurements, the sample flow was conditioned with a pre-cooler, which was set to -10 °C to remove excess moisture and the CFDC was operated at -55 ± 0.2 °C and 51 ± 2.3 % SS_i (-11 ± 1.5 % SS_{water}). Under these conditions, we can ensure that all particles larger than the 2 µm size cut were frozen, which is the goal of this experiment.

For clarity, the CASPOL measurements of the VOAG droplets, ambient aerosols collected at SPL, and

ice crystals generated in homogeneous conditions are referred to as droplet, aerosol, and ice crystal training datasets, respectively.

5

3 Results

3.1 Discriminating water droplets, aerosols, and ice crystals with optical signatures

This analysis used optical differences between ice crystals, droplets, and aerosols in order to identify and quantify ice crystals that form in the TAMU CFDC. The CASPOL has been used previously to discriminate between different aerosol populations using an empirical tool known as an optical signature (Glen et al., 2013). In an analogous method, optical signatures produced from CALIPSO satellite data of various types of clouds have been reported by Hu et al., (2009).

Optical signatures for the training datasets are displayed in Fig. 1. The optical signatures are generated by defining a 50 x 50 Cartesian grid with depolarization ratio on the x-axis and total backscatter (calculated as the sum of the CASPOL's parallel and perpendicular signal intensities) on the y-axis. Each particle detected by the CASPOL is placed in the appropriate grid cell. The color scale displays the fraction of particles in a dataset that populate that grid cell. Optical signatures for ice training, droplet and aerosol training data are shown in Fig. 1 a-c, respectively. These signatures show depolarization ratio (as defined in Eq. (2)) versus total backscatter. The optical signatures are generated by defining a 50 x 50 Cartesian grid with depolarization ratio on the x-axis and total backscatter (calculated as the sum of the CASPOL's parallel and perpendicular signal intensities) on the y-axis. Each particle detected by the CASPOL is placed in the appropriate grid cell. The color scale displays the fraction of particles in a dataset that populate that grid cell. As discussed, the ice crystal and droplet training data shown in Fig. 1 only includes particles with diameters ≥ 2 μm and ≥ 1 μm, respectively. Each training dataset contains some members particles that are highly backscattering (> 75,) or highly depolarizing (> 0.1), but only the ice crystal population contains particles that have both a high depolarization ratio and high backscatter signal. In Fig. 1 d-f, normalized optical signatures with respect to forward scatter, F, are displayed. Here

81

~~the total backscatter signal to forward scatter signal ratio is plotted against the back perpendicular signal to forward signal ratio. The back perpendicular to forward ratio is a measure of depolarizing ability normalized by size (which is determined by the forward signal, *F*). In Fig.s 1 d-f, we see that very few aerosols and droplets achieve a back perpendicular to forward ratio > 0.05.~~ . ~~In contrast, many of the ice~~

5 ~~crystal training dataset particles exceed that value.~~

~~Consistent with the findings of Glen et al (2013), CASPOL optical signatures can be used as an empirical tool to detect differences in the bulk optical properties of different particle populations. However, in order to design a new analysis method, it is necessary to gain a quantitative understanding of how the CASPOL detects single particles as opposed to bulk populations of particles.~~

10

3.2 Modelling the depolarization ratio of water droplets, aerosols, and ice crystals

Model calculations can provide insight on how particles depolarize light in the CASPOL. To ~~perform model~~perform model calculations, we first must define the relation between the CASPOL depolarization

15 ratio (Eq. 2) and the scattering phase matrix. The ~~It is assumed that the~~ CASPOL laser emits an incident beam that propagates along the z direction in the form,

$$\boldsymbol{E}_i = \begin{pmatrix} E_{\|i} \\ E_{\perp i} \end{pmatrix} e^{i(kz-\omega t)} = \begin{pmatrix} E_{\|i} \\ 0 \end{pmatrix} e^{i(kz-\omega t)}, \tag{3}$$

where $\boldsymbol{E}_i$ is the incident electric field, $E_{\|i}$ and $E_{\perp i}$ (=0) are the parallel and perpendicular components with

20 respect to the scattering plane, k is wavenumber, ω is frequency, and t is time. The scattering plane is defined as a plane through the z-axis and the line linking the particle and detection point. ~~.~~ The scattered light at a sufficiently large distance (i.e., in the far-field zone) is related to the incident light in the form

$$\boldsymbol{E}_s = \frac{e^{ik(r-z)}}{-ikr} \begin{pmatrix} S_2 & S_3 \\ S_4 & S_1 \end{pmatrix} \begin{pmatrix} E_{\|i} \\ 0 \end{pmatrix} = \frac{e^{ik(r-z)}}{-ikr} \begin{pmatrix} S_2 \\ S_4 \end{pmatrix} E_{\|i}, \tag{4}$$

~~where r is the distance between the particle and detector, and $S_{i,j}$ i(i=1,2,3,4) are s theelements of the amplitude matrix. Note that $e^{i(\omega t)}$ term is omitted since the scattering is assumed to be elastic. The model depolarization ratio δ_{Model} can be expressed as follows,.~~

$$\delta_{Model}(\theta) = \frac{B_{\perp,Model}(\theta)}{B_{\perp,Model}(\theta) + B_{\parallel,Model}(\theta)} = \frac{|S_4(\theta)|^2}{|S_4(\theta)|^2 + |S_2(\theta)|^2} \qquad (5)$$

5 ~~where θ is the detection angle, and $B_{\parallel,Model}$ and $B_{\perp,Model}$ are the modelled parallel and perpendicular backscattered intensities. Using the following relations between the the elements of scattering phase matrix , P_{ij}(i,j=1,2,3,4) and thethe elements of amplitude matrix S_{ij} and the scattering cross section C_{sca} (i=1,2,3,4) bbelow,~~

$$|S_4(\theta)|^2 + |S_2(\theta)|^2 = (P_{11}(\theta) + P_{12}(\theta)) \times C_{sca}, \qquad (6)$$

$$|S_4(\theta)|^2 - |S_2(\theta)|^2 = (P_{21}(\theta) + P_{22}(\theta)) \times C_{sca}, \qquad (7)$$

10 ~~where C_{sca} is the scattering cross section of a particle, we can define the depolarization ratio from the CASPOL that is analogous to the mean modeled depolarization ratio over the angular range of 168° to 176° and is expressed below in Eq. (8).~~

where r is the distance between the particle and detector and S_i (i=1,2,3,4) are elements of the amplitude matrix. The model depolarization ratio, $\delta_{Model,}$ can be expressed as follows,

15

$$\delta_{Model}(\theta) = \frac{B_{\perp,Model}(\theta)}{B_{\perp,Model}(\theta) + B_{\parallel,Model}(\theta)} = \frac{|S_4(\theta)|^2}{|S_4(\theta)|^2 + |S_2(\theta)|^2} \qquad (5)$$

where θ is the detection angle, and $B_{\parallel,Model}$ and $B_{\perp,Model}$ are the modelled parallel and perpendicular backscattered intensities. Using the following relations between the elements of scattering phase matrix, P_{ij}(i,j=1,2,3,4), and the elements of amplitude matrix, S_i (i=1,2,3,4), below,

$$|S_4(\theta)|^2 + |S_2(\theta)|^2 \sim (P_{11}(\theta) + P_{12}(\theta)) \times C_{sca}, \qquad (6)$$

$$|S_4(\theta)|^2 - |S_2(\theta)|^2 \sim (P_{21}(\theta) + P_{22}(\theta)) \times C_{sca}. \quad (7)$$

where C_{sca} is the scattering cross-section of a particle. As described above, the CASPOL detects light over a narrow range of back scattering angles, 168° to 176°. To compare to the CASPOL measurements, we define the mean modelled depolarization ratio over the angular range of 168° to 176° and is expressed below in Eq. (8).

5

$$\bar{\delta}_{Model}(168°:176°) = \frac{\int_{168°}^{176°}(P_{11}(\theta) + P_{12}(\theta) - P_{21}(\theta) - P_{22}(\theta))\,\sin(\theta)\,d\theta}{2\int_{168°}^{176°}(P_{11}(\theta) + P_{12}(\theta))\,\sin(\theta)\,d\theta} \quad (8)$$

To compute the scattering phase matrices of these models with specific sizes at CASPOL wavelength, we apply so-called improved geometric optics method (IGOM) for particle with relatively large size and the invariant imbedding T-matrix method (II-TM) for particles with relatively small sizes (Yang et al., 1996; Bi et al., 2013; Bi and Yang, 2014; Johnson, 1988). The combination of these two methods is

10 chosen because of the different size parameters of the aerosol and ice crystal populations. The T-matrix method is a highly accurate method for calculating scattering properties of atmospheric particles (Koepke et al., 2015; Brooks et al., 2004). However, it becomes impractical for large particles due to its excessive demands on the computational power. In contrast, the IGOM is accurate over the range of particle sizes over which the particle size to be much larger than the incident wavelength (Xu et al, 2017).

15 Three idealized ice crystal habits were modeled: a hexagonal column, a hexagonal plate, and a droxtal. These shapes represent generalizations of common ice crystal habits (Bailey and Hallett, 2009). An idealized dust-like particle with fractal facets was used to model aerosols (Liu et al., 2013). These particles are nonspherical irregularly shaped and thus will yield different measured depolarization ratios depending on their orientation in the CASPOL. The model provides the mean depolarization ratio over all

20 orientations with respect to the laser beam. In contrast, the theoretical depolarization of water droplets is zero at all sizes.

Fig. 2 shows the depolarization ratios as a function ofvs. size for the three ice crystal habits, dust-like aerosol, and water droplets. The aerosol calculations provided in this analysis provide depolarization ratios for aerosols up to 1.75 μm diameter, representing an approximate upper size limit for aerosols

entering the CFDC. and do not reach a non-zero value 0.005 nominal For hexagonal columns, hexagonal plates, and droxtals, the depolarization ratio increases from less than 0.05 to as high as 0.35 as the optical diameter increases from 0.5 to 8 μm diameter. Above 8 μm, the depolarization ratio for droxtals and columns continue to rise, while the values for plates decrease to ~0.25. The droxtal depolarization ratios are quite low.. Thus, while columns and plates could be distinguished from water droplets based on depolarization ratio alone, droxtals could not be distinctly identified. It is not known which of these habits best represents individual ice crystals nucleated and grown in the CFDC. Fortunately, if it is assumed that only particles of 2 μm diameter or larger are ice crystals in the CFDC, these theoretical results shown that discrimination between water droplets and ice particles on any of the three habits of ice crystals is possible. Thus, consideration of depolarization ratio should provide a large improvement in particle discrimination.

Similar to ice crystals, depolarization ratios of the modeled dust aerosols increase with particle diameter. At most sizes, the aerosol data falls within the range of depolarizations rations reported for the 3 ice crystal shapes. This indicates that the use of depolarization ratios will not improvemake an improvement in differentiating between aerosols and ice crystals. Fortunately, the traditional CFDC method incorporates theinvolves includes use of an impactor to physically removes aerosols greater than 1.75 μm from the sample flow prior to entering the chamber combined coupled with with the analysis strategy of only countingwhich only counts particles thatwhich are larger than the nominal size cut-off (at least 2 μm diameter) as ice crystals. Thus, the traditional method is already sufficient for differentiating between aerosols and ice crystals.

We notice that ice crystals have a relatively high depolarization ratio in comparison to aerosols and water droplets, which confirms the bulk population observations from optical signatures in Fig. 1. For ice crystals larger than 4 μm, crystals of any habit are predicted to have higher depolarization ratios than aerosols. However, between 2 and 4 μm, it can be seen that depolarization ratio varies strongly with habit. Hexagonal columns are predicted to have depolarization ratios higher than aerosols, but hexagonal plates and droxtals may have depolarization ratios equivalent to or even lower than aerosols.
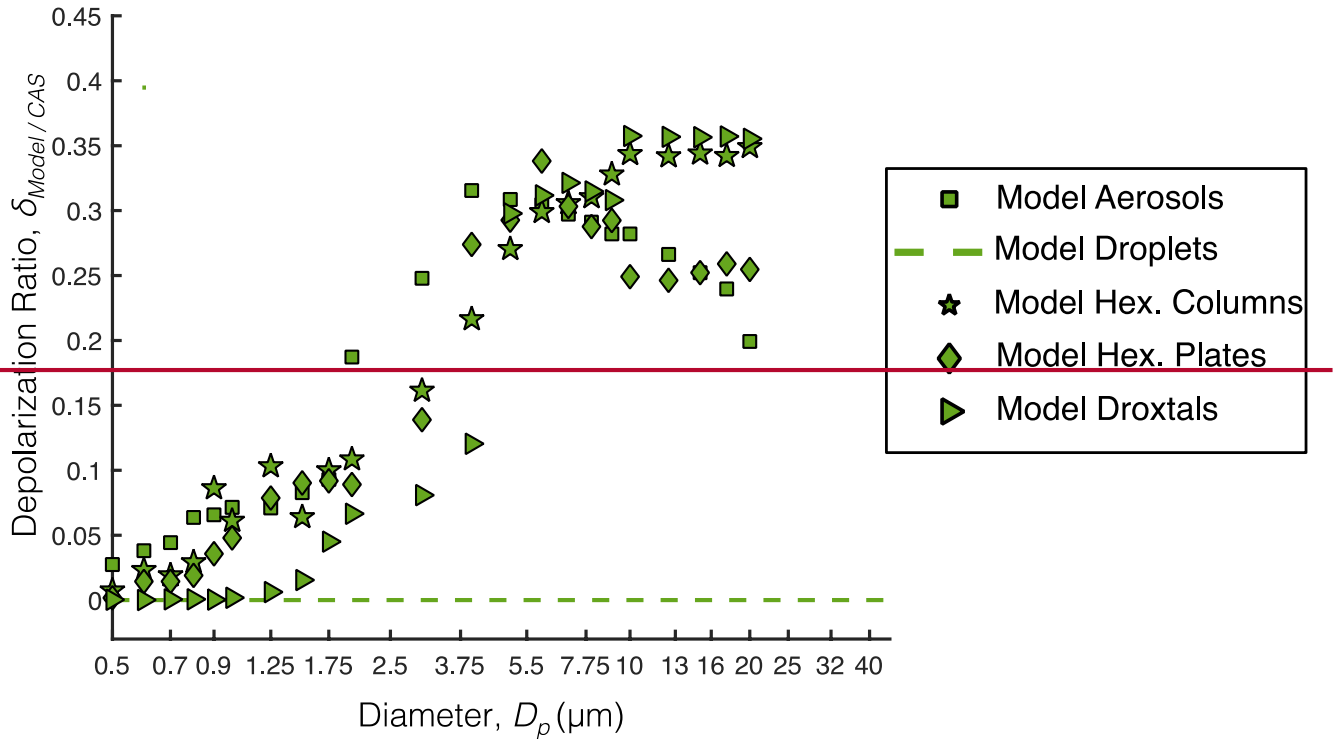
3.3 Determination of optical properties of aerosols, droplets, and ice crystals

In this section, we empirically test the assertion that the CASPOL depolarization ratio can be used to
discriminate ice crystals from aerosols and water droplets. To accomplish this, the training datasets of
droplets, aerosols, and ice crystals shown above (Fig. 1) are examined further. The lognormal size
distributions (shown as a percent of population) observed by the CASPOL for the droplet, aerosol, and
ice crystal training data are shown in Fig. 3a. Each VOAG size in the droplet training dataset is treated as
a separate population and plotted as a separate line in the figure. As seen in Ffig. 1athe Fig., the size
distributions of droplets, aerosols and ice crystals overlap. This demonstrates the primary disadvantage
to using particle diameter as the sole criteria to identify ice crystals.

   For each training data set, the frequency distribution of depolarization ratio reported as a percentage
of the total particles in the data set is shown in Fig. 3b. As seen in the figure, droplets have depolarization
ratios up to 0.3. Therefore, we visually assign 0.3 as the nominal depolarization threshold cut-off for
differentiating between ice crystals and non-ice particles. The choice on 0.3 is further evaluated in Section

86

3.7 below. Unfortunately, a small percentage of aerosols do have depolarizations greater than this threshold. However, since aerosols with sizes above 1.75 micron diameter are physically removed from the sample upstream of the CFDC chamber, the combined consideration of size and depolarization may prove a robust strategy for avoiding the miscounting of aerosols as INP as further discussed below.

5   In Fig. 3c, the percent of particles that achieve a depolarization ratio ≥ 0.3 (the nominal selection criteria for depolarizing ice crystals) as a function of particle diameter is shown. In Fig. 3c, the droplet training data collected for all sizes of olive oil droplets is combined and displayed as one line for simplicity. In contrast to the size distributions (Fig. 3a), in which the training datasets cannot be discriminated, the depolarization ratio distributions show notable differences between droplets, aerosols,

10 and ice crystals. Fig. 3b and c reveal that only 0.3% of droplets and 1.6% of aerosol particless achieve a depolarization ratio ≥ 0.3. The exception to this is aerosols with diameters of 5 to 10 μm. In this size range, 3.9 % percent of aerosols achieve a depolarization ratio of 0.3. However, 5 to 10 μm particles are not abundant in nature, cannot easily be sampled by real-time instruments having the inlet complexity of a CFDC, and only represent 0.3% of the aerosol training dataset. Furthermore, particles in this size range

15 were not generated during the FIN-02 campaign. In contrast, 13.5 % of particles in the ice crystal training dataset achieve a depolarization ratio of at least 0.3. This natural break in the depolarization ratio distributions can be considered as a threshold for which particles above the threshold are ice. Below the threshold, the identity of particles is unknown since the majority of all three populations have depolarization ratios between 0 and 0.3.

20

3.4 Determining WDBT conditions in CFDC runs

As discussed in Ssection 2.45, WDBT can be difficult to identify when relying on the traditional analysis method. To better determine periods when WDBT conditions are occurring in the CFDC, particle size

25 distributions and mean depolarization ratio can be considered. In this manuscriptHere, the onset of water droplet breakthrough is analytically defined as the time period where a continuous size distribution extends from the small size bins past the 2 μm threshold. For example, we consider a CFDC run from the FIN-02 campaign where Snomax® aerosols were generated by atomization of suspensions and introduced

to the AIDA chamber at concentrations of ~2000 cm^{-3}. The CFDC was operated at -15 °C ± 1.5 °C, and scanned from low to high SS_w. A time series of the normalized size distribution is shown in Fig. 4a. Figures .s 4b and c show the mean depolarization ratio of all particles larger than 2 μm and the CFDC supersaturation (with respect to water and with respect to ice), respectively. In addition, supplemental Figure S1 shows the number lognormal size distribution of Snomax® aerosols generated during this sample period. No Snowmax particles greater than 2 μm diameter are present. Under normal operating conditions, such as those occurring during 10:45 to 11:55 CET (Central European Time Zone), the size distribution is clearly a bimodal distribution with an aerosol population at diameters of ~ 0.5 to 1.5 μm and the ice crystal population at diameters of ~3 to 25 μm. In the Fig. 4Fig., water droplet breakthrough is observed between 11:55 to 12:15 CET as the upper limit of the CASPOL size distribution mode increases from 1.5 to ~10 μm.

In Figure 4, the CFDC begins sampling at relatively low supersaturations. During this time period, the few ice crystals nucleate in the chamber as particles are mostly larger than 5 μm in diameter (Fig. 4a). Initially, there is a wide range of mean depolarization ratios reported. In Fig. 4b, Aas more ice crystals begin to grow in the chamber at higher SS_w (at -3% SS_w), the mean depolarization ratio becomes more uniform, with a range of ~ 0 to 0.22 before 10:45 to a range of ~ 0.09 to 0.12 after 10:45. These values are similar to, but slightly lower than the mean depolarization for training dataset ice crystals. Then at 11:55 CET (at 4 % SS_w) water droplet breakthrough initiates and the mean depolarization ratio decreases to approximately zero, consistent with the theoretical depolarization ratio of water droplets. This is similar to the low mean depolarization ratio of training dataset droplets. Taken together, these results show that the mean depolarization ratio of particles larger than 2 μm has a strong dependence on whether or not WDBT is occurring in the CFDC. This makes the mean depolarization ratio a useful tool for confirmation of the onset of water droplet breakthrough.

3.5 Optical properties of particles present in the CFDC

In this section, the frequency distribution of depolarization ratios of particle populations present in the CFDC are investigated for comparison to the training datasets. First, all data from the FIN-02 campaign

was classified as WDBT conditions or normal operating conditions. Then particle diameters were used to determine the particle type. Aerosol particles during the FIN-02 campaign were generally smaller than< 2 μm in size. Since water droplets can bias~~pollute~~ this population during WDBT conditions, only those particles smaller than~~that are <~~ 2 μm in diameter during normal operating conditions are defined as

5   aerosols. Particles ≥ 2 μm in diameter during normal operating conditions are identified as ice crystals. A third population is defined as "WDBT particles" and consists of particles ≥ 2 μm in diameter during WDBT conditions. This population typically consists of mostly water droplets, but can also include ice crystals. These three populations are referred to as "CFDC populations" in this manuscript.

Figure 5 shows the depolarization ratio distributions of the CFDC populations interpreted to be ice

10   crystals, water droplets, and aerosols. For the analysis completed to produce Fig. 5, 19 normal operating condition periods and 17 WDBT periods with variable time lengths were classified. Ice crystals achieve higher depolarization ratios than water droplets and aerosol. 13.5~~2~~ % of ice crystals in the CFDC achieve a depolarization ratio larger than> 0.3, compared to 1.5 % percent of water droplets and 0.3 % of aerosols. These values are very similar to the percentages of training data particles that achieve a depolarization

15   ratio greater than 0.3. Ice crystals achieve depolarization ratios larger than> 0.3 more than 10 times more frequently than aerosol or water droplets. One interesting feature in the CFDC observations are the two Snomax® cases (cases 13 and 14 in Table 1 at -33 °C and -21 °C respectively) in Fig. 5. More particles with high depolarization ratios were observed than during the other 15 WDBT cases. These particles are most likely ice crystals. Since Snomax® bacteria are a particularly active INP it is not surprising that ice

20   crystals dominate the population of particles in the CFDC even during WDBT (Wex et al., 2015), ~~particularly at~~ particularly for runs with lower temperatures~~colder temperatures of these runs~~.

3.6 Comparing CASPOL observations to model calculations

25

In this section, modeled and observed particles discussed in the preceding results section are compared. Fig. 6 shows modeled and observed mean depolarization ratios of particles as a function of diameter. The modeled results (green) are shown with the same shape conventions as Fig. 2. Observed results include

training (blue shapes) and CFDC (red shapes) ice crystals (pentagrams), aerosols (squares), and droplets/WDBT particles (circles). Observed values are accompanied by error bars representing the standard deviation of depolarization ratios of particles at the respective diameters plotted. The CFDC populations presented here include particles sampled from all FIN-02 experiments, and not only those discussed in Section 3.5 above. The same conventions are used here to process these particles: CFDC ice crystals are those larger than 2 μm sampled under normal operating conditions, CFDC aerosols are those smaller than 2 μm sampled under normal operating conditions, and CFDC WDBT particles are those larger than 2 μm sampled under WDBT conditions.

In Fig. 6, both the model calculations and the observed results indicate that ice crystals have higher mean depolarization ratios than water droplets and aerosols on average at diameters above 5 μm. However, error bars show that the standard deviations of depolarization ratios at these sizes are very large and that differences in the mean depolarization ratios of the observed particles displayed are not statistically significant from each other. This represents a major challenge in designing a new analysis method that uses depolarization ratio to quantify INP.

In Section 3.5, the complex WDBT population was discussed. WDBT particles consist of both water droplets and ice crystals. Diffusional growth theory dictates that ice crystals will grow to larger sizes in the CFDC than water droplets (Pruppacher and Klett, 2010). Fig. 6 shows an increase in the depolarization ratio from ~ 0 to 0.25 in the CFDC WDBT population region starting at ~6 μm. At diameters greater than> 10 μm the mean depolarization ratio of WDBT particles is greater than or equal to the depolarization of CFDC ice crystals and training dataset ice crystals suggesting that these large particles are mostly or all ice crystals. It is inferred that particles in the 6 to 10 μm range are a mixture of water droplets and ice crystals.

There are significant differences between modeled particles and their observed counterparts. Observations show water droplets apparently depolarizing light, but the observed mean depolarization ratio of water droplets is almost zero ($\delta \leq 0.05$). Another significant difference is that for both ice crystals and aerosols, the mean observed depolarization ratios are approximately 30% lower than the modeled depolarization ratio. One possible reason for the discrepancies between the model and observations is that the CASPOL depolarization detector underestimates the depolarization of particles due to the weak

90

depolarization of particles and relatively high detection limit of the CASPOL perpendicularly polarized detector. In general, particles scatter relatively little perpendicularly polarized light in the backward 1 raw count which translates roughly a scattering cross section of ~1 x10^{-13} cm^2. This limit results in the CASPOL registering a perpendicular signal below the CASPOL's detection limit for 45 % of training ice crystals, 76 % of training aerosols, and 57 % of training droplets. In the training data sets, all particles with undetected perpendicularly polarized detector were assigned depolarization ratio of zero. Another possibility is that the idealized model particles do not accurately depict the shape, composition, or other microphysical properties of the observed particles. Smith et al. (2016) found that after an ice crystal has nucleated, the geometry of the ice crystal can be modified leading to drastic differences in the observed depolarization ratio. To investigate this, Smith et al. (2016) operated the Manchester Ice Cloud Chamber at different temperatures and supersaturations to produce an assortment of ice crystal morphologies including solid and hollow columns, plates, sectored plates and dendrites. During that study, Smith et al. (2016)they also compared observed and modeled depolarization ratio results and found that on average the difference between modeled and observed depolarization ratios was ~120% (2016). The CFDC results reported in Fig. 6 include data from all of the runs sampled during FIN-02. The data set of the campaign represents ice nucleation events over a broad range of temperature (-15 °C to -35 °C) and supersaturation (0 % to 40 % SS$_i$) conditions. Thus, many different habits of ice crystals likely formed in the CFDC, in part, contributing to the wide range of depolarization ratios reported in Fig. 6. Nicolet et al. (2007) reported modeling results of single-particles that confirm that a wide range of depolarization ratios can be detected for a single shape depending on the orientation. Non-preferential orientation of particles in the CFDC is likely to contribute to the breadth of depolarization ratios detected.

The observations are qualitatively consistent with the model in that ice crystals depolarize more light than water droplets and aerosols. However, the discrepancies between the observed and modeled mean depolarization ratios and the wide distributions of observed depolarization ratios dictate that we cannot rely on a mean modeled depolarization ratio to identify and quantify ice crystals in the CFDC. Rather than designing a theoretical model based on model calculations, we move forward by designing an empirical model based on the CASPOL observed signals.

3.7 Designing an empirical model to quantify INP with depolarization ratio

The results above show that counting ice crystals in the CFDC using depolarization ratio can be challenging since only ~13.5 % of ice crystals achieve a depolarization ratio greater than 0.3 (Fig. 3). A depolarization ratio threshold of 0.3 is a favorable criterion to detect ice crystals because less than 2% of the water droplets and aerosols achieve this depolarization ratio. However, when there are extreme concentrations of water droplets, such as those experienced during water droplet breakthrough conditions, the water droplet concentration may be 10^3 times greater than the ice crystal concentration in the CFDC effectively reducing the signal (ice crystals) to noise (water droplets with $\delta \geq 0.3$) ratio ~1:1 or worse. Therefore, an INP concentration cannot be determined by simply applying a depolarization ratio criterion to detect ice crystals with the CFDC-CASPOL.

To obtain a more accurate INP concentration, we used a linear regression model to fit the number of particles with depolarization ratios above the threshold (0.3) to the number of ice crystals in the CFDC. Linear regressions are frequently used to interpret the signal(s) of new instrumentation or new techniques by validating the signal with a "ground truth" measurement (e.g. Li et al., 2016; Zimmerman et al., 2017; Brunner et al., 2015; Choi et al., 2016).

In our case, ground truth is provided by the aerosol-only (Storm Peak), ice-only (homogeneous) and droplet-only (VOAG) training data populations discussed above. To create a linear regression model which relates the number of particles with depolarization ratios above the threshold (0.3) to ice crystals concentration, CASPOL data set containing a known number of ice crystal and non-ice particles is required. Here, aerosol-only, ice-only, and droplet-only data are added together to create artificial data sets in which the number of each type of particle is known. The aerosol, ice crystal, and droplet training datasets are randomized in time before particles are selected from each population to create the simulated datasets. (This analysis is possible because the data point for each individual particle detected by the CASPOL includes forward scattering, backward scattering and depolarization).

In total fifty simulated datasets are generated. Supplemental Table 1 summarizes the concentration of ice crystals, water droplets and aerosols in each dataset. Each simulated dataset is divided into 120 segments, containing a number of ice crystals ranging from 0 to 350. The number of water droplets and aerosols are constant throughout all segments in a single dataset. All 50 data sets contain segments with

the same number of randomly selected ice crystals. The upper range of M values here represents an extreme sampling condition where there are many aerosols and many cloud condensation nuclei that will form cloud droplets, but few INP. Given the relatively high number of aerosols and droplets, this would represent the most challenging sampling scenario for proposed new method.

5   The quantity of aerosols and water droplets in each dataset is determined by a multiplication factor M, such that the number of water droplets = $100M$ and the number of aerosols = $300M$. For example, the first simulated data set ($M = 1$) contains 100 water droplets and 300 aerosols. For each iteration, M is increased by 1. In summary, 50 data sets were generated containing 100 to 5,000 water droplets and 300 to 15,000 aerosol particles.

10   As discussed above, particles in the INP data sets smaller than the CFDC size cut of 2 μm diameter were removed. Next, for each of the 120 segments in the simulated dataset, the number of particles with a depolarization ratio greater than or equal to a selected depolarization ratio threshold (ranging from 0 to 0.75 in increments of 0.05) is determined. A linear fit is determined for the relationship between the known ice crystal concentration and the number of particles detected greater than or equal to the depolarization ratio threshold for the first dataset ($M = 1$). The linear regression fit is applied to all of the

15   simulated datasets over the entire range of M. Only one fit is determined for each threshold because we cannot feasibly design a model that adapts to water droplet and aerosol concentration in the CFDC An R^2 value is determined to assess the goodness of the linear regression fit over all of the simulated datasets.

    Figure 7 shows the R^2 values as a function of M and depolarization ratio threshold for each of the

20   simulated datasets. The figure reveals that high choices of depolarization ratio thresholds perform poorly, since because very few particles will achieve a high depolarization ratio. In contrast, the figure shows that R^2 values are quite high for cases where aerosol and droplet concentrations are low and the depolarization ratio threshold is low. However, as the concentration of droplets and aerosol increase, the R^2 value for a given threshold decreases. This is especially true for lower depolarization ratio thresholds

25   that are more sensitive to increases in droplets and aerosols. An optimal choice for depolarization ratio threshold is defined as a threshold that retains high R^2 values across the entire range of M. The threshold should be chosen such that it is sufficiently high that it's not sensitive water droplets and aerosols that may be highly depolarizing and low enough that particles are still detected. Figure 7 shows that a threshold

value of 0.35 out performs all other thresholds when *M* is larger than 20, including our initial visually chosen threshold value of 0.3. The mean R^2 value for the 0.35 threshold is 0.46. The next best performing threshold is 0.3 with a mean R^2 value of 0.44. However, aerosol and water droplet concentrations in CFDC experiments are typically in the range $1 < M < 20$. The mean R^2 value in this range of *M* for the 0.3

5   and 0.35 thresholds 0.71 and 0.7 respectively. While the performance of these thresholds perform comparably over this range, we selected the 0.3 threshold because it will slightly outperform the 0.35 threshold, especially when detecting lower INP concentrations.

The linear regression for the 0.3 threshold is provided in Eq. 9,

$$N_{INP} = 6.11 \, N_\delta + 22.20 \qquad\qquad (9)$$

10   where N_δ is the number of particles that have a depolarization ratio greater than 0.3 and N_{INP} is the derived INP number. Next, Eq. 9 is applied to all CFDC-CASPOL data collected during the FIN-02 campaign, and the accuracy of this model is assessed.

3.8 Application of the new analysis method to CFDC data collected during FIN-02

15

INP concentrations were obtained using both the depolarization ratio method (Eq. 9) and the traditional method on CFDC data collected during the FIN-02 campaign. Three representative CFDC runs of Snomax® at -15 °C and at -20 °C and Arizona Test Dust at -25 °C are shown in Fig. 8. Each humidity scan starts in subsaturated conditions with respect to water. Supersaturation is gradually increased until ice

20   nucleation initiates and then further increased until WDBT occurs (represented by the red symbolspoints in Fig. 8b). The reported concentrations reveal that the traditional (circles) and depolarization ratio (*) methods generally agree during "ice only" periods (blue symbols in Fig. 8). The reported concentrations reveal that the traditional and depolarization ratio methods generally agree during "ice only" periods (blue symbols in Fig. 8b). In most cases there is clear disagreement between concentrations in WDBT periods,

25   for example in the cases of Snomax® at -15 °C and Arizona Test Dust at -25 °C. This is expected since the traditional concentration is sensitive to an increase in water droplets that grow larger than the size cut

applied in WDBT conditions, where INP concentrations are usually not reported. An exception to this can be seen in Fig. 8b, the Snomax® at -20 $^{\circ}$C. The concentrations from the two methods remain in good agreement as the supersaturation is increased into the WDBT period. In this case, the ice crystal concentration is dominating the population in WDBT. The evidence for this is the high concentration of

5   ice crystals that from ~~orm the period that starts around~~ 13:15 CET as observed in the size distribution time series i~~n bottom pane~~nl ~~of~~ center panel Fig. 8b~~8b~~.

Fig. 9 summarizes the mean concentrations obtained through the traditional and new method for all periods when the CFDC was operational during FIN-02. In total, 27 "ice only" periods and WDBT cases are included. A description of the date and time, aerosol composition, and temperature of each case is

10   detailed in Table 1. In cases 24, 25, and 26 WDBT did not occur, so no data is reported. The error bars report the CFDC-CASPOL uncertainty in INP concentration, which is 39% based on combined instrumental uncertainties (Glen and Brooks, 2014 & 2013), Fig. 9 shows that in all but 4 cases out of 27 (cases 2, 7, 9, and 23), the mean concentration of the new analysis method is in agreement with traditional analysis method for the "ice only" periods. Fig. 9 also shows that only 9 out of 24 WDBT cases have

15   statistical agreement between the new and traditional analysis method. At the onset of WDBT, the impact of water droplets on the INP concentration determined by the 2 μm size cut may not be very large and the concentration may closely resemble the true INP concentration, but as the SS_w is increased more water droplets will be incorrectly counted in the traditional INP concentration. This phenomenon gives rise to the large error bars reported in some of the WDBT cases. In general, the observations reported in Fig. 9

20   are consistent with the assertion that the traditional method and new method are in agreement during the "ice only" periods, and that during WDBT the traditional method is elevated in response to large water droplets miscounted as ~~polluting the~~ INP ~~concentration~~ while the depolarization ratio method remains accurate.

To summarize the comparison between our new method and the traditional method during the "ice

25   only" periods, the INP concentrations determined using the traditional method vs. new method are plotted in Fig. 10~~a~~. Each point on the plot represents data for a 1-minute segment. The black line in Fig. 10 is a 1:1 line. Since the analysis used to generate Fig. 10 only uses data collected under normal operating conditions (not WDBT), the traditional concentration can be considered ground truth. The data closely

follows the 1:1 line, confirming that the depolarization ratio can be used to reliably retrieve an INP concentration when no or few water droplets/aerosols are larger than 2 µm. To assess the performance of the new method we use mean percent error (MPE) defined here as:

$$MPE = \frac{New\ Concentration - Traditonal\ Concentration}{Traditional\ Concentration} \times 100\% \qquad (10)$$

5

The mean percent error of the method is dependent on the INP concentration. Due to the high detection limit of concentration for the CASPOL, the mean percent error of the new method is ±500% when the traditional concentration is between 0 and 50,000 L^{-1}. However, at higher concentrations the MPE is typically ± 50 % or less. Additionally, Fig. 10 shows that at concentrations in the range 0 to 3×10^6 L^{-1}, the new method typically undercounts INPs, but over counts INPs at higher concentrations (greater than> 3×10^6 L^{-1}). The mean percent error for the new method for all concentrations is ± 32.1 %.

Based on Fig. 10, the new analysis method provides very accurate results when INP concentrations are greater than 50,000 L^{-1}, which is only achievable in laboratory settings. For this reason, the method is not suitable to be used in a field setting where concentrations typically range from 0.1 to 100 L^{-1} (e.g. Mason et al., 2016; Jiang et al., 2015; DeMott et al., 2003; Kanji et al. 2017). Nonetheless, the new method is considered an improvement for use during water droplet breakthrough, when the traditional method cannot be used.

As a final test of the new method during water droplet breakthrough periods, a reliable measure of INP at higher supersaturation conditions (when the TAMU CFDC is experiencing WDBT) is needed. Due to design and flow rate differences, the Colorado State University (CSU) CFDC does not experience the onset of WDBT until higher supersaturations than the TAMU CFDC, up to 108% or higher depending on temperature (DeMott et al., 2015). Thus, inclusion of the CSU data provides a test of the new method at higher relative humidities under conditions when data obtained through the TAMU CFDC's traditional method is spurious due to water droplet breakthrough. Fig. 11 shows the comparison of the TAMU CFDC's traditional (2 µm size cut) and new method INP concentrations and the CSU CFDC INP

concentration, collected during the FIN-02 campaign. Because CASPOL sizing of nonspherical ice crystals nucleated and grown in the chamber is uncertain, the data was also analyzed using a 5 μm size cut to provide an estimate of the lower limit of INP concentration. As discussed above, the CSU CFDC has a longer chamber, a different evaporation region design, a different detector, and a chosen size cut of

5   3 μm. Results of INP percent activated are reported from three CFDC runs discussed earlier including Snomax® at -15 °C and -20 °C and Arizona test dust at -25 °C. Concentrations used to calculate the percent activation are average concentrations of samples in a 1% range of SS_w conditions in the CFDC. Though not previously discussed in the manuscript, a 5 μm size cut has also been used to report an INP concentration for the TAMU CFDC and is used here to provide an upper estimate for the INP

10 concentration. Large symbols show data collected under normal operating conditions. Small symbols show data collected during WDBT conditions in the TAMU CFDC. The CSU CFDC did not experience WDBT in the data reported in Fig. 11. The traditional concentration from TAMU and CSU and the new method concentration all are in reasonable agreement during "ice only" conditions for all three cases. During WDBT, the TAMU traditional concentrations increase in response to the water droplets that grow

15 larger than the size criteria (2 μm or 5 μm). FortunatelyHowever, the new method remains in agreement with the CSU concentration. Fig. 11b shows thea special case of mentioned in previous discussion that has high activation of INP shown in Figure 8b. This case involves a highly active INP, Snomax® at -20 °C, a significantly colder temperature than required for the Snomax® to activate as INP. In this case Since most particles activated prior to the onset of WDBT, there is negligible difference in the concentrations

20 reported during "ice only" and WDBT periods since most particles activated prior to the onset of WDBT. In conclusion, the new method accurately determines the INP concentration in the presence of water droplets and can thus extend the range of operating conditions of the TAMU CFDC.

4. Conclusions

25

This manuscript presents a new analysis method that uses depolarization ratio to quantify INP concentrations in the TAMU CFDC using single-particle depolarization measured by the CFDC's CASPOL detector. This paper presents a new analysis method that uses the depolarization ratio to

quantify INP concentrations in the TAMU CFDC in terms of single-particle depolarization measured by the CFDC's CASPOL detector. Ice crystal, droplet and aerosol training populations were used to build simulated datasets with known concentrations of aerosols, droplets, and ice crystals. The simulated datasets were evaluated ~~determine an optimal~~ depolarization ratio threshold of 0.3 ~~observed by the CFDC CASPOL~~ above which all particles were classified as ice crystals. A linear regression fit ~~between ice~~ between ice crystal concentration and ~~the~~ number of particles detected greater than or equal to the depolarization ratio threshold of 0.3 ~~was trained on~~ was determined ~~simulated CFDC dataset using the 0.3 threshold~~ and applied to CFDC data collected during the FIN-02 campaign. Concentrations of INP determined by the new analysis method agree reasonably well with the traditional method (ice detection by size-segregation) under normal operating temperatures and supersaturations (with no large water droplets present) with a mean percent error of $\pm$32.1 %. However, at INP concentrations less than $<$50,000 L^{-1}, the mean percent error of the new method is greater than$>$ 500 % due to a high concentration detection limit of the CASPOL. While high INP concentrations of 10^4 to 10^6 L^{-1} can be generated in laboratory settings, typical ambient INP concentrations range from 0 to 100 L^{-1}. For this reason, the new CASPOL depolarization method is recommended for CFDC laboratory experiments only. A comparison between the CSU CFDC INP concentration and TAMU CFDC INP concentration derived from the new analysis method show agreement even under conditions in which the TAMU CFDC experiences WDBT and CSU does not experience WDBT. We conclude that the new method can be used to extend the range of operating conditions in the CFDC. However, under conditions encountered in field studies, the traditional method is still preferred analysis method for counting ice nucleating crystals with the TAMU CFDC.

5

References

Amato, P., Joly, M., Schaupp, C., Attard, E., Möhler, O., Morris, C. E., Brunet, Y., and Delort, A.-M.: Survival and ice nucleation activity of bacteria as aerosols in a cloud simulation chamber, Atmos. Chem. Phys., 15, 6455-6465, 2015.

Atkinson, J. D., Murray, B. J., Woodhouse, M. T., Whale, T. F., Baustian, K. J., Carslaw K. S., Dobbie S., O'Sullivan, D., and Malkin, T. L.: The importance of feldspar for ice nucleation by mineral dust in mixed-phase clouds, Nature, 498(7454), 355-358, 2013.

Bailey, M. P., and J. Hallett: A comprehensive habit diagram for atmospheric ice crystals: Confirmation from the laboratory, AIRS II, and other field studies, J. Atmos. Sci., 66(9), 2888-2899, 2009.

Bi, L., P. Yang, G. W. Kattawar, and M. I. Mishchenko: Efficient implementation of the invariant imbedding T-matrix method and the separation of variables method applied to large nonspherical inhomogeneous particles, J. Quant. Spectrosc. Radiat. Transfer, 116, 169-183, 2013.

Bi, L., and Yang, P.: Accurate simulation of the optical properties of atmospheric ice crystals with the invariant imbedding T-matrix method, J. Quant. Spectrosc. Radiat. Transfer 138, 17-35, 2014.

Bohren. C.F.; Huffman, D.R.:Absorption and Scattering of Light by Small Particles. John W. Wiley and Sons, Inc. : 1983.

Boucher, O., Randall, D., Artaxo, P., Bretherton, C., Feingold, G., Forster, P., Kerminen, V.M., Kondo, Y., Liao, H., Lohmann, U. and Rasch, P.: Clouds and Aerosols, in Climate Change: The Physical Science Basis. Contribution of Working Group I to the Fifth Assessment Report of the Intergovernmental Panel on Climate Change, Cambridge University Press, Cambridge, United Kingdom and New York, NY, USA. 571-657, 2013.

Brooks, S. D., Toon, O. B., Tolbert, M. A., Baumgardner, D., Gandrud B. W., Browell E. V., Flentje, H., and Wilson, J. C.:, Polar stratospheric clouds during SOLVE/THESEO: Comparison of lidar observations with in situ measurements, J. Geophys. Res.-Atmos., 109(D2), 2004.

Brooks, S. D., Suter, K., & Olivarez, L.: Effects of chemical aging on the ice nucleation activity of soot and polycyclic aromatic hydrocarbon aerosols, J. Phys. Chem. A, 118(43), 10036-10047, 2014.

Brunner, J., Pierce, R. B., and Lenzen, A.: Development and validation of satellite-based estimates of surface visibility, Atmos. Meas. Tech., 9, 409-422, https://doi.org/10.5194/amt-9-409-2016, 2016.

Choi, M., Kim, J., Lee, J., Kim, M., Park, Y.-J., Jeong, U., Kim, W., Hong, H., Holben, B., Eck, T. F., Song, C. H., Lim, J.-H., and Song, C.-K.: GOCI Yonsei Aerosol Retrieval (YAER) algorithm and validation during the DRAGON-NE Asia 2012 campaign, Atmos. Meas. Tech., 9, 1377-1398, 2016.

Clauss, T., Kiselev, A., Hartmann, S., Augustin, S., Pfeifer, S., Niedermeier, D., Wex, H., and Stratman, F.: Application of linear polarized light for the discrimination of frozen and liquid droplets in ice nucleation experiments, Atmos. Meas. Tech., 6(4), 1041-1052, 2013.

Collier, K. N., and Brooks, S. D., Role of organic hydrocarbons in atmospheric ice formation via contact freezing, J. Phys. Chem. A, 120(51), 10169–10180, 2016.

Coluzza, I., Creamean, J., Rossi, M. J., Wex, H., Alpert, P. A., Bianco, V., Y. Boose, C. Dellago, L. Felgitsch, J. Fröhlich-Nowoisky, H. Herrmann, S. Jungblut, Z.A. Kanji, G. Menzl, B. Moffett, C. Moritz, A. Mutzel, U. Pöschl, M. Schauperl, J. Scheel, E. Stopelli, F. Stratmann, H. Grothe, and D. Schmale III. Perspectives on the Future of Ice Nucleation Research: Research Needs and Unanswered Questions Identified from Two International Workshops. Atmosphere, 8(8), 138, 2017.

Creamean, J. M., Suski, K. J., Rosenfeld, D., Cazorla, A., DeMott, P.J., Sullivan, R.C., White, A. B., Ralph, F.M., Minnis P., and Comstock, J.M.: Dust and biological aerosols from the Sahara and Asia influence precipitation in the western US, Science, 339(6127), 1572-1578, 2013.

Cziczo, D. J., Ladino, L., Boose, Y., Kanji, Z. A., Kupiszewski, P., Lance, S., Mertes, S., and Wex, H.: Measurements of Ice Nucleating Particles and Ice Residuals, Meteor. Mon., 58, 8.1-8.13, 2017.

De Boer, G., Morrison, H., Shupe, M., and Hildner, R.: Evidence of liquid dependent ice nucleation in high-latitude stratiform clouds from surface remote sensors, Geophys. Res. Lett., 38(1), 2011.

DeMott, P. J., Sassen, K., Poellot, M.R., Baumgardner, D., Rogers, D. C., Brooks, S. D., Prenni, A. J., and Kreidenweis, S. M.: African dust aerosols as atmospheric ice nuclei, Geophys. Res. Lett., 30(14), 2003.

DeMott, P. J., Möhler, O., Stetzer, O., Vali, G., Levin, Z., Petters, M. D., Murakam, M., Leisner, T., Bundke, U., Klein, H., Kanji, Z., Cotton, R., Jones, H., Petters, M., Prenni, A., Benz, S., Brinkmann, M., Rzesanke, D., Saathoff, H., Nicolet, M., Gallavardin, S., Saito, A., Nillius, B., Bingemer, H., Abbatt, J., Ardon, K., Ganor, E., Georgakopoulos, D. G., and Saunders, C.: Resurgence in ice nucleation research. Bull. Amer. Meteor. Soc., **92**, 1623-1635, 2011.

DeMott, P. J., Prenni, A. J., McMeeking, G. R., Sullivan, R. C., Petters, M. D., Tobo, Y., Niemand, M., Möhler, O., Snider, J. R., and Wang, Z.: Integrating laboratory and field data to quantify the immersion freezing ice nucleation activity of mineral dust particles, Atmos. Chem. Phys., 15(1), 393-409, 2015.

DeMott, P. J., Hill, T. C., McCluskey, C. S., Prather, K. A., Collins, D. B., Sullivan, R. C., Ruppel, M. J., Mason, R. H., Irish, V. E., and Lee, T.: Sea spray aerosol as a unique source of ice nucleating particles, P. Natl. Acad. Sci.,113(21), 5797-5803, 2016.

DeMott, P. J. et al., Overview of results from the Fifth International Workshop on Ice Nucleation, Part 2 (FIN-02): Laboratory intercomparisons of ice nucleation measurements, in preparation for submission to Atmos. Chem. Phys., 2017.

Durant, A. J., and Shaw, R. A.: Evaporation freezing by contact nucleation inside-out, Geophys. Res. Lett., 32(20), 2005.

Fornea, A. P., Brooks, S. D., Dooley, J. B., and Saha, A.: Heterogeneous freezing of ice on atmospheric aerosols containing ash, soot, and soil, J. Geophys. Res.-Atmos., 114(D13), 2009.

Garimella, S., Kristensen, T., Ignatius, K., Welti, A., Voigtländer, J., Kulkarni, G., Sagan, F., Kok, G., Dorsey, J., and Nichman, L.: The SPectrometer for Ice Nuclei (SPIN): An instrument to investigate ice nucleation, Atmos. Meas. Tech. Discuss. 9(7), 278, 2016.

Glen, A., and Brooks, S. D.: A new method for measuring optical scattering properties of atmospherically relevant dusts using the Cloud and Aerosol Spectrometer with Polarization (CASPOL), Atmos. Chem. Phys., 13(3), 1345-1356, 2013.

Glen, A., and Brooks, S.D.: Single particle measurements of the optical properties of small ice crystals and heterogeneous ice nuclei, Aerosol Sci. Tech., 48(11), 1123-1132, 2014.

Glen, A.: The development of measurement techniques to identify and characterize dusts and ice nuclei in the atmosphere. Diss. Texas A&M University, 2014.

Hecht E, Zajac A: Optics 4th (International) edition. Addison Wesley Publishing Company, 2002.

Hoose, C., and Möhler, O.: Heterogeneous ice nucleation on atmospheric aerosols: a review of results from laboratory experiments, Atmos. Chem. Phys., 12(20), 9817-9854, 2012.

Hu, Y., Winker, D., Vaughan, M., Lin, B., Omar, A., Trepte, C., Flittner, D., Yang, P., Nasiri, S. L., and Baum, B.: CALIPSO/CALIOP cloud phase discrimination algorithm, J. Atmos. Ocean Tech., 26(11), 2293-2309, 2009.

Jiang, H., Yin, Y., Yang, L., Yang, S., Su, H., and Chen, K.: The characteristics of atmospheric ice nuclei measured at different altitudes in the Huangshan Mountains in Southeast China, Adv. Atmos. Sci., 31(2), 396 0256-1530, 2014.

Johnson, B. R.: Invariant imbedding T matrix approach to electromagnetic scattering, Appl. Optics, 27(23), 4861-4873, 1988.

Kanji, Z.A., Ladino, L., Wex, H., Boose, Y., Burkert-Kohn, M., Cziczo, D.J., and Krämer, M.: Overview

of Ice Nucleating Particles, Meteor. Mon., 58, 1.1-1.33, 2017

Koepke, P., Gasteiger, J., and Hess, M.: Technical Note: Optical properties of desert aerosol with non-spherical mineral particles: data incorporated to OPAC, Atmos. Chem. Phys., 15(10), 5947-5956, 2015.

5

Korolev, A.: Limitations of the Wegener–Bergeron–Findeisen mechanism in the evolution of mixed-phase clouds. J. Atmos. Sci., 64(9), 3372-3375, 2007.

10 Levin, E., McMeeking, G., DeMott, P., McCluskey, C., Carrico, C., Nakao, S., Jayarathne, T., Stone, E., Stockwell, C., and Yokelson, R.: Ice-nucleating particle emissions from biomass combustion and the potential importance of soot aerosol, J. Geophys. Res.-Atmos., 121(10), 5888-5903, 2016.

Li, S., Joseph, E., and Min, Q.: Remote sensing of ground-level PM2. 5 combining AOD and
15 backscattering profile, Remote Sens. Environ., 183, 120-128, 2016.

Linke, C., Möhler, O., Veres, A., Mohacsi, A., Bozóki, Z., Szabó, G., and Schnaiter, M.: Optical properties and mineralogical composition of different Saharan mineral dust samples: a laboratory study, Atmos. Chem. Phys., 6(11), 3315-3323, 2006.

20

Liu, C., Panetta, R. L., Yang, P., Macke, A., and Baran, A. J.: Modeling the scattering properties of mineral aerosols using concave fractal polyhedra, Appl. Optics, 52(4), 640-652, 2013.

Mason, R. H., Si, M., Chou, C., Irish, V., Dickie, R., Elizondo, P., Wong, R., Brintnell, M., Elsasser, M.,
25 and Lassar, W.: Size-resolved measurements of ice-nucleating particles at six locations in North America and one in Europe, Atmos. Chem. Phys., 16(3), 1637-1651, 2016.

Marcolli, C.: Deposition nucleation viewed as homogeneous or immersion freezing in pores and cavities, Atmos. Chem. Phys., 14, 2071–2104, 2014.

30

McCluskey, C. S., DeMott, P. J., Prenni, A. J., Levin, E. J., McMeeking, G. R., Sullivan, A. P., Hill, T. C., Nakao, S., Carrico, C. M., and Kreidenweis, S. M.: Characteristics of atmospheric ice nucleating particles associated with biomass burning in the US: Prescribed burns and wildfires, J. Geophys. Res.-Atmos., 119(17), 10458-10470, 2014.

35

McCluskey, C. S., Hill, T. C., Malfatti, F., Sultana, C. M., Lee, C., Santander, M. V., Beall, C. M., Moore, K. A., Cornwell, G. C., and Collins, D. B.: A dynamic link between ice nucleating particles released in nascent sea spray aerosol and oceanic biological activity during two mesocosm experiments, J. Atmos. Sci., 74.1, 151-166, 2016.

40

McFarquhar, G. M., Ghan, S., Verlinde, J., Korolev, A., Strapp, J.W., Schmid, B., Tomlinson, J., Wolde, M., Brooks, S.D., Collins, D., Cziczo, D., Dubey, M., Fan, J. D., Flynn, C., Gultepe, I., Hubbe, J., Gilles.

M., Kok, G., Laskin, A., Lawson, P., Liu, P., Liu, X., Lubin, D., Mazzoleni, C., Macdonald, A., Moffet, R., Morrison, H., Ovtchinnikov, M., Ronfeld, D., Shupe, M., Turner, D., Xie, S., Zelenyuk, A., and Glen, A.: Indirect and Semi-Direct Aerosol Campaign (ISDAC): The impact of arctic aerosols on clouds, Bull. Amer. Meteor. Soc., 92(2), 183-201, 2011.

Mishchenko, M. I., and Sassen, K.: Depolarization of lidar returns by small ice crystals: An application to contrails, Geophys. Res. Lett., 25, 309-312, 1998.

Murray, B., O'sullivan, D., Atkinson, J., and Webb, M.: Ice nucleation by particles immersed in supercooled cloud droplets, Chem. Soc. Rev., 41(19), 6519-6554, 2012.

Nicolet, M., Stetzer, O., and Lohmann, U.: Depolarization ratios of single ice particles assuming finite circular cylinders, Appl. Optics 46.20: 4465-4476, 2007.

Nicolet, M., Stetzer, O., Lüönd, F., Möhler, O., and Lohmann, U.: Single ice crystal measurements during nucleation experiments with the depolarization detector IODE, Atmos. Chem. Phys., 10(2), 313-325, 2010.

Niemand, M., Möhler, O., Vogel, B., Vogel, H., Hoose, C., Connolly, P., Klein, H., Bingemer, H., DeMott, P., and Skrotzki, J.: A particle-surface-area-based parameterization of immersion freezing on desert dust particles, J. Atmos. Sci., 69, 3077-3092, 2012.

Noel, V., and Sassen, K.: Study of planar ice crystal orientations in ice clouds from scanning polarization lidar observations, J. Appl. Meteorol., 44, 653-664, 2005.

Pinto, J. O.: Autumnal mixed-phase cloudy boundary layers in the Arctic. J. Atmos. Sci., 55(11), 2016-2038, 1998.

Pithan, F., Medeiros, B., & Mauritsen, T.: Mixed-phase clouds cause climate model biases in Arctic wintertime temperature inversions. Clim. Dynam., 43(1-2), 289-303, 2014.

Prenni, A., Tobo, Y., Garcia E., DeMott, P., Huffman J., McCluskey, C., Kreidenweis, S., Prenni, J., Pöhlker, C., and Pöschl, U.: The impact of rain on ice nuclei populations at a forested site in Colorado, Geophys. Res. Lett., 40(1), 227-231, 2013.

Pruppacher, H. R., and Klett, J. D.: Microphysics of Clouds and Precipitation, Second revised and expanded edition, Springer Science & Business Media, 2010.

Richardson, M. S., DeMott, P. J., Kreidenweis, S. M., Cziczo, D. J., Dunlea, E. J., Jimenez, J. L., Thomson, D. S., Ashbaugh, L. L., Borys, R. D., Westphal, D. L. and Casuccio, G. S.: Measurements of heterogeneous ice nuclei in the western United States in springtime and their relation to aerosol characteristics. J. Geophys. Res., 112(D2), 2007.

Rogers, D. C.: Development of a continuous flow thermal gradient diffusion chamber for ice nucleation studies, Atmos. Res., 22(2), 149-181, 1988.

5   Rogers, D. C., DeMott, P. J., Kreidenweis, S. M., and Chen, Y.: A continuous-flow diffusion chamber for airborne measurements of ice nuclei, J. Atmos. Ocean Tech., 18(5), 725-741, 2001.

Schnaiter, M., Järvinen, E., Vochezer, P., Abdelmonem, A., Wagner, R., Jourdan, O., Mioche, G., Shcherbakov, V. N., Schmitt, C. G., and Tricoli, U.: Cloud chamber experiments on the origin of ice 10   crystal complexity in cirrus clouds, Atmos. Chem. Phys., 16(8), 5091-5110, 2016.

Smith, H. R., Connolly, P. J., Webb, A. R., and Baran, A. J.: Exact and near backscattering measurements of the linear depolarisation ratio of various ice crystal habits generated in a laboratory cloud chamber, J. Quant. Spectrosc. Radiat. Transfer, 178, 361-378.

15

Tan, I., Storelvmo, T., & Zelinka, M. D.: Observational constraints on mixed-phase clouds imply higher climate sensitivity. Science, 352(6282), 224-227, 2016.

Vali, G. (1985), Nucleation terminology, Bull. Amer. Meteorol., 66, 1426-1427, 1985.
20

Vali, G., DeMott, P. J., Möhler, O., and Whale, T. F.: Technical Note: A proposal for ice nucleation terminology, Atmos. Chem. Phys., 15, 10263–10270, 2015.

Volten, H., Munoz, O., Rol, E., Haan, J. D., Vassen, W., Hovenier, J., Muinonen, K., and Nousiainen, T.: 25   Scattering matrices of mineral aerosol particles at 441.6 nm and 632.8 nm, J. Geophys. Res.-At mos., 106(D15), 17375–17401, 2001

Wagner, R., Ajtai, T., Kandler, K., Lieke, K., Linke, C., Müller, T., Schnaiter, M., and Vragel, M.: Complex refractive indices of Saharan dust samples at visible and near UV wavelengths: a laboratory 30   study, Atmos. Chem. Phys., 12, 2491–2512, 2012.

Wagner, R., Höhler, K., Möhler, O., Saathoff, H., and Schnaiter, M.: Crystallization and immersion freezing ability of oxalic and succinic acid in multicomponent aqueous organic aerosol particles, Geophys. Res. Lett., 42(7), 2464-2472, 2015.

35

Warren, S. G., and Brandt, R. E.: Optical constants of ice from the ultraviolet to the microwave: A revised compilation. J. Geophys. Res., 113(D14220), 2008.

Wendisch, M., Pilewskie, P., Pommier, J., Howard, S., Yang, P., Heymsfield, A. J., Schmitt, C. G., 40   Baumgardner, D., and Mayer, B.: Impact of cirrus crystal shape on solar spectral irradiance: A case study for subtropical cirrus, J. Geophys. Res.-Atmos., 110, 2156-2202, 2005.

Wex, H., Augustin-Bauditz, S., Boose, Y., Budke, C., Curtius, J., Diehl, K., Dreyer, A., Frank, F., Hartmann, S., and Hiranuma, N.: Intercomparing different devices for the investigation of ice nucleating particles using Snomax® as test substance, Atmos. Chem. Phys., 15(3), 1463-1485, 2015.

5   Wylie, D. P., and Menzel, W. P.: Eight years of high cloud statistics using HIRS. J. Climate, 12, 170–184, 1999.

Xu, G., Sun,, B., Brooks, S. D., Yang P., Kattawar G. W., and Zhang, X.: Modeling the inherent optical properties of aquatic particles using an irregular hexahedral ensemble, J. Quant. Spectrosc. Ra., 191, 30-
10   39, 2017.

Yakobi-Hancock, J., Ladino, L., and Abbatt, J.: Feldspar minerals as efficient deposition ice nuclei, Atmos. Chem. Phys., 13(22), 11175-11185, 2013.

15   Yang, P., and Liou, K.: Geometric-optics–integral-equation method for light scattering by nonspherical ice crystals, Appl. Optics, 35(33), 6568-6584, 1996.

Yang, P., Bi, L., Baum, B. A., Liou, K.-N., Kattawar, G. W., Mishchenko, M. I., and Cole, B.: Spectrally consistent scattering, absorption, and polarization properties of atmospheric ice crystals at wavelengths
20   from 0.2 to 100 μ m, J. Atmos. Sci., 70(1), 330-347, 2013.

Yang, P., Liou, K.-N., Bi, L., Liu, C., Yi, B., and Baum, B. A.: On the radiative properties of ice clouds: Light scattering, remote sensing, and radiation parameterization, Adv. Atmos. Sci., 32, 32-63, 2015.

25   Yoshida, R., Okamoto, H., Hagihara, Y., and Ishimoto, H.: Global analysis of cloud phase and ice crystal orientation from Cloud Aerosol Lidar and Infrared Pathfinder Satellite Observation (CALIPSO) data using attenuated backscattering and depolarization ratio, J. Geophys. Res.-Atmos., 115(D4), 2010.

Zhang, Y., Macke, A., and Albers, F.: Effect of crystal size spectrum and crystal shape on stratiform cirrus
30   radiative forcing, Atmos. Res., 52(1–2), 59-75, 1999.

Zimmerman, N., Presto, A. A., Kumar, S. P. N., Gu, J., Hauryliuk, A., Robinson, E. S., Robinson, A. L., and Subramanian, R.: Closing the gap on lower cost air quality monitoring: machine learning calibration models to improve low-cost sensor performance, Atmos. Meas. Tech. Discuss.,
35   https://doi.org/10.5194/amt-2017-260, in review, 2017.

Zolles, T., Burkart, J., Häusler, T., Pummer, B., Hitzenberger, R., and Grothe, H.: Identification of ice nucleation active sites on feldspar dust particles, J. Phys. Chem. A, 119, 2692-2700, 2015.
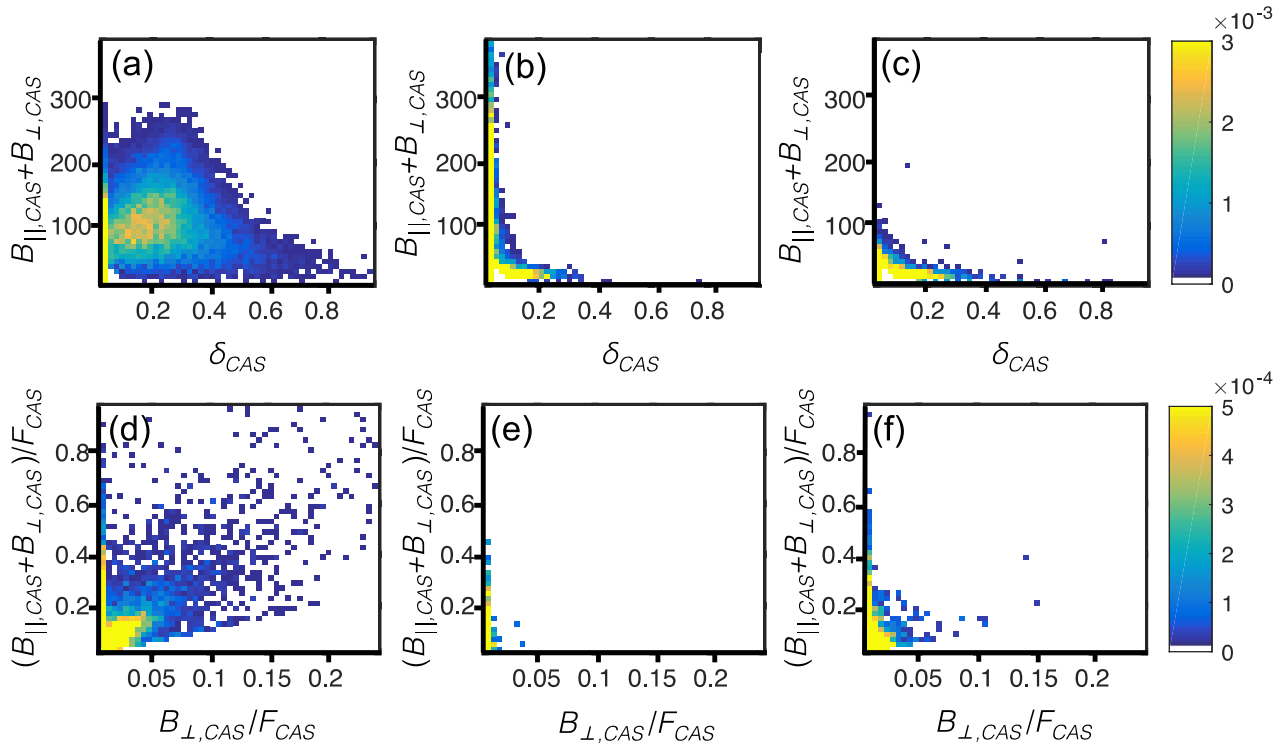
Figure 1: Optical signatures of training data populations: ice crystals (a, d), droplets (b, e), and aerosol (c, f). The CASPOL signals used to generate these signatures are parallel back scatter ($B_{\|CAS}$), perpendicular back scatter ($B_{\perp,CAS}$), and forward scatter (F_{CAS}). The shading scales indicate the fraction of the training dataset that populates a grid cell.
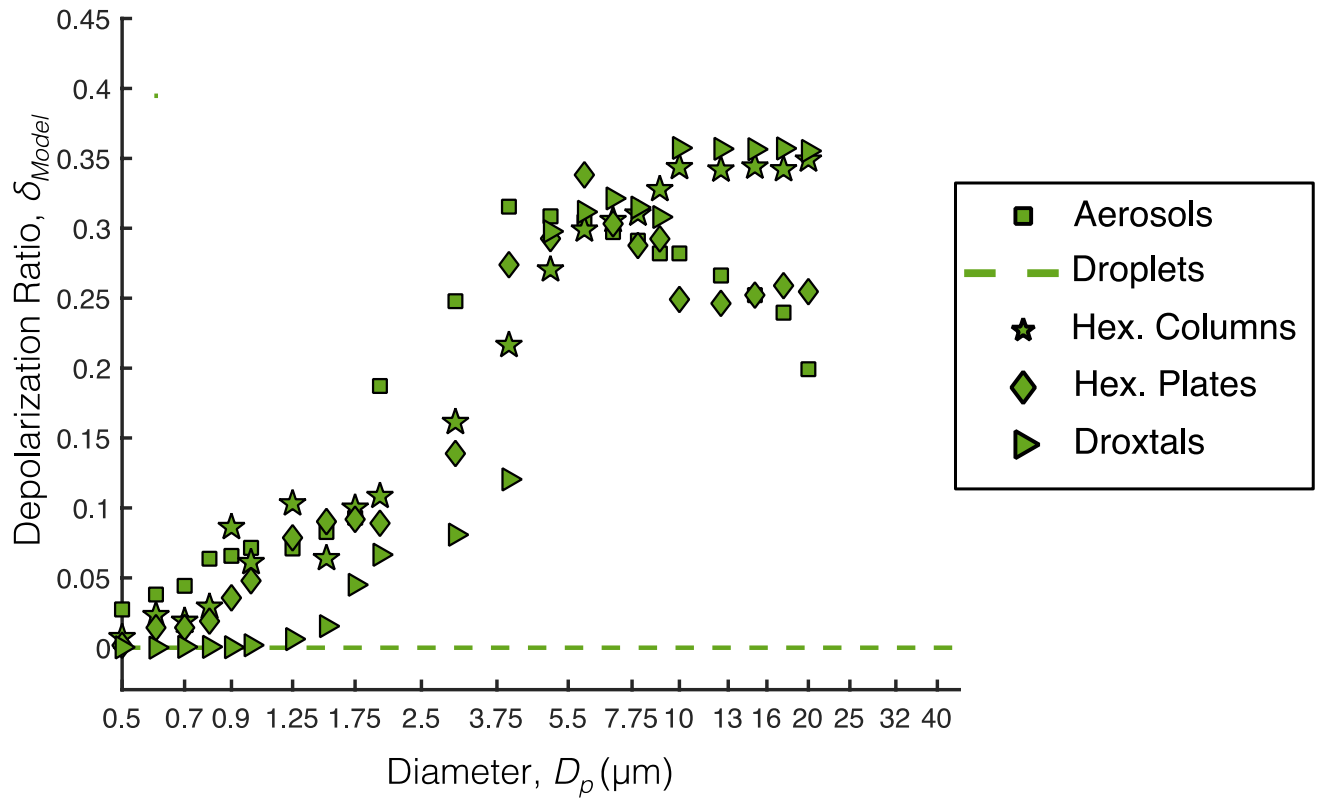
Figure 2. Depolarization ratio vs. diameter for modeled particles: droplets, aerosols, hexagonal column ice crystals, hexagonal plate ice crystals, and droxtals.

5
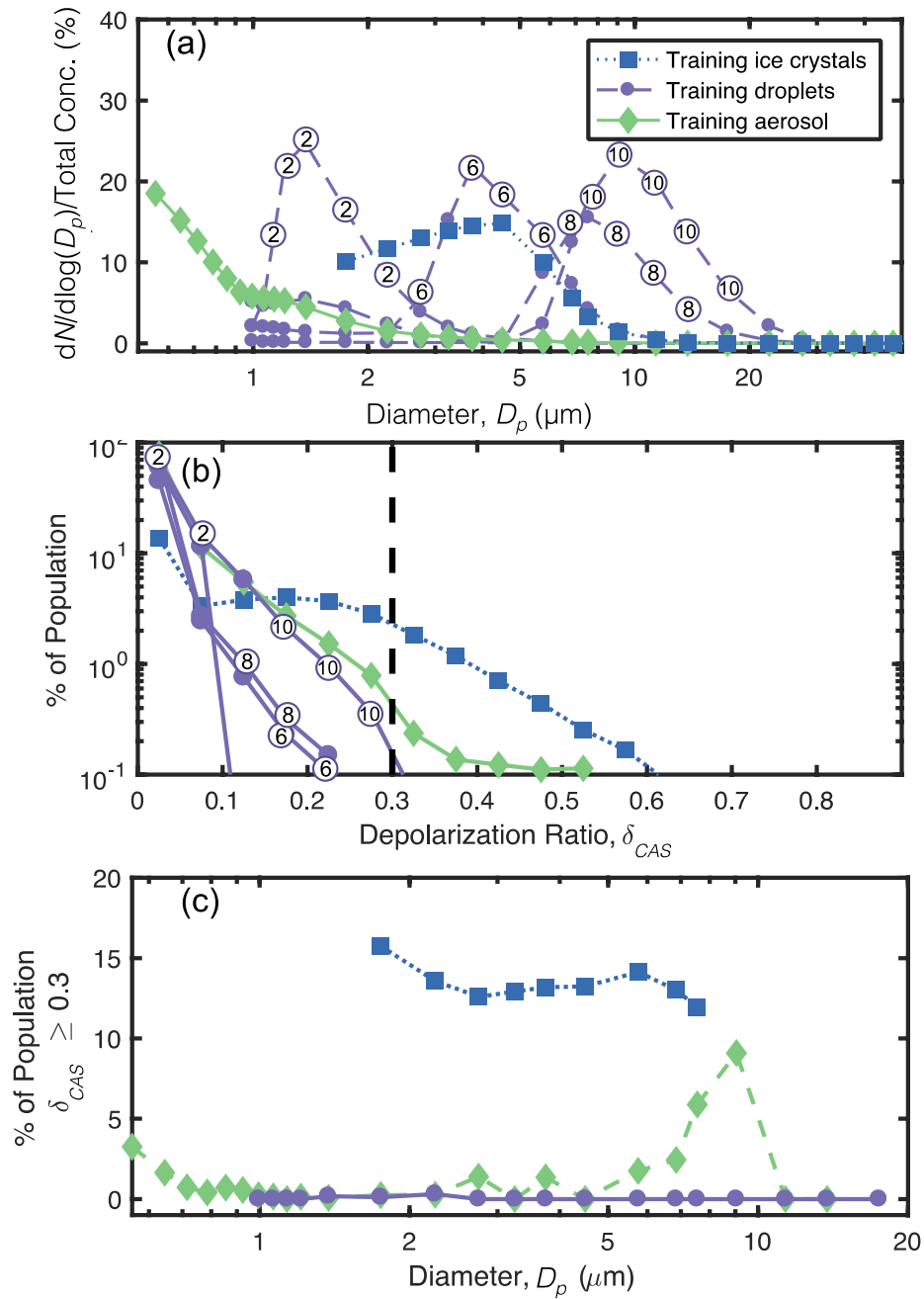
Figure 3: (a) Percent lognormal size distribution, (b) frequency distribution of depolarization ratios, and (c) the percentage of the particles with depolarization ratios above the threshold of 0.3 are shown for training data droplets, aerosols, ice crystals as detected by the CASPOL. In 1b, the depolarization ratio threshold value of 0.3 is indicated by the dashed line. In 1a and b, the numbers displayed in circles provide the diameter in µm of the VOAG data represented by that line.
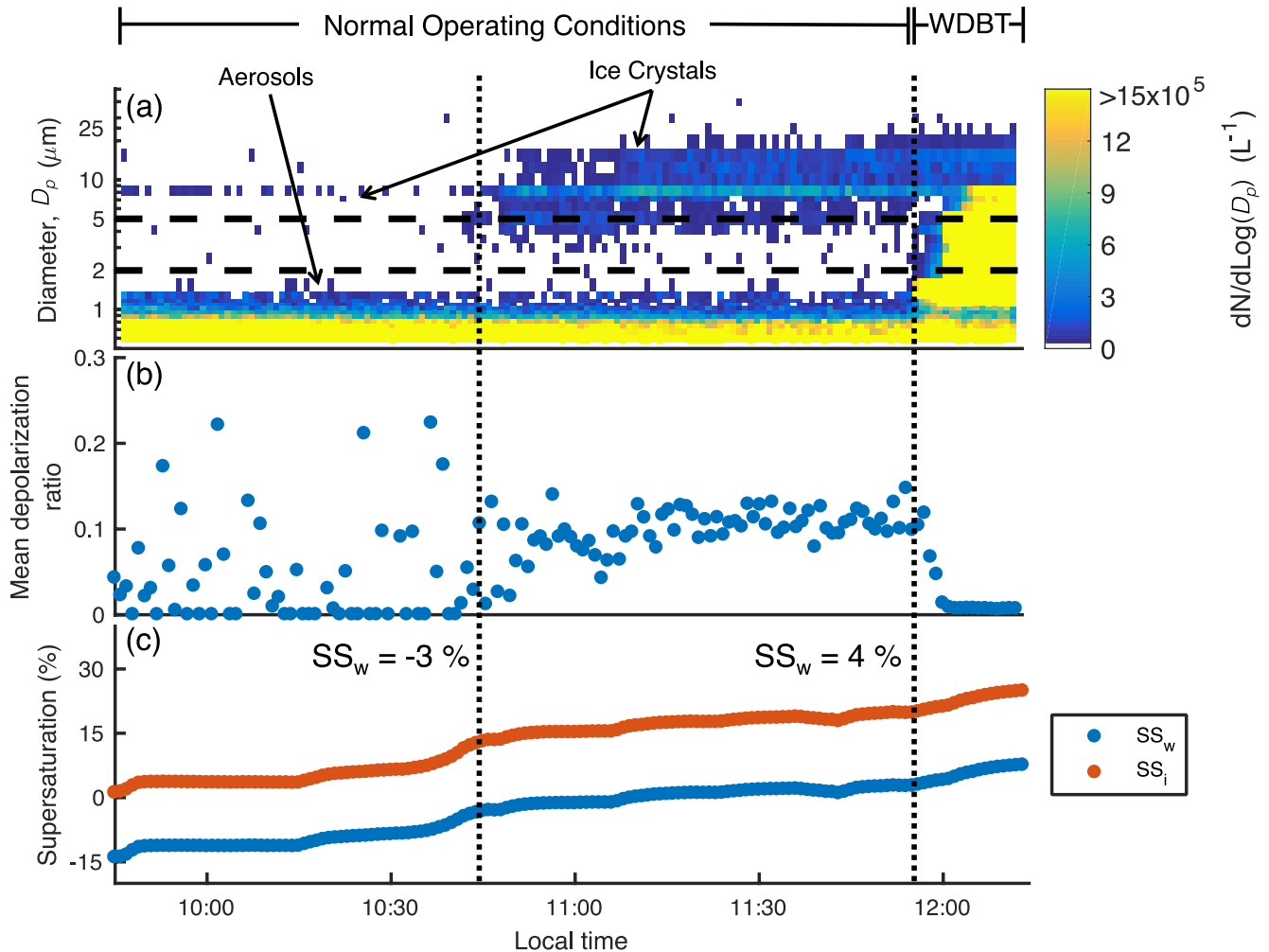
Figure 4. (a) The normalized size distribution, (b) mean depolarization ratio of particles in CFDC with diameter~~D~~D_p > 2 μm, and (c) supersaturation conditions with respect to ice (SS_i) and water (SS_w) for a Snomax® scan on March 27 at -15 °C ± 1.5 °C (case no. 27 in Table 1). The dashed lines in the figure denote the onset of abundant ice nucleation (10:45) and the onset of WDBT (11:55)
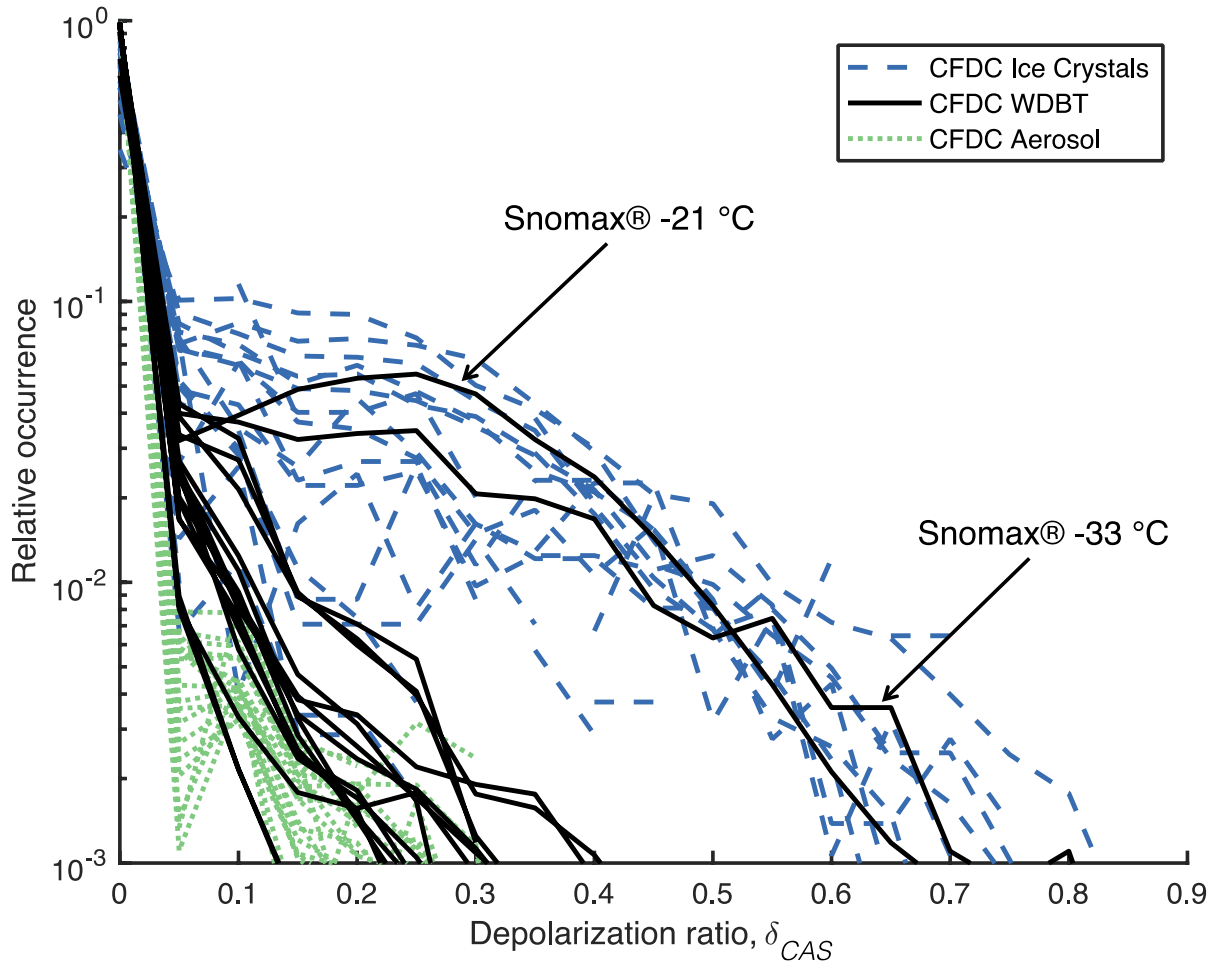
Figure 5: Frequency distribution of depolarization ratios for CFDC populations: ice crystal periods (19 periods classified), WDBT periods (17 periods classified), and aerosol periods (19 periods classified). Mean temperatures of periods included range from -15 to -35 °C.
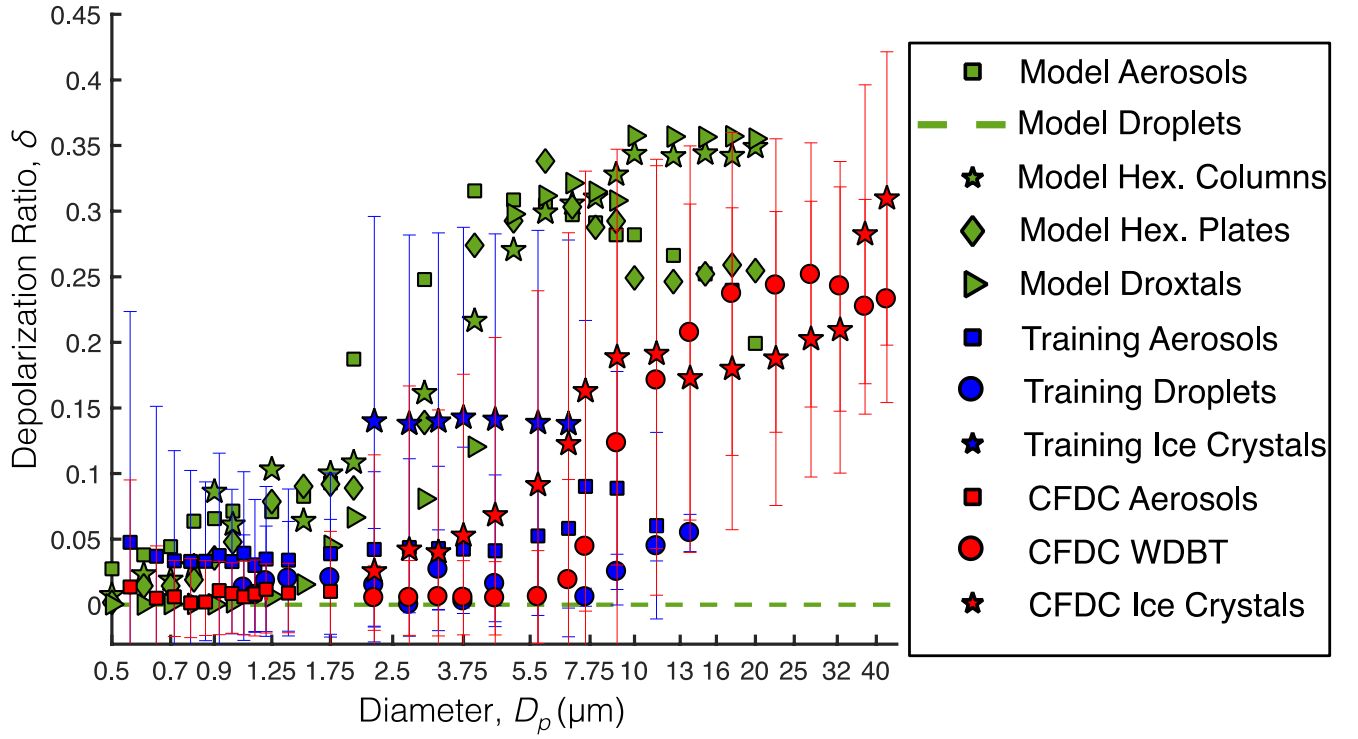
Figure 6: Mean depolarization ratios vs. particle diameter for modeled and observed particles. Observed error bars provide a standard deviation on the depolarization ratios of particles at each reported size. No error bars are reported for model calculations.
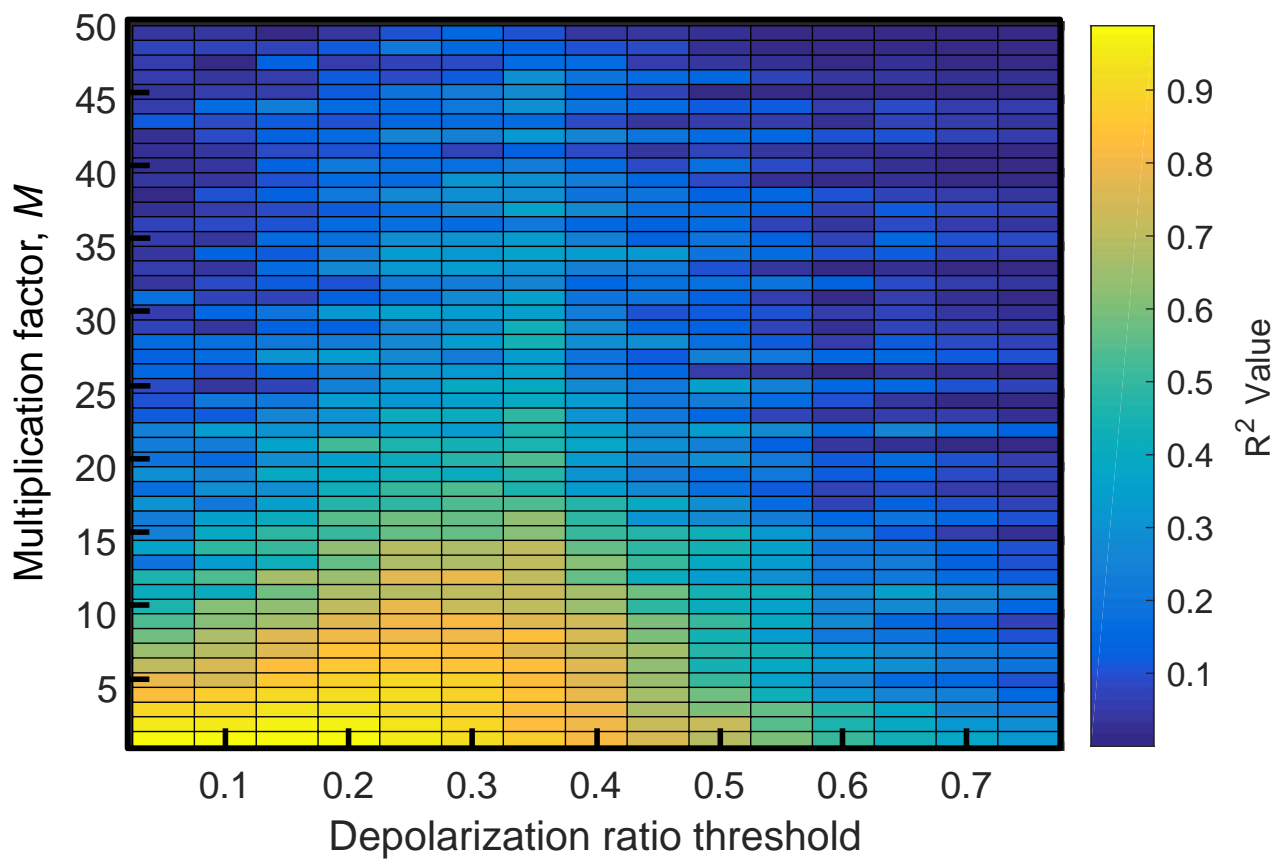
Figure 7. R^2 values for linear regression fit as a function of depolarization ratio threshold for optimizing ice crystal differentiation and water droplet/aerosol concentration multiplication factor, M.
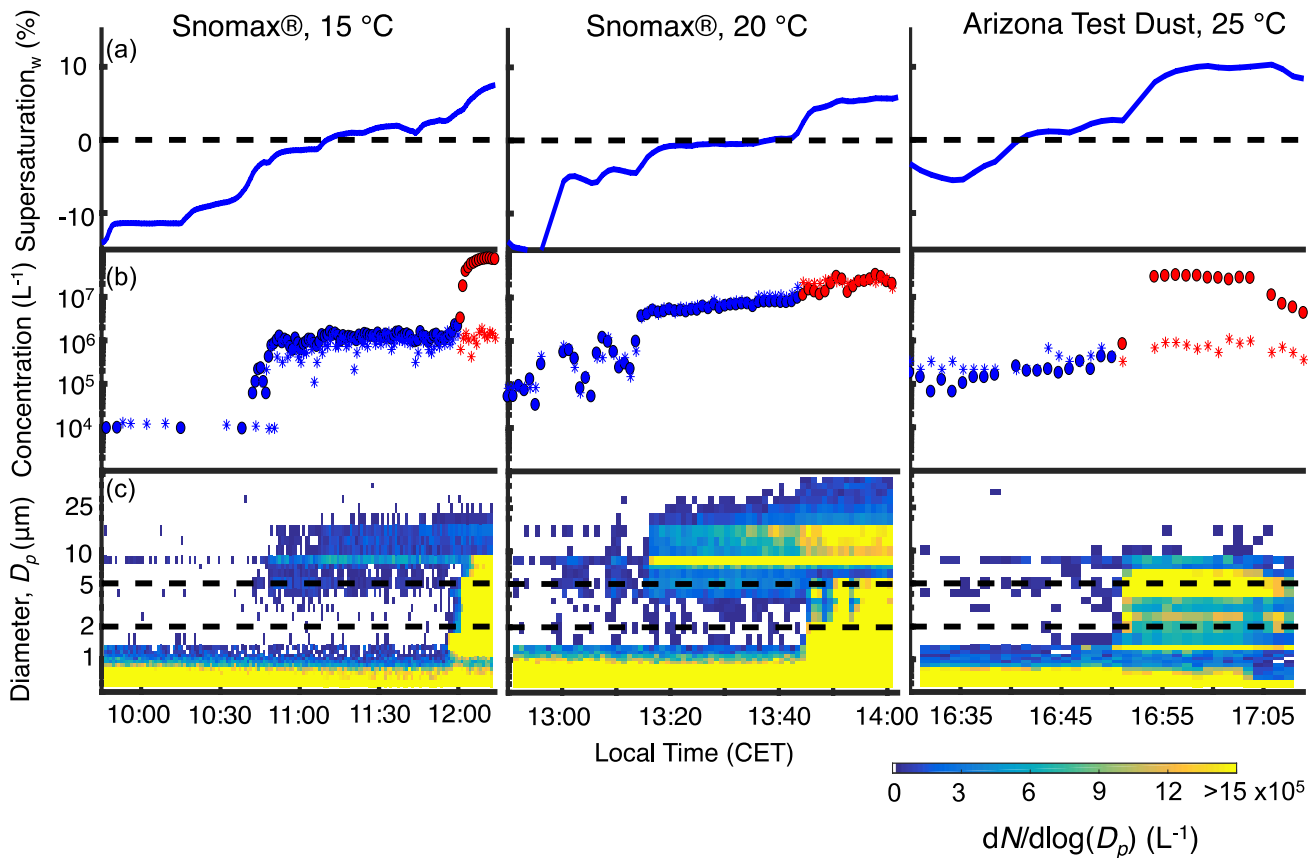
5

Figure 8: Application of depolarization ratio method on three CFDC runs. Aerosol composition and temperature are labeled in the title. (a) Time series of supersaturation with respect to water. (b) INP Concentrations under normal (blue) and WDBT (red) conditions are shown for the traditional (circle) and new (asterisk) analysis methods. (c) The normalized number distributions of all particles detected by the CASPOL. Time is reported in local time (CET).
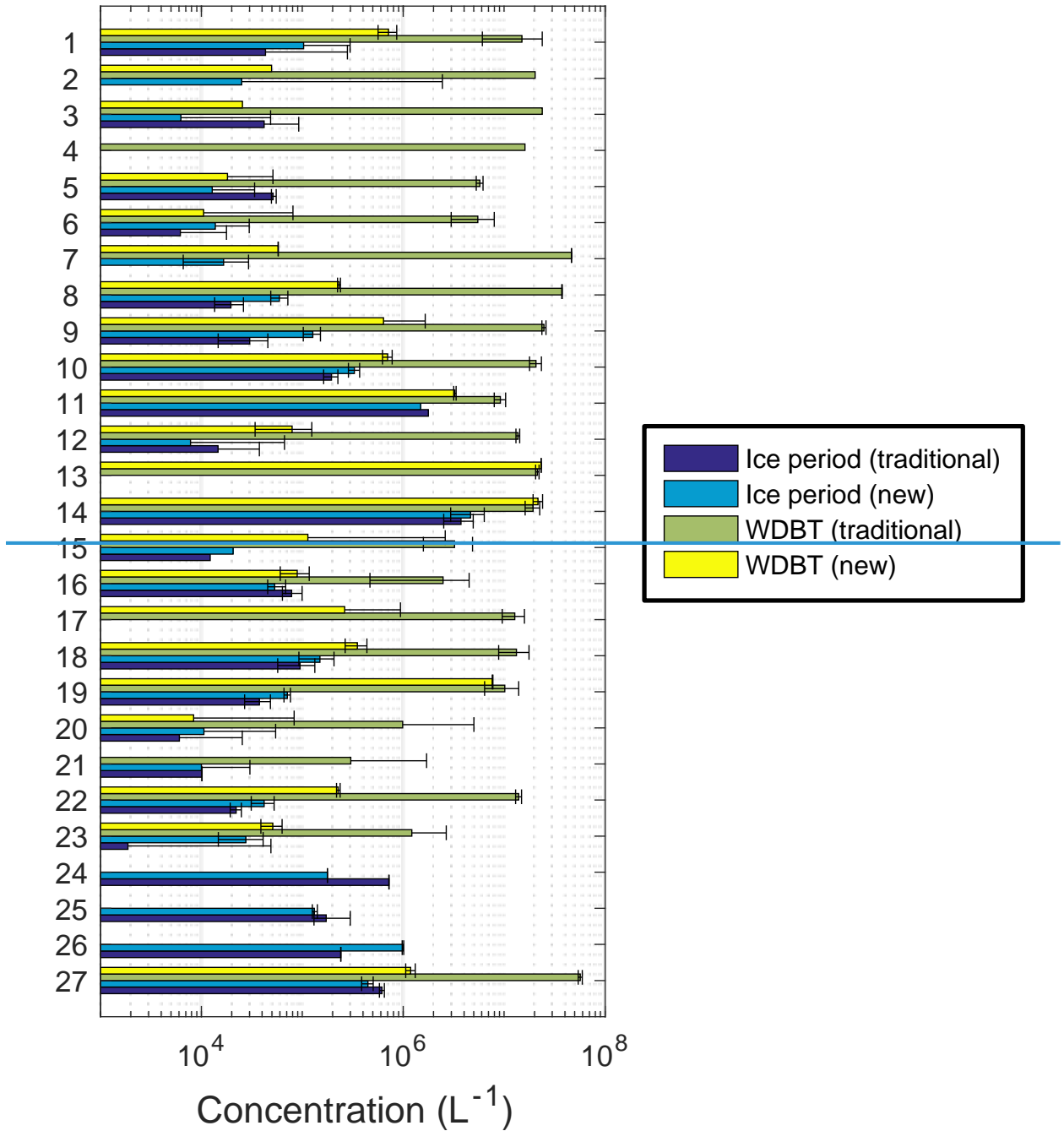
Ice period (traditional)
Ice period (new)
WDBT (traditional)
WDBT (new)
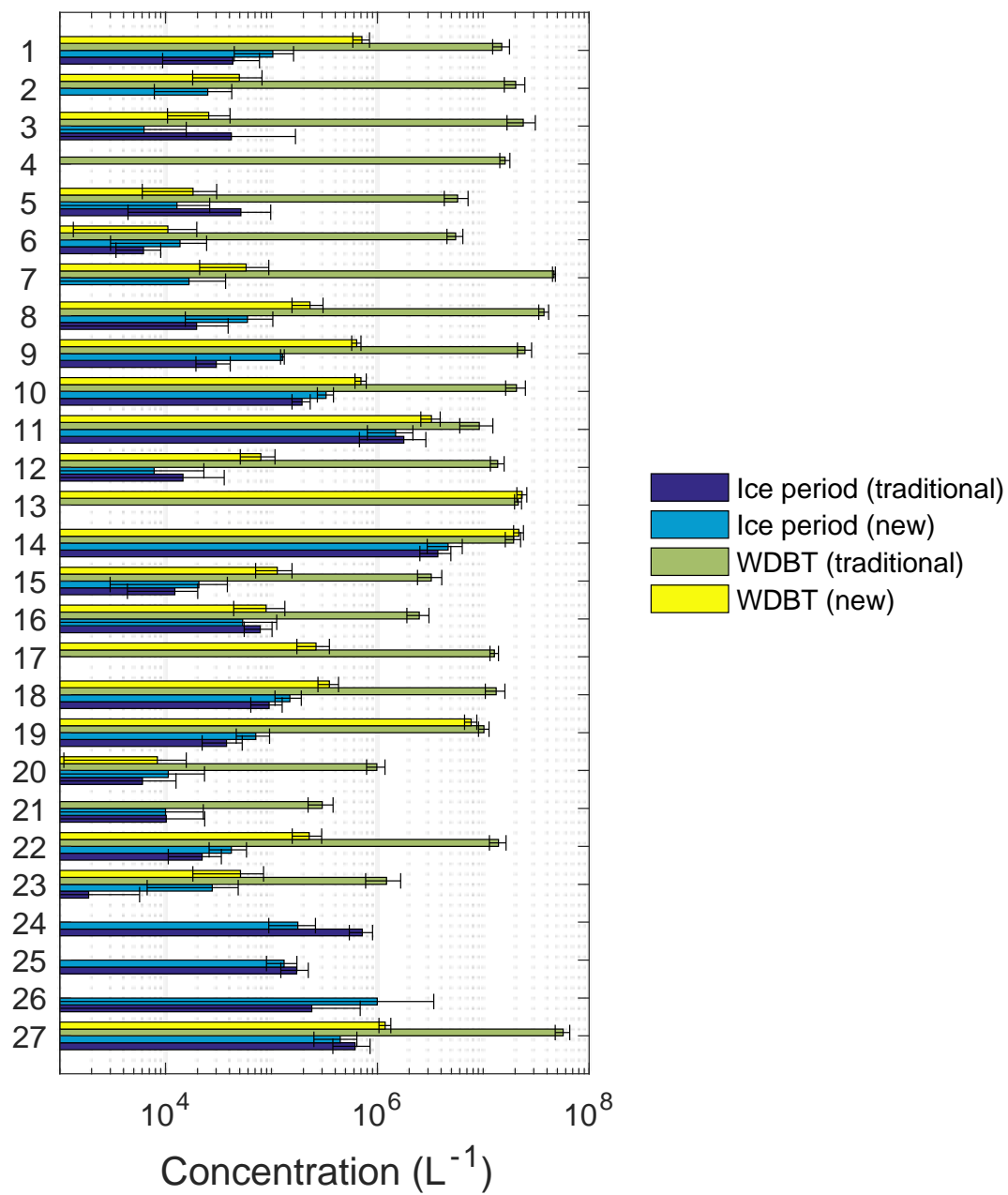
Concentration (L^{-1})

Figure 9: Individual cases of "Ice Only" and "WDBT" INP concentration comparisons with the traditional size-cut and depolarization ratio methods. Error bars report the CFDC-CASPOL counting error of 39%.
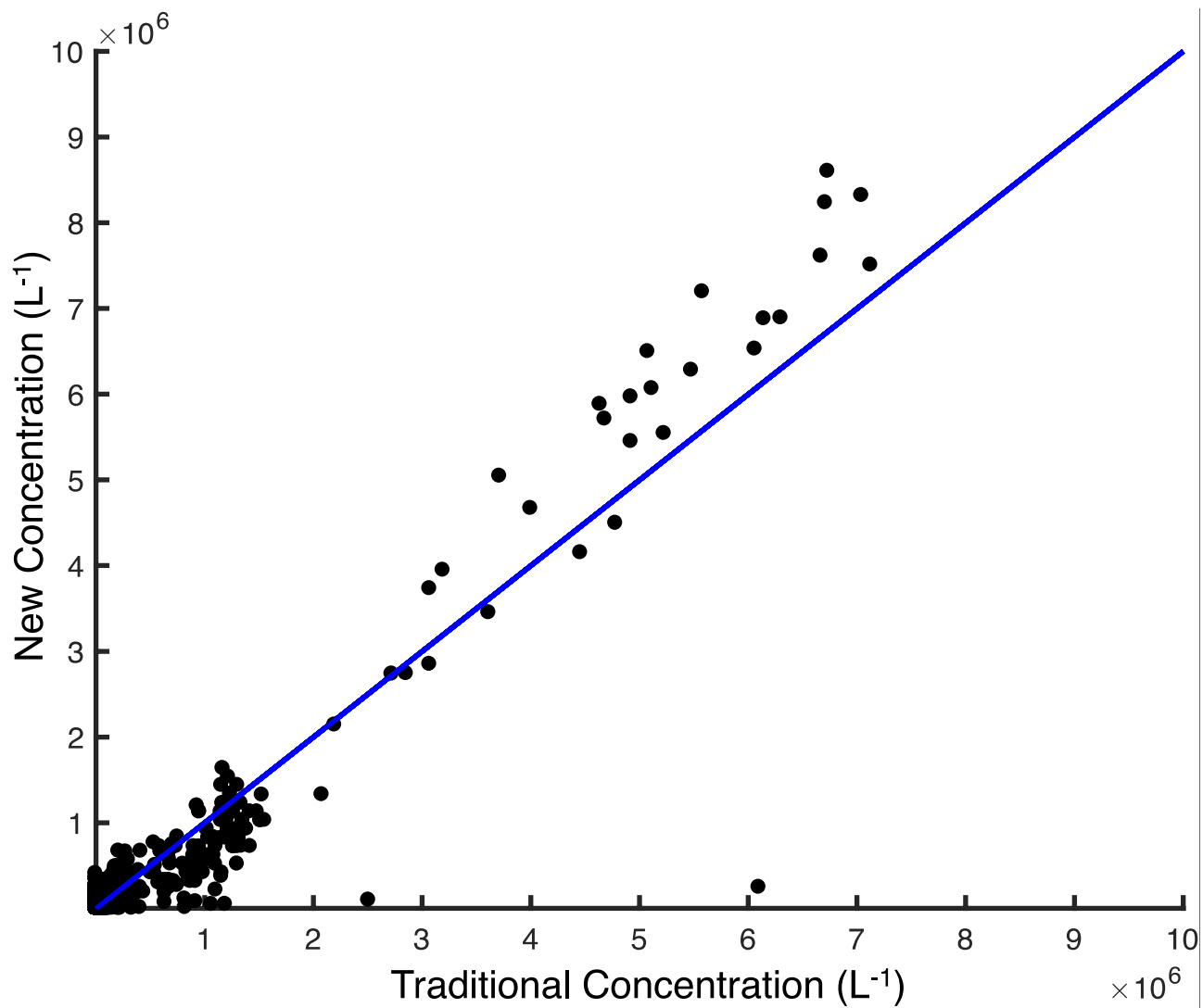
5

Figure 10: Traditional INP concentration vs. new INP concentration with 1:1 line for "ice only" periods.
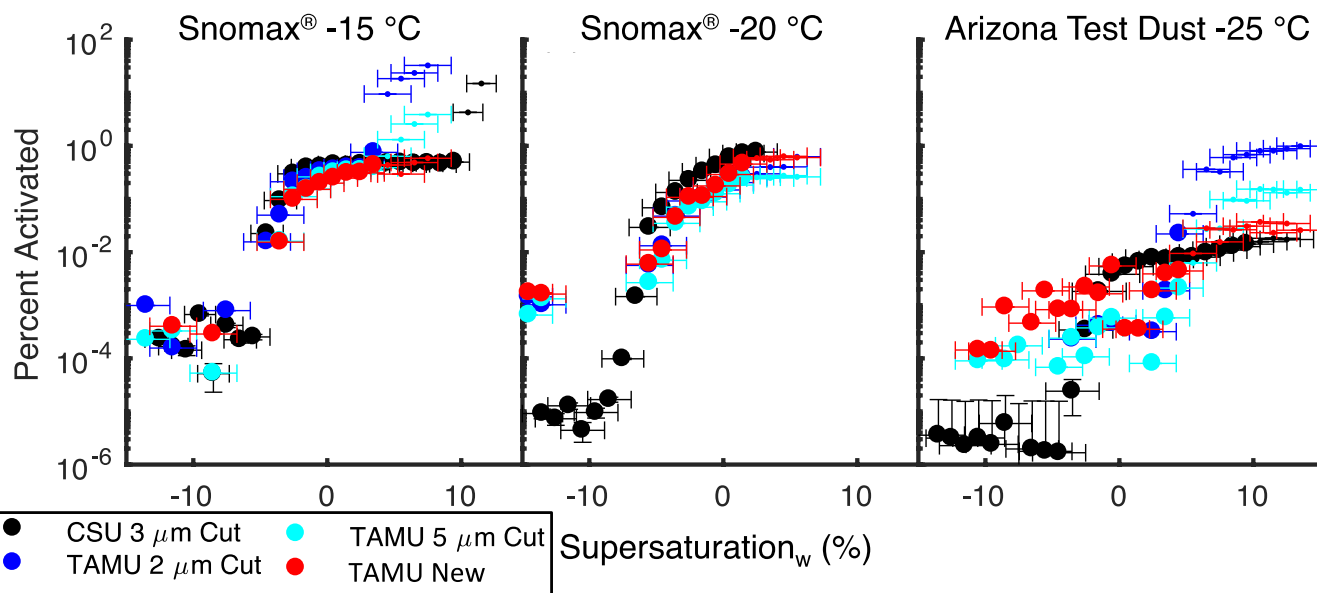
117

Figure 11: TAMU CFDC versus CSU CFDC comparison: (a) Snomax® at -15 °C, (b) Snomax® at -20 °C, and (c) Arizona Test Dust at -25 °C. Small symbols indicate that those points were sampled in WDBT. TAMU 2 µm cut and 5 µm cut traditional INP fraction activated are shown in blue and cyan respectively. The TAMU new analysis method INP fraction activated is shown in red. The CSU 3 µm INP fraction activated is shown in black.

5

Case No.	Date Time	Composition	Chamber	Temperature ($^\circ$C)
1	3/24/15 10:13	Arizona Test Dust*	AIDA	-25
2	3/24/15 11:25	Arizona Test Dust*	AIDA	-20
3	3/24/15 12:48	Arizona Test Dust*	APC	-19
4	3/24/15 16:02	Argentinian Soil Dust*	AIDA	-19
5	3/24/15 17:29	Argentinian Soil Dust*	AIDA	-18
6	3/24/15 18:28	Argentinian Soil Dust*	AIDA	-24
7	3/25/15 10:15	Argentinian Soil Dust*	AIDA	-25
8	3/25/15 11:22	Argentinian Soil Dust*	AIDA	-28
9	3/25/15 12:35	Argentinian Soil Dust*	APC	-28
10	3/25/15 16:48	Arizona Test Dust*	AIDA	-25
11	3/25/15 17:51	Arizona Test Dust*	AIDA	-28
12	3/19/15 17:45	Arizona Test Dust	AIDA	-34
13	3/20/15 11:49	Snomax®	APC	-33
14	3/20/15 13:28	Snomax®	APC	-21
15	3/21/15 10:28	Snomax®	AIDA	-16
16	3/21/15 11:12	Snomax®	AIDA	-19
17	3/21/15 11:47	Snomax®	AIDA	-20
18	3/21/15 12:54	Snomax®	APC	-15
19	3/23/15 10:55	K-Feldspar (Contaminated with Snomax®)	AIDA	-30
20	3/23/15 16:48	K-Feldspar (Contaminated with Snomax®)	AIDA	-25
21	3/23/15 18:17	K-Feldspar (Contaminated with Snomax®)	AIDA	-21
22	3/26/15 10:05	Illite NX	AIDA	-25
23	3/26/15 11:09	Illite NX	AIDA	-25
24	3/26/15 12:04	Illite NX	AIDA	-28
25	3/26/15 12:44	Illite NX	AIDA	-30
26	3/26/15 16:39	Desert Dust	APC	-29
27	3/27/15 10:59	Snomax®	APC	-16

Table 1: Date and time (CET), the composition of aerosol sampled, and the CFDC operating temperature (± 1.5 $^\circ$C).
*Data collected during "blind tests" Sample composition was provided by the referees after the experiment was completed.
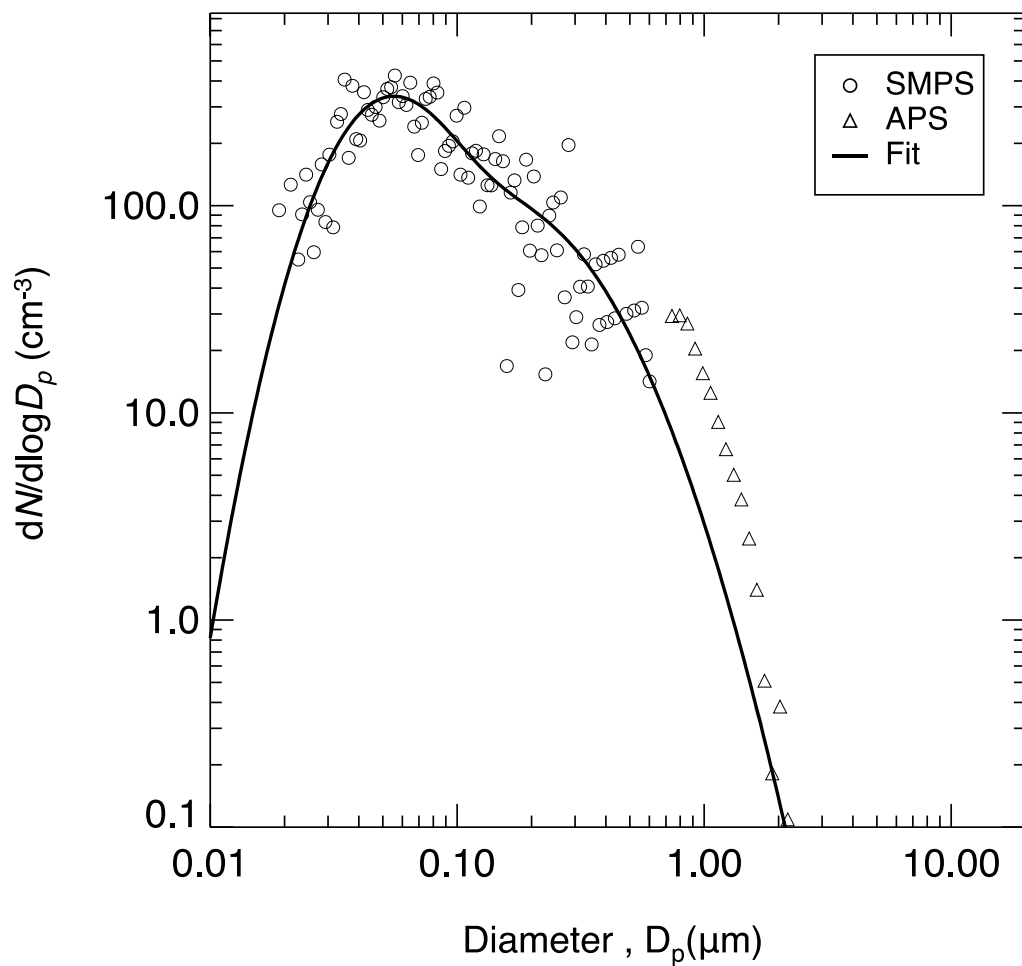
Figure S1. The number lognormal size distribution for Snomax® run on March 27th (case 27 in table) and featured in Fig. 4. SMPS data is reported as ~~cirlees~~circles, APS data is reported as ~~trianlges~~triangles, and a fit is reported as a black line.

5

10

Simulation M

Segment No.	Ice crystals	Droplets	Aerosol	$\geq \delta$ -Threshold
1	0	$M \times 100$	$M \times 300$	.
2	2	$M \times 100$	$M \times 300$	.
3	5	$M \times 100$	$M \times 300$	.
.	.	$M \times 100$	$M \times 300$	.
.	.	$M \times 100$	$M \times 300$	.
.	.	$M \times 100$	$M \times 300$	.
120	350	$M \times 100$	$M \times 300$	.

Simulation $M+1$

Segment No.	Ice crystals	Droplets	Aerosol	$\geq \delta$ -Threshold
1	0	$(M+1) \times 100$	$(M+1) \times 300$	.
2	2	$(M+1) \times 100$	$(M+1) \times 300$	.
3	5	$(M+1) \times 100$	$(M+1) \times 300$	.
.	.	$(M+1) \times 100$	$(M+1) \times 300$	.
.	.	$(M+1) \times 100$	$(M+1) \times 300$	.
.	.	$(M+1) \times 100$	$(M+1) \times 300$	.
120	350	$(M+1) \times 100$	$(M+1) \times 300$	.

5   **Supplemental Table 1. This table illustrates how the simulated data sets are constructed as detailed in section 3.7 for M and $M+1$.**